Properties of vitreous and molten alkali molybdates and tungstates

Document Version:
Publisher's PDF, also known as Version of Record (includes final page, issue and volume numbers)

Please check the document version of this publication:

• A submitted manuscript is the version of the article upon submission and before peer-review. There can be important differences between the submitted version and the official published version of record. People interested in the research are advised to contact the author for the final version of the publication, or visit the DOI to the publisher's website.
• The final author version and the galley proof are versions of the publication after peer review.
• The final published version features the final layout of the paper including the volume, issue and page numbers.

[Link to publication](#)

PROPERTIES OF VITREOUS AND MOLTEN ALKALI MOLYBDATES AND TUNGSTATES

R. G. GOSSINK

PROPERTIES OF VITREOUS AND MOLTEN ALKALI MOLYBDATES AND TUNGSTATES

PROEFSCHRIFT

DOOR

ROBERT GEORG GOSSINK

GEBOREN TE EINDHOVEN

aan Liesbeth
aan mijn ouders

CONTENTS

1. INTRODUCTION

1.1. Glasses containing MoO_3 or WO_3

This thesis describes an investigation of the structures of glasses containing MoO_3 or WO_3 as the only glass-forming oxide. In a narrower sense this means: the structures of vitreous alkali molybdates and tungstates. In the pure state, neither MoO_3 nor WO_3 forms a glass unless it is quenched extremely rapidly with the aid of a special technique. Both oxides can form glasses only in combination with certain other oxides.

Among the classical glass-forming oxides, only P_2O_5 allows the preparation of stable glasses having high MoO_3 or WO_3 contents.

For this reason, most investigations of glasses containing considerable amounts of MoO_3 or WO_3 concern phosphomolybdate or phosphotungstate glasses.

Glasses having high WO_3 contents were prepared first by Rothermel et al. [1-1]) in the system $PbO–WO_3–P_2O_5$ (up to 85 weight% WO_3). These glasses possess interesting X-ray-absorbing properties.

Franck [1-2]) prepared both $MoO_3–P_2O_5$ and $WO_3–P_2O_5$ glasses, which strongly coloured on melting. The colour is due to oxygen loss, which causes transition of part of the Mo^{6+} and W^{6+} ions to lower valency states. By this reduction the glasses become semiconducting.

An investigation of electrical conductivities of phosphotungstate glasses was described by Caley and Murthy [1-3]), their glasses containing up to 80 mole% WO_3. The electrical conductivity is improved when the WO_3 content is increased. Obviously, the semiconducting character of the phosphomolybdate and phosphotungstate glasses can be optimalised by application of a sensibly selected melting atmosphere. In this connection the investigations of Hirohata et al.[1-4]) should be mentioned, which demonstrate that the specific resistance of WO_3 decreases when the oxygen deficiency is increased by hydrogen treatment.

Stable glasses can also be prepared in the system $MoO_3–WO_3–MgO–BaO$[1-5]) which indicates that MoO_3 and WO_3 show a greater tendency to glass formation when melted together. The glasses formed in the latter system are infrared-transmissive between 1·5 and 5 μm.

A systematic investigation of the tendency to glass formation in a large number of binary oxide systems with MoO_3 or WO_3 as one of the components, was carried out by Baynton et al.[1-6]): MoO_3 was found to form glass in combination with Li_2O, Na_2O, K_2O, BaO, P_2O_5 and TeO_2, indications of glass formation also being observed in the systems $MoO_3–PbO$ and $MoO_3–Bi_2O_3$; WO_3 formed glass in combination with Na_2O, K_2O, P_2O_5 and TeO_2, whilst indications of glass formation were also found in the systems $WO_3–BaO$ and $WO_3–PbO$.

In all these cases the glass-formation tendency was measured by heating a paste of a mixture of the two components (10–20 mg) on a V-kinked platinum-alloy resistance wire, followed by abruptly switching off the heating current. Baynton et al. give no values for the cooling rates obtained in their experiments.

With the exception of those containing P_2O_5 or TeO_2, the glasses were qualified as devitrifying easily and could only be prepared in narrow composition regions (a few mole% MoO_3 or WO_3) around the compositions listed in table 1-I*).

TABLE 1-I

Compositions of glasses obtained by Baynton et al.[1−6])

system	mole% MoO_3 or WO_3 in the glass
Li_2MoO_4–MoO_3	57
Na_2MoO_4–MoO_3	65
K_2MoO_4–MoO_3	10
$BaMoO_4$–MoO_3	76
Na_2WO_4–WO_3	6
K_2WO_4–WO_3	54

1.2. Vitreous alkali molybdates and tungstates

When the properties and behaviour of MoO_3 and WO_3 as glass-forming oxides are to be studied, problems are caused by the fact that both oxides only form glass under extremely rapid quenching conditions. The stable glasses which can be obtained by a combination with P_2O_5 or TeO_2 present the difficulty of the introduction of a second glass-forming oxide. This difficulty is avoided if oxides are added of a typically modifying character, such as the alkali oxides.

The work of Baynton et al.[1−6]) shows that glass formation in alkali-molybdate and -tungstate systems is possible, provided that the melt is rapidly cooled.

Gelsing et al.[1−7,8]) investigated the glass-formation tendencies of alkali-tungstate systems, the alkali metal being Li, Na, K, Rb or Cs. Their method, though resembling superficially that of Baynton, shows a few essential differences:

---

*) In the systems M_2O–MoO_3 and M_2O–WO_3 (M = alkali metal) glasses are formed exclusively at compositions containing an excess of trioxide (MoO_3 or WO_3). For this reason only the systems M_2MoO_4–MoO_3 and M_2WO_4–WO_3 will be considered in this thesis. Compositions will be expressed, whenever possible, in mole% MoO_3 and WO_3 respectively. For example, $(100 - x) M_2MoO_4 . x MoO_3$ will be referred to as "x mole% MoO_3". It should be stressed here that "0 mole% MoO_3" does not refer to pure M_2O, but to the monomolybdate M_2MoO_4.

(a) Gelsing's samples were prepared before being melted on the resistance wire;
(b) cooling rates could be varied, and high cooling rates were obtained by directing a current of air onto the sample;
(c) the apparatus used permitted an accurate determination of cooling rates.
This experimental method, also applied in our work, will be described in more detail in chapter 2.

As the cooling rates could be measured, Gelsing et al. were able to describe quantitatively the glass-formation tendency in the systems considered. They express this tendency by the value of the critical cooling rate (CCR, $°C\ s^{-1}$) defined as *the minimum cooling rate necessary to prevent crystallisation entirely.* A low value of CCR corresponds with a high tendency to glass formation.

The results of the investigations of Gelsing et al. are shown in fig. 1.1. This figure also contains the results of an analogous investigation of the glass formation in alkali-molybdate systems performed by Van der Wielen et al.[1-9]. A comparison between the glass-formation phenomena in both groups of systems produces a number of striking similarities and dissimilarities.
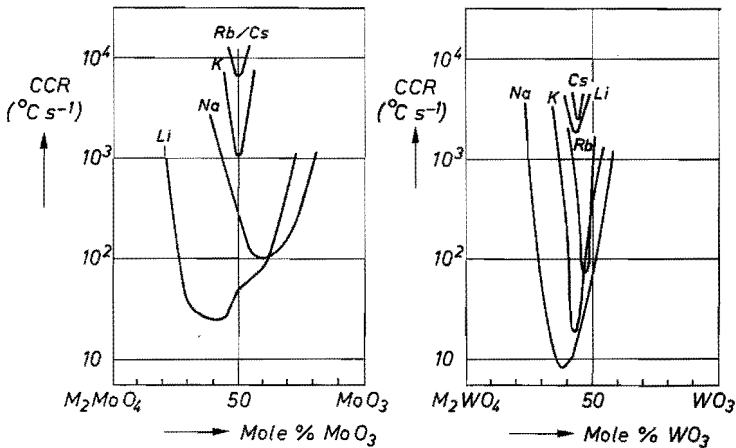
Fig. 1.1. Relation between critical cooling rate CCR ($°C\ s^{-1}$) and composition for alkali-molybdate and -tungstate systems (after Van der Wielen et al.[1-9] and Gelsing et al.[1-7,8]).

The similarities can be summarised as follows:
(a) There is a sharp minimum in all systems between 40 and 60 mole % trioxide, i.e. round the compositions $M_2Mo_2O_7$ and $M_2W_2O_7$.
(b) The tendency to glass formation strongly depends on the nature of the alkali ion present; in general this tendency increases when the radius of the alkali ion decreases.

The differences are the following:
(a) The minimum CCR value of any alkali-tungstate system is lower than that of the corresponding molybdate system, with the remarkable exception of the system $Li_2WO_4-WO_3$.

(b) The CCR-composition curves of the tungstate systems are narrower and show a greater mutual similarity than those of the molybdate systems.

The overall minimum CCR value reached in these systems is approximately $9\,°C\,s^{-1}$ (at the composition $0·62\ Na_2WO_4 . 0·38\ WO_3$).

The compositions of the glasses prepared by Baynton et al. (see table 1-I) deviate appreciably from the compositions of minimum CCR, found by Gelsing et al. and Van der Wielen et al. This should be attributed to Baynton's preparation method, which may cause serious errors in composition.

In fig. 1.1 it is seen that a cooling rate of $10^4\,°C\,s^{-1}$ is still insufficient to bring MoO_3 or WO_3 into the vitreous state. Sarjeant and Roy [1-11]), however, obtained partly vitreous MoO_3 and WO_3, using the splat-cooling method with cooling rates of $10^6–10^7\,°C\,s^{-1}$. The latter method will also be described in chapter 2.

1.3. Phase diagrams and crystal structures

For our investigation, knowledge of the phase diagrams of alkali-molybdate and alkali-tungstate systems, and the crystal structures of the compounds found in these phase diagrams, is indispensable. Therefore, a short survey of the literature data available will be given. Phase diagrams of alkali-tungstate and alkali-molybdate systems have been reported by a great number of authors. However, the results obtained are often contradictory, owing to the various experimental methods applied.

In our opinion the phase diagrams determined by Gelsing et al.[1-12]), Caillet [1-13]), Van der Wielen et al.[1-9]) and Salmon and Caillet [1-14]) are the most reliable for reasons of sample-preparing and measuring methods. The above-mentioned authors obtained their samples by a slow solid-state reaction.

Figure 1.2 shows the phase diagrams of the alkali-tungstate and -molybdate systems. The $Li_2WO_4–WO_3$ phase diagram included is based on non-published data obtained by Gelsing [1-15]). Some uncertainty exists as to the melting behaviour of $K_2W_2O_7$, which compound should melt incongruently according to Gelsing et al.[1-12]), whereas Caillet [1-13]) reports congruent melting. Gelsing's diagram has been included in fig. 1.2. A comparison between the phase diagrams of fig. 1.2 prompts to the following remarks:

(a) The melting point of a monotungstate (M_2WO_4) shows only a slight difference from that of the corresponding monomolybdate (M_2MoO_4). However, the melting points of WO_3 and MoO_3 lie far apart.

(b) The crystalline compounds in the Li-, Rb- and Cs-tungstate systems appear less frequently than those in the corresponding molybdate systems. Moreover, the stability of the tungstate compounds generally is lower than that of the corresponding molybdates, which is demonstrated by a smaller number of compounds formed and a smaller number of congruently melting phases observed in the case of the tungstate systems.

(c) In general the stability of the ditungstates and dimolybdates tends to decrease in the order Li→Cs, whereas for the trimolybdates and tritungstates the opposite order appears to be valid.

The crystal structures of only some of the compounds found by phase-diagram studies have been determined.

To begin with, all monomolybdate and monotungstate structures are known [1-20,38]). The structures of all these compounds consist of nearly regular MoO_4 and WO_4 tetrahedra respectively, held together by the alkali ions. Monomolybdates and monotungstates having the same alkali ion are isomorphous. However, the coordination number of the alkali ion depends on the radius of this ion. At room temperature, Li^+ ions are coordinated by 4 oxygen ions [1-16,17]), while Cs^+ ions occupy 9- and 10-coordinate positions [1-20]). Further, an elevation of temperature appears to give rise to a higher coordination number of the alkali ions [1-39]).

Among the crystalline alkali molybdates and tungstates of higher trioxide contents, only the structures of $Na_2Mo_2O_7$ [1-18,21]), $Na_2W_2O_7$ [1-18]), $K_2Mo_3O_{10}$ [1-22,23]), $Rb_2Mo_3O_{10}$ [1-23]) and $Cs_2Mo_3O_{10}$ [1-23]) have been determined. The structures of all these compounds consist of infinite chains without cross-links.

The chains found in the $Na_2Mo_2O_7$ structure — this compound being isomorphous with $Na_2W_2O_7$ — are built up by MoO_6 octahedra sharing corners, with MoO_4 tetrahedra bridging adjacent octahedra. This structure is shown in fig. 1.3. Tetrahedral groups are nearly regular, whereas the octahedra are clearly distorted. Sodium ions, occupying interchain positions, are 6-coordinated.

The chains found in the $K_2Mo_3O_{10}$ structure consist of distorted MoO_6 octahedra interconnected by pairs of polyhedra which form a transition between MoO_4 tetrahedra and MoO_5 pyramids. Seleborg [1-22]) makes no choice, while Gatehouse and Leverett [1-23]) express a preference for 5-coordination. The structure as described by the latter authors is shown in fig. 1.3. In the $K_2Mo_3O_{10}$ structure, the polyhedra share not only corners but also edges. Potassium ions occupy interchain positions, which are 6-coordinated according to Seleborg, whereas Gatehouse and Leverett propose 10-coordination. $Rb_2Mo_3O_{10}$ and $Cs_2Mo_3O_{10}$ are isostructural with $K_2Mo_3O_{10}$ [1-23]).

Finally, the structures of MoO_3 and WO_3 are essentially different. Although both structures contain exclusively distorted octahedra, these octahedra form a three-dimensional network in the case of WO_3, while MoO_3 has a layer structure, without cross-links. The WO_6 groups only share corners. In the MoO_3 structure, however, each octahedron shares edges with its two neighbours, forming zig-zag chains; octahedra in the chain share corners with octahedra in parallel chains, thus forming layers.

Three oxygens of each MoO_6 group are common to three octahedra within a

Fig.1.2a.
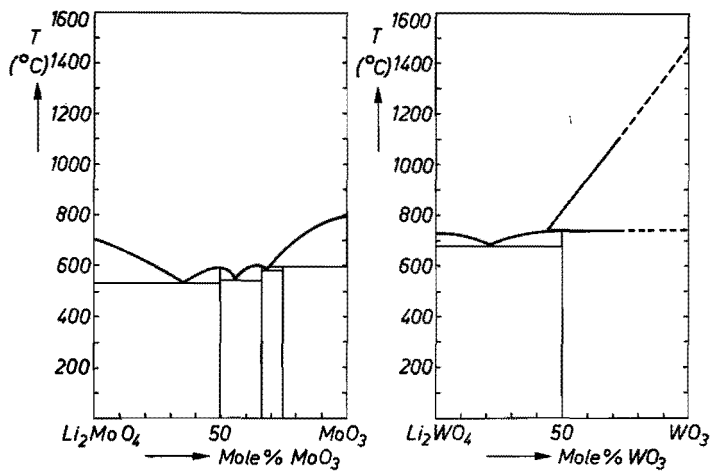
Fig.1.2b.
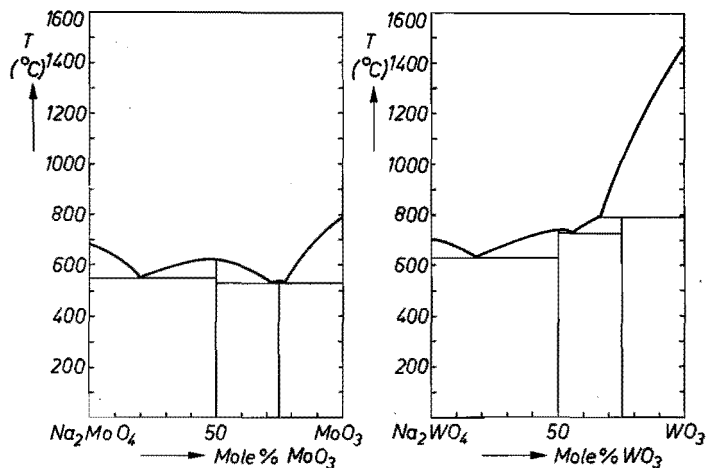
Fig.1.2c.
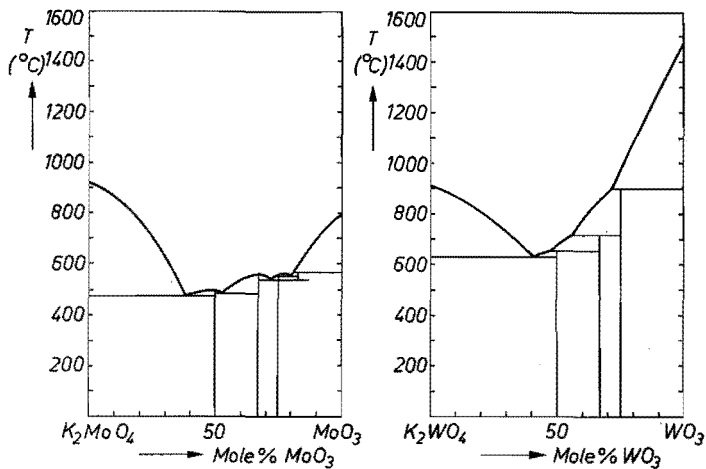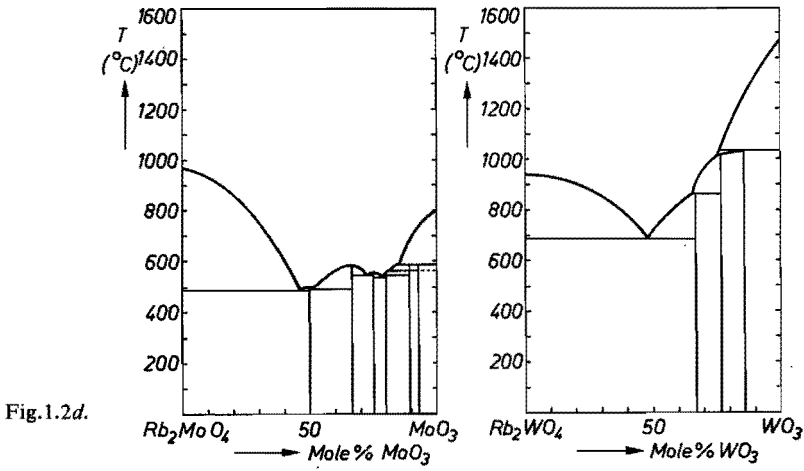
Fig.1.2d.
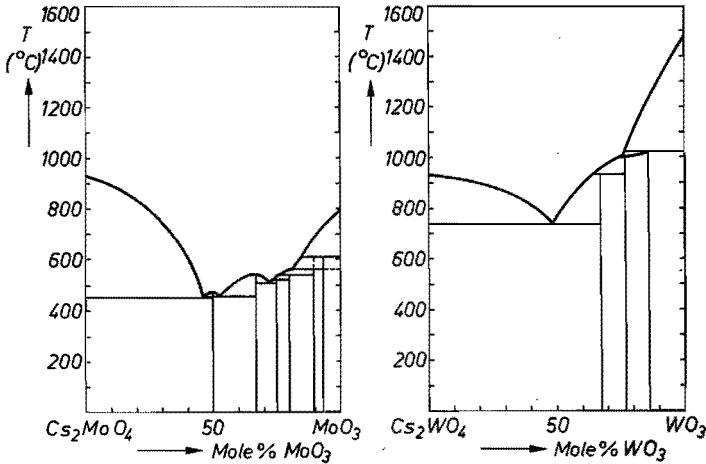
Fig. 1.2e.

Fig. 1.2. Phase diagrams of alkali-molybdate and -tungstate systems.
(a) System Li_2MoO_4–MoO_3 (ref. 1–9); system Li_2WO_4–WO_3 (ref. 1–15).
(b) System Na_2MoO_4–MoO_3 (ref. 1–13); system Na_2WO_4–WO_3 (ref. 1–13).
(c) System K_2MoO_4–MoO_3 (ref. 1–13); system K_2WO_4–WO_3 (ref. 1–12).
(d) System Rb_2MoO_3–MoO_3 (ref. 1–14); system Rb_2WO_4–WO_3 (ref. 1–14).
(e) System Cs_2MoO_4–MoO_3 (ref. 1–14); system Cs_2WO_4–WO_3 (ref. 1–14).
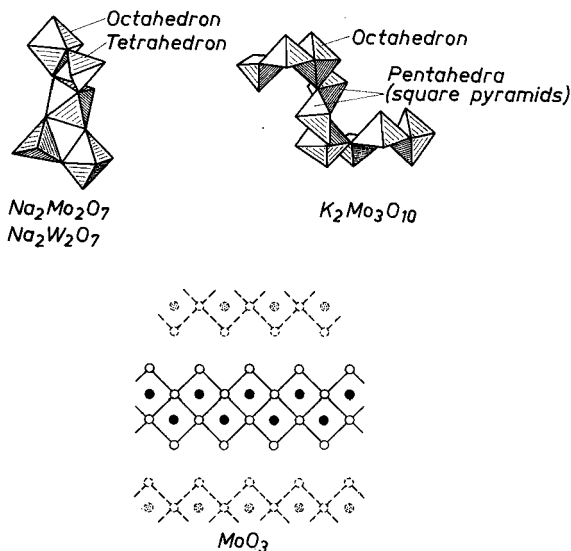
Fig. 1.3. Schematic diagrams of the crystal structures of $Na_2Mo_2O_7/Na_2W_2O_7$ (ref. 1–18), $K_2Mo_3O_{10}$ (ref. 1–23), and MoO_3 (ref. 1–24).

chain, while two oxygens are common to two octahedra in adjacent chains, one oxygen being non-bridging. The structure of MoO_3 is elucidated in fig. 1.3.

The dependence of the stability of di- and trimolybdates (and corresponding tungstates) on the radius of the alkali ion is obvious when we consider the above-described crystal structures. The large rubidium and caesium ions do not fit into the 6-coordinated alkali positions of the $Na_2Mo_2O_7$ ($Na_2W_2O_7$) structure. On the other hand the small lithium ions would "rattle" in the $K_2Mo_3O_{10}$ structure.

In the molybdate systems a sharp transition between tetrahedral and octahedral coordinations is absent. The same conclusion does not seem to be justified in the case of the tungstates, at least not on the basis of crystal-structure data. On the contrary, the lower stabilities of the tritungstates as compared with those of the trimolybdates may indicate that the W atoms are not liable to assume 5-coordination and prefer either strictly tetrahedral or strictly octahedral coordinations, if necessary in combination (cf. $Na_2W_2O_7$). (Seleborg [1-22]) reports that $K_2W_3O_{10}$ and $K_2Mo_3O_{10}$ are not isomorphous; no further data are given.)

1.4. The structures of vitreous and molten alkali tungstates and molybdates

As a first approach towards the elucidation of the structure of vitreous tungstates, Gelsing et al. [1-7,8]) applied infrared spectroscopy in the frequency range 1700–650 cm^{-1}. The spectra of all glasses measured were found to be similar, the frequency of the band of maximum absorption being approximately

equal to that of the crystalline monotungstates. From this the authors concluded that the oxygen coordination of the W atoms in all alkali-tungstate glasses is the same, viz. tetrahedral.

However, the value of the W/O ratio in the glass-formation regions forces isolated tetrahedra to combine in the form of chains, the average chain length being 2 at the composition 50 mole% WO_3 ($M_2W_2O_7$). According to Gelsing et al. it is highly improbable that the chain length in glass or melt should be uniform. Disproportionation may occur by reactions of the type

$$2 W_2O_7^{2-} \rightleftharpoons WO_4^{2-} + W_3O_{10}^{2-}.$$
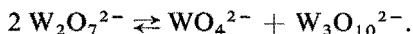
The relatively high glass-formation tendency found at compositions around 45 mole% WO_3 is explained qualitatively in the following way. Addition of WO_3 to an M_2WO_4 melt forces isolated tetrahedra to combine, thus favouring glass formation. However, an increase of WO_3 content also engenders a growing tendency to octahedral coordination. According to the above authors, the formation of octahedra implies the creation of three-dimensional units with strong internal bonds, in which adjacent polyhedra share edges (this is not supported by the structure of crystalline $Na_2W_2O_7$, a compound containing two-dimensional units built up by both tetrahedra and octahedra not sharing edges). By this mechanism the positions of polyhedra with respect to neighbouring polyhedra become more and more fixed, so reducing the glass-formation tendency.

The dependence of CCR on the nature of the alkali ion is, as Gelsing et al. point out, based on different influencing of the disproportionation equilibrium. The remarkable position of the Li^+ ion in tungstate glasses (cf. fig. 1.1) is attributed to the "well-known ordering effect exerted by Li^+ on all kinds of melts".

It should be stressed that this glass structure, also thought to be valid for the melt, is essentially different from that of crystalline $Na_2W_2O_7$, the only compound formed in a glass-formation region the structure of which is known. The proposed glass structure is only possible if the infinite $Na_2W_2O_7$ chains undergo nearly complete dissociation on melting.

Partial support for this can be found in the cryometric studies of Kordes and Nolte [1-25,26,27]). In the first place, these authors point out that $Na_2W_2O_7$ possesses an unusually high melting enthalpy of 22·7 kcal mole^{-1} (cf. $K_2Cr_2O_7$: 8·9 kcal mole^{-1}). This, together with the fact that the liquidus temperature of $Na_2W_2O_7$ shows no noticeable decrease when a few mole% Na_2WO_4 or WO_3 are added, is attributed to a nearly complete dissociation in Na_2WO_4 and WO_3 on melting. In our opinion, however, Kordes and Nolte make too rigorous a distinction between dissociation of $Na_2W_2O_7$ in either W_2O_7 dimers or a mixture of monotungstate and WO_3. Intermediate situations, such as chains of tetrahedra that are subject to disproportionation, may equally

well account for the phenomena found. The only condition which must be fulfilled is that dissociation should give rise to an appreciable concentration of $WO_4{}^{2-}$ ions.

Finally, it should be remarked that for diluted solutions of $Na_2W_2O_7$ in $K_2Cr_2O_7$ and nitrate melts, Kordes and Nolte[1-25,27] and Kust [1-28] respectively accept the existence of dimers W_2O_7.

At first sight, the structure of molten alkali tungstates and their tendency to glass formation seems to be explained. However, the evidence put forward by Gelsing et al. that vitreous alkali tungstates contain exclusively tetrahedral WO_4 groups, is rather limited. In the infrared frequency range 1700–650 cm^{-1} both crystalline an vitreous alkali tungstates only show important absorption maxima at frequencies lower than 1000 cm^{-1}. In this rather narrow region the similarity between the spectra of vitreous tungstates and those of the crystalline monotungstates reported by Gelsing et al. is not so obvious as was suggested. The spectra of the tungstate glasses show strong absorption at frequencies lower than 770 cm^{-1}, contrary to the spectra of the monotungstates. This makes it worthwhile to know the spectra of glasses and crystals in lower frequency regions. Moreover, an infrared-spectroscopic study of more glasses of different compositions would be of great interest.

Alkali-molybdate glasses were subjected by Van der Wielen et al. [1-9] to an analogous infrared-spectroscopic investigation. At the same time, the densities of molten lithium, sodium and potassium molybdates were measured.

The infrared spectra of vitreous molybdates were found to differ appreciably from those of the crystalline monomolybdates, indicating that the coordination of the Mo atom in the molybdate glasses is more complicated than that of the W atom in the corresponding tungstate glasses (according to Gelsing's hypothesis). From density isotherms, Van der Wielen et al. concluded that the densities of the alkali-molybdate melts in the glass regions are relatively low. Van der Wielen et al. assume the MoO_4 group to be more liable to distortion than the WO_4 group. In connection with this, the structure proposed for the molybdate glasses differs from Gelsing's structure only in that it contains distorted polyhedra (it is even suggested that the distortion is so strong that the limits of 5- and 6-coordination are approached). This explains the infrared-absorption spectra found and also the fact that the Li^+ ion does not occupy any special position in the molybdate glasses: the ordering effect of Li^+ is counteracted by the distortion of the MoO_4 tetrahedron.

The structure proposed by Van der Wielen et al. likewise differs essentially from the structures of crystalline compounds in the glass-formation regions, viz. $Na_2Mo_2O_7$ and $K_2Mo_3O_{10}$ (the glass regions do not as yet include $Rb_2Mo_3O_{10}$ and $Cs_2Mo_3O_{10}$).

Again, this implies a dissociation on melting. Some support for this is found in the work of Navrotsky and Kleppa [1-29] on the enthalpies of mixing in the

system Na_2MoO_4–MoO_3. The results obtained suggest that $Na_2Mo_2O_7$ undergoes significant dissociation on melting, this dissociation, however, being incomplete. Dissociation is expected to increase in the order $K_2Mo_2O_7 \rightarrow Na_2Mo_2O_7 \rightarrow Li_2Mo_2O_7$.

Our remarks concerning Van der Wielen's structure are partly analogous to those expressed with respect to Gelsing's. An infrared-spectroscopic investigation only involving the frequency range 1700–650 cm^{-1} forms an uncertain basis for a structure determination. Also, Van der Wielen et al. point out that the formation of octahedra is inherent in the occurrence of three-dimensional units, this being contrary to the crystal structures of compounds found in the glass-formation regions.

Turning to the density isotherms, we are of the opinion that little argument is put forward to render plausible the view that on the average short chains of tetrahedra effect a lower density than units containing octahedra.

And, finally, no attention is given to the fact that a distortion of the MoO_4 group to such a degree that the limits of 5-coordination are approached or passed implies the formation of larger structural units.

1.5. General glass-formation theories

Various theories have been put forward on the basis of which it should be possible to predict which inorganic oxidic systems will form glasses and which will not. None of these theories seems to be valid without exception. In order to indicate the position of the glasses under consideration in relation to these theories, a brief survey will be given.

Zachariasen [1-30]) assumed the existence of a "random network" to be a necessary condition for glass formation. The existence of such a network was considered to be restricted to oxides in which the glass-forming cations were 3- or 4-coordinated, with adjacent polyhedra having not more than 1 oxygen in common. Obviously, MoO_3 and WO_3 do not obey Zachariasen's rules, and in fact these oxides only form glasses if extremely rapid quenching is applied. The limitation of Zachariasen's theory is that it only concerns systems which are liable to form a three-dimensional network. However, on the addition of alkali oxide to MoO_3 and WO_3 the network is no longer three-dimensional, so that the structure of the system is no longer covered by Zachariasen's theory.

Hägg [1-31]), one of the first of Zachariasen's critics, did not require a specific coordination number of the glass-forming cation. Emphasizing the importance of the presence of large and irregular complex anions in the melt, Hägg pointed out that structures consisting of layers of chains can also form a glass. His theory may also apply to the molybdate and tungstate glasses. A drawback of Hägg's theory is its qualitative character.

Smekal [1-32]) expressed the view that the presence of mixed bonds is a necessary condition for glass formation. Calculation of the amount of ionic character

of Mo–O and W–O bonds from electronegativity values gives 51 and 55% of ionic character respectively.

According to the classification of *Stanworth* [1-33]), MoO_3 should, therefore, belong to the intermediates, while WO_3 should be classed among the select group of glass formers. Obviously, the latter classification does not correspond to reality.

Sun [1-34]) suggested the importance of a strong bond between the glass-forming cation and the oxygens surrounding it. During crystallisation a rearrangement process must take place, this frequently involving the breaking of cation–oxygen bonds. According to Sun's criterion both MoO_3 and WO_3, having values of the "single-bond strength" (B_{M-O}) of 92 and 103 kcal mole^{-1} respectively, should be reckoned among the glass-forming oxides.

Rawson [1-35]) modified Sun's criterion in that he also took the value of the liquidus temperature into account. His theory is based on the view that the chance of breaking a bond is not only related to the strength of the bond, but also to the amount of thermal energy available. If the ratio $B_{M-O}/T_{liqu.}$ (where $T_{liqu.}$ = liquidus temperature, K) is taken as a criterion, WO_3, as a result of its high melting point (1473 °C), passes over to the group of intermediates.

The merit of Rawson's theory is that it can also be used for binary systems and that it gives an explanation of the fact that a number of oxides (called conditional glass formers) which do not form glass when melted alone, can easily be vitrified in combination with other oxides. On the other hand, Rawson's criterion gives only a rough indication of glass-formation ranges to be expected. For instance, in most of the alkali-molybdate and -tungstate systems, the composition of minimum CCR deviates considerably from that of the lowest liquidus temperature (cf. figs 1.1 and 1.2).

Furthermore, it is doubtful whether Rawson's argumentation is quite correct. Both liquidus temperature and glass-formation tendency are affected by the structure of the melt. The liquidus temperature, however, is a thermodynamical-equilibrium value, whereas glass formation presupposes the very absence of equilibrium.

Dietzel [1-36]) considers the reciprocal value of the maximum linear crystal-growing rate, represented by the term "Glasigkeit" (glassiness), to be a criterion for the prediction of glass formation. The lowest glassiness is expected to occur at compositions corresponding with congruently melting phases, since at these compositions the structural units in the melt should be identical to those in the crystal lattice to be formed.

In the systems under consideration, however, it is not seldom that the minimum CCR value is found exactly at the composition of a congruently melting phase (cf. figs 1.1 and 1.2). This may indicate that, at least at these compositions, structural units appearing in the melt are not identical to those in the crystal

to be formed (this would be in conformity with the ideas discussed in the previous section).

The views put forward by *Turnbull* [1-37]) and *Sarjeant and Roy* [1-10]), which are based on a theoretical consideration of nucleation and crystal growth, are not suitable for the prediction of glass formation in complex systems and, moreover, require the knowledge of viscosity values. These theories, however, will be briefly discussed in chapter 6.

1.6. Purposes of the investigation

In the previous section we have seen that a number of questions with regard to glass formation in alkali-molybdate and -tungstate systems and in particular with regard to the structures of the glasses formed, are still unsatisfactorily answered.

This thesis is an attempt to solve some of the problems, at least in part.

In *chapter* 2 the questions will be discussed whether the composition regions of glass formation may still be extended, and whether the glass-formation tendency is enhanced by the mixing either of two different alkali ions or of molybdate and tungstate. Further, an investigation of crystallisation phenomena, which was undertaken in view of the ideas expressed by Dietzel (see sec. 1.5), is described. In *chapter* 3 attention will be paid to the question whether by an extension of the infrared-spectroscopic studies with respect to both frequency and composition ranges, new structural information can be obtained.

The structure of a glass is seldom understood completely if the investigation is one-sided in its approach. The problem should be approached from various directions, e.g. by means of spectroscopic methods and by measuring certain properties of the glass as a function of composition. The latter method, however, is not applicable in the case of vitreous alkali molybdates and tungstates, as samples of reasonable amount can only be prepared over small composition regions.

A way of avoiding this difficulty is the method in which measurement is made of the properties of the same system in the molten state, the basis of which is the concept that the structures of melt and glass will not be essentially different.

Such an investigation has been started by Van der Wielen et al. [1-9]) by means of determination of the densities of molten lithium-, sodium- and potassium-molybdate systems as a function of composition and temperature.

This thesis is largely devoted to this method of obtaining indirect information on the structures of the vitreous alkali molybdates and tungstates.

In *chapters* 4, 5 and 6 respectively the determinations of density, surface-tension and viscosity values of both molten alkali-molybdate and -tungstate systems will be discussed, the alkali ions being lithium, sodium and potassium. Special attention will be paid to mutual comparisons of property/composition

isotherms of molten molybdates on the one hand, and molten tungstates on the other. From the similarities and dissimilarities observed, conclusions will be drawn concerning the structures of the corresponding glasses.

Finally, in *chapter* 7, an attempt will be made to give a synthesis of the results found by the various methods applied.

One observation should be made in concluding this introductory chapter. In the previous section it was shown that vitreous molybdates and tungstates do not obey dissimilar theories advanced in respect of glass formation. Conversely, these theories do not describe the facts as found for vitreous molybdates and tungstates. Therefore, an investigation of glass formation in these systems is at the same time a study of the fundamental mechanisms governing glass formation.

REFERENCES

[1-1] J. J. Rothermel, K. H. Sun and A. Silverman, J. Am. ceram. Soc. **32**, 153-162, 1949.
[1-2] H. H. Franck, Tag. Ber. chem. Ges. DDR, 119-122, 1955.
[1-3] R. H. Caley and M. K. Murthy, J. Am. ceram. Soc. **453**, 254-257, 1970.
[1-4] H. Hirohata, K. Shimada and Y. Iida, Funtai Oyobi Funmatsuyakin **16**, 86-89, 1969.
[1-5] Brit. Pat. Spec. 1,444,153; No. 23872/66.
[1-6] P. L. Baynton, H. Rawson and J. E. Stanworth, Nature **178**, 910-911, 1956. Trav. du IVᵉ congr. internat. du verre (Paris 1956), Imprimerie Chaix, Paris, 1957, pp. 62-69.
[1-7] R. J. H. Gelsing, H. N. Stein and J. M. Stevels, Phys. Chem. Glasses **7**, 185-190, 1966.
[1-8] R. J. H. Gelsing, Klei en Keramiek **17**, 183-189, 1967.
[1-9] J. C. Th. G. M. van der Wielen, H. N. Stein and J. M. Stevels, J. non-cryst. Solids **1**, 18-28, 1968.
[1-10] P. T. Sarjeant and R. Roy, Mat. Res. Bull. **3**, 265-280, 1968.
[1-11] P. T. Sarjeant and R. Roy, J. Am. ceram. Soc. **50**, 500-503, 1967.
[1-12] R. J. H. Gelsing, H. N. Stein and J. M. Stevels, Rec. Trav. chim. **84**, 1452-1458, 1965.
[1-13] P. Caillet, Bull. Soc. chim. 4750-4755, 1967.
[1-14] R. Salmon and P. Caillet, Bull. Soc. chim. 1569-1573, 1969.
[1-15] R. J. H. Gelsing, personal communication.
[1-16] W. H. Zachariasen, Norsk geol. Tidsskrift **9**, 65-73, 1926.
[1-17] W. H. Zachariasen and H. A. Plettinger, Acta cryst. **14**, 229-230, 1961.
[1-18] I. Lindqvist, Acta chem. Scand. **4**, 1066-1074, 1950.
[1-19] B. M. Gatehouse and P. Leverett, J. chem. Soc. (A), 849-854, 1969.
[1-20] A. S. Koster, F. X. N. M. Kools and G. D. Rieck, Acta cryst. **B25**, 1704-1708, 1969.
[1-21] M. Seleborg, Acta chem. Scand. **21**, 499-504, 1967.
[1-22] M. Seleborg, Acta chem. Scand. **20**, 2195-2201, 1966.
[1-23] B. M. Gatehouse and P. Leverett, J. chem. Soc. (A), 1398-1405, 1968.
[1-24] A. F. Wells, Structural inorganic chemistry, Clarendon Press, Oxford, 1962, 3rd ed., pp. 468-469.
[1-25] G. Nolte, Thesis, Bonn, 1967.
[1-26] G. Nolte and E. Kordes, Z. anorg. allgem. Chem. **371**, 149-155, 1969.
[1-27] E. Kordes and G. Nolte, Z. anorg. allgem. Chem. **371**, 156-171, 1969.
[1-28] R. N. Kust, Inorg. Chem. **6**, 157-160, 1967.
[1-29] A. Navrotsky and O. J. Kleppa, Inorg. Chem. **6**, 2119-2121, 1967.
[1-30] W. H. Zachariasen, J. Am. chem. Soc. **54**, 3841-3851, 1932.
[1-31] G. Hägg, J. chem. Phys. **3**, 42-49, 1935.

[1-32] A. S m e k a l, J. Soc. Glass Technol. **35**, 411-420, 1951.

[1-33] J. E. S t a n w o r t h, J. Soc. Glass Technol. **32**, 366-372, 1948.

[1-34] K. H. S u n, J. Am. ceram. Soc. **30**, 277-281, 1947.

[1-35] H. R a w s o n, Trav. du IVe congr. internat. du verre (Paris 1956), Imprimerie Chaix, Paris, 1957, pp. 62-69; Inorganic glass-forming systems, Academic Press, London, 1967, pp. 25-29.

[1-36] A. D i e t z e l and H. W i c k e r t, Glastechn. Ber. **29**, 1-4, 1956.

[1-37] D. T u r n b u l l, Contemp. Phys. **10**, 473-488, 1969.

[1-38] F. X. N. M. K o o l s, A. S. K o s t e r and G. D. R i e c k, Acta cryst. **B 26**, 1974-1977, 1970.

[1-39] A. W. M. v a n d e n A k k e r, A. S. K o s t e r and G. D. R i e c k, J. appl. Cryst. **3**, 389-392, 1970.

2. GLASS-FORMATION AND CRYSTALLISATION PHENOMENA

2.1. Extension of glass-formation regions

Enlargement of the glass-formation regions, found so far [2−1,2,3]), is necessary if the infrared-spectroscopic study of vitreous molybdates and tungstates is to be extended as far as composition is concerned.

The consequence of this is that higher cooling rates have to be realised. Several methods exist by which extremely high cooling rates can be attained, all being based on dividing a quantity of a melt into a great number of small droplets, which are caught in a cool liquid or on a cool substrate.

2.1.1. *The splat-cooling technique*

The splat-cooling technique, the principle of which was described by Tammann and Elbrächter as early as 1932 [2−4]), was employed in the experiments leading to the present thesis. A small quantity of a melt is divided into a great number of droplets by a strong current of air. The droplets are splatted onto a cool substrate. In order to generate a current of air having enough force, a shock tube as described by Sarjeant [2−5]) was used (for a schematic diagram, see fig. 2.1). The vertical tube consisted of stainless steel with an inner diameter of 1·8 cm. The upper section of the tube, 18 cm long, was connected to a compressed-air cylinder. The lower section was 13 cm long. Between upper and lower part of the tube a cellophane diaphragm was inserted, held tightly by two rubber rings.
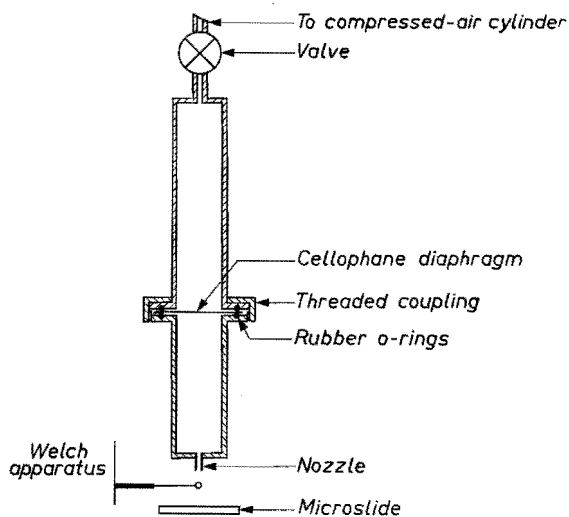
Fig. 2.1. Schematic diagram of the shock tube used for splat-cooling.

The nozzle at the lower end of the tube was placed at a distance of 0·5 cm from the substance under study, the substance being melted into the loop of a V-kinked thermocouple (Pt 5% Rh/Pt 20% Rh).

The thermocouple was switched alternately into a heating circuit and a measuring circuit, the frequency of switching being 50 c/s (a diagram of the circuits is given in fig. 2.3; see also sec. 2.2.1).

Samples of 2–4 mg were used. The temperature was maintained at approximately 100 °C above the liquidus.

The air shock was produced by raising the pressure beyond the bursting pressure of the diaphragm. Application of cellophane of two different thicknesses (bursting pressures being 2·5 and 4 ato respectively) did not have a markedly different effect on glass formation.

The melt was driven off the thermocouple by the shock and shot onto a microscope slide which was placed at a distance of 1 cm below the thermocouple.

Our experiments confirm Sarjeant's experience that metal substrates, though better heat-conducting, are unsuitable for the purpose, because an oxidic melt does not attach itself to a metal surface. Only glass substrates give satisfactory results in this respect and, moreover, show no signs of reaction with the sample.

The samples obtained — referred to as splats — were examined for the occurrence of crystallisation with a Carl Zeiss WL Pol microscope, using both normal and polarised light (magnification 125 and $500\times$).

Although visual examination using normal light gives reliable information on the extent of crystallisation, the distinction between vitreous and crystalline regions was even clearer between crossed nicols. In general, this method can be safely used in the systems under investigation, since among the crystal structures known, only the structures of Na_2MoO_4 and Na_2WO_4 possess cubic symmetry.

A few splats which were classified as "glass with very slight crystallisation" were also examined by X-ray diffraction (Debije–Scherrer technique; $CuK\alpha$ radiation). It was established that the crystals seen under the microscope, which were few in number and small in size, were not observed by X-ray-diffractiometric examination.

For calculation of the cooling rate, a number of material properties such as layer thickness, heat-transfer coefficient and thermal conductivity must be known. The latter two properties have not been determined for the systems under consideration. However, Sarjeant and Roy [2–6] demonstrated that the cooling rate is mainly dependent on the layer thickness. In our experiments the droplets were found to have a thickness of 1–2 μm (measured under the microscope, using a micrometer). For this thickness, we estimate the cooling rate to have an order of magnitude of 10^6 °C s^{-1}, this being the value calculated

by Sarjeant and Roy for a few very dissimilar compounds, viz. SiO_2, $MgAl_2O_4$, NaCl and Pb.

2.1.2. *Preparation of samples*

Samples were made from alkali carbonates, MoO_3 and WO_3. The following chemicals were used:

Li_2CO_3	Merck, extra pure
Na_2CO_3	anhydrous, Merck, pro analysi
K_2CO_3	Merck, pro analysi
Rb_2CO_3	Merck
$Cs_2CO_3 + H_2O$	BDH
MoO_3	Merck, pro analysi
WO_3	Merck

Before being weighed the alkali carbonates were dried for a few hours at 300 °C.

Calculated quantities of alkali carbonate and trioxide were mixed intimately and melted together in a platinum dish for several hours at 900–1000 °C.

Tungstates having a WO_3 content higher than 75 mole % were excluded from the experiments because of their high liquidus temperatures and tendency to oxygen loss, which gave rise to greying or blackening.

2.1.3. *Results and discussion*

The results of the splat-cooling experiments are shown in tables 2-I and 2-II and in fig. 2.2.

The results obtained demonstrate that application of the splat-cooling technique gives a considerable extension of the glass-formation regions in the direction of higher trioxide content, especially in the case of the molybdate systems, which have relatively low liquidus temperatures, irrespective of trioxide content.

The observation of Sarjeant and Roy [2-7]) that even pure MoO_3 can be made partly vitreous was confirmed.

In trying to extend the glass-formation regions to a lower trioxide content, splats were obtained which rapidly attracted moisture. Since it was the purpose of the experiments to prepare samples for infrared-spectroscopic measurements, no further attempts were made in this direction.

From table 2-I and fig. 2.2 it is seen that addition of a small quantity of any alkali monomolybdate to MoO_3 considerably raises the tendency to glass formation. It seems unlikely that the addition of, for instance, 10 mole % of an alkali monomolybdate produces a glass structure analogous to that described by Van der Wielen et al.[2-3]) (see sec. 1.4), as this would involve a sudden and complete transition to distorted tetrahedral coordination.

Addition of monomolybdate (or rather alkali oxide) means the introduction of extra oxygen atoms, which will be used for the partial breaking of oxygen bridges in the MoO_3 layers (see sec. 1.3) and the creation of new oxygen bridges.

TABLE 2-I

Results of splat-cooling of alkali molybdates

system	glass region acording to Van der Wielen et al.[2-3] (mole % MoO_3)	composition (mole % MoO_3)	classification
$Li_2MoO_4–MoO_3$	20–75	80	glass
		90	glass
$Na_2MoO_4–MoO_3$	35–80	90	glass
		95	most droplets 100% glass; in largest droplets many small crystals
$K_2MoO_4–MoO_3$	45–55	65	glass
		73	glass
		80	glass
		90	some crystallisation in largest droplets
$Rb_2MoO_4–MoO_3$	50	55	glass
		60	glass
		70	glass
		90	glass
$Cs_2MoO_4–MoO_3$	50	60	glass
		90	some conglomeration of small crystals in largest droplets
MoO_3	—	100	small droplets partly glass; vaporises easily

Probably, oxygen atoms shared by two octahedra are the first to be affected, rather than those shared by three octahedra. Since breaking of oxygen bridges will be easier at sites where extra non-bridging oxygen atoms have already been introduced, further addition of alkali oxide will "cleave" the MoO_3 layers.

TABLE 2-II

Results of splat-cooling of alkali tungstates

system	glass region indicated by Gelsing et al.[2-1,2] (mole % WO$_3$)	composition (mole % WO$_3$)	classification
Li$_2$WO$_4$–WO$_3$	41–49	40	glass
		50	glass
		55	glass
Na$_2$WO$_4$–WO$_3$	23–61	23	glass, hygroscopic
		50	glass
		60	glass
		61·5	glass
		70	glass
K$_2$WO$_4$–WO$_3$	36–57	20	crystal, hygroscopic
		35	glass
		56	glass
		70	glass
Rb$_2$WO$_4$–WO$_3$	42–52	52·3	glass
		58·3	glass
		71·4	glass
		75	largest droplets partly crystalline
Cs$_2$WO$_4$–WO$_3$	44–47	40	glass, hygroscopic
		50	glass
		60	glass
		70	largest droplets for the greater part crystalline

Essentially, this process may continue until chains of octahedra only, without cross-links, are left. However, a stoichiometric calculation shows that to effect this, so much trioxide has to be added that the monomolybdate composition is reached. Naturally, long before this is realised a tendency to the formation of 5- and 4-ocordinations has occurred.

For the alkali-tungstate systems (see table 2-II and fig. 2.2), application of the splat-cooling technique gives an extension of the glass-formation regions
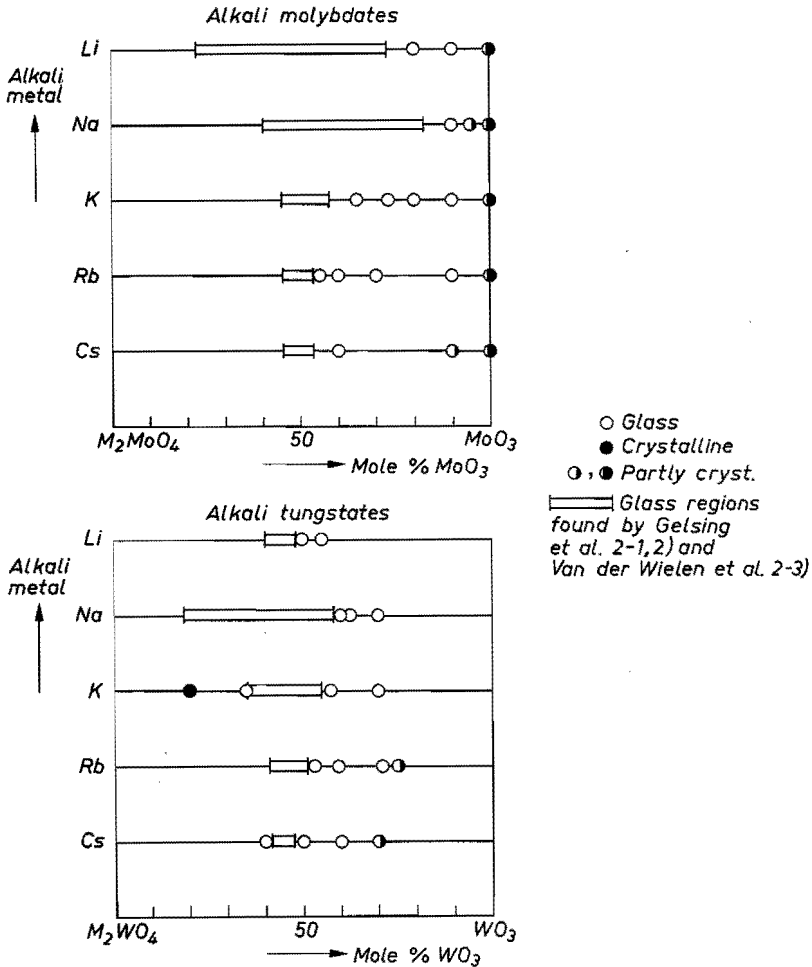
Fig. 2.2. Glass formation by the splat-cooling technique.

to approximately 70 mole% WO_3. An exception is formed by the lithium-tungstate system as a result of its relatively high liquidus temperatures for a WO_3 content higher than 50 mole% (cf. fig. 1.2a).

2.2. Glass formation in mixed alkali molybdates and tungstates

The measurements described in this section were performed with a view to ascertaining the effect which the mixing of two different alkali species, or Mo and W, exerts on the glass-formation tendency. It was not our intention to find the composition most favouring glass formation.

Since the maximum glass-formation tendencies in both molybdate and tungstate systems were found round a trioxide content of 50 mole%, only the compositions $M_2Mo_2O_7$ and $M_2W_2O_7$ were taken into account.

As a criterion of the tendency to glass formation, we considered the value of the critical cooling rate (CCR), in accordance with the work of Gelsing et al.[2-1,2]) and Van der Wielen et al.[2-3]).

The question may arise whether CCR forms a valuable criterion of the tendency to glass formation, as its value is liable to be dependent on factors influencing the occurrence of heterogeneous nucleation, such as impurities, materials in contact with the sample, and quantity of the sample.

The answer is that the experiments were performed under conditions which were kept constant as much as possible. Furthermore, in the course of CCR measurements on various systems [2-1,3,11,12]) it was observed that the value of CCR was reproducible within ± 50%, when various thermocouples and crucibles were used and the quantity of the sample was varied from some milligrammes to several grammes. An error of ± 50% may seem to be extremely large. Generally, however, the value of CCR strongly varies with composition, so that such an error has virtually no effect on the relation between CCR and composition.

2.2.1. *Experimental method*

Values of CCR were determined using the apparatus described by Welch [2-8]). A diagram is shown in fig. 2.3. A Pt 5% Rh/Pt 20% Rh thermocouple was switched by means of a Siemens high-speed relay alternately into a heating circuit and a measuring circuit. The relay vibrated at the mains frequency of 50 c/s, making it possible to apply the thermocouple both as a resistance heater and a temperature-measuring device.

The selection of the unusual thermocouple composition was based on Welch's experience that this combination is very insensitive to cold-junction temperature variation. The thermocouple was bent into a loop near its hot junction.
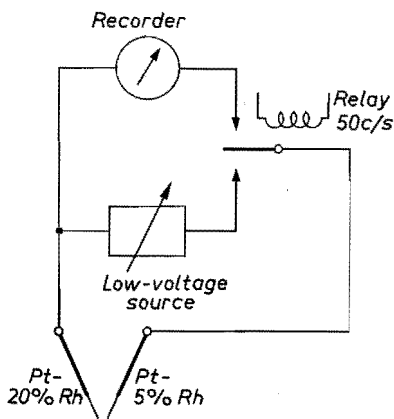
Fig. 2.3. Diagram of the Welch apparatus for the determination of cooling rates.

A quantity of 2–4 mg of the sample to be studied was melted into the loop. The sample was observed through a Vernier measuring microscope (James Swift & Sons), using a magnification of $24\times$.

The heating current was turned down by means of a servomotor with variable speed. The cooling rate, therefore, could be varied within wide limits. If the heating current was switched off abruptly a cooling rate of approximately $200\ ^{\circ}\mathrm{C\ s^{-1}}$ was observed. Higher cooling rates could be attained by simultaneously directing a current of air onto the sample.

Cooling rates were determined with the aid of a Goerz Servogor Type RE 511 compensation recorder or (at high cooling rates) with a Tektronix Type 546 storage oscilloscope.

CCR values reported are the arithmetic mean of the lowest cooling rate preventing crystallisation entirely, and the highest cooling rate producing a sample in which traces of crystallisation could still be observed.

Samples were prepared by the method described in sec. 2.1.2.

2.2.2. Results and discussion

The results of the measurements are shown in figs 2.4–2.7.

Figure 2.4 demonstrates the effect which the replacement of Mo atoms by
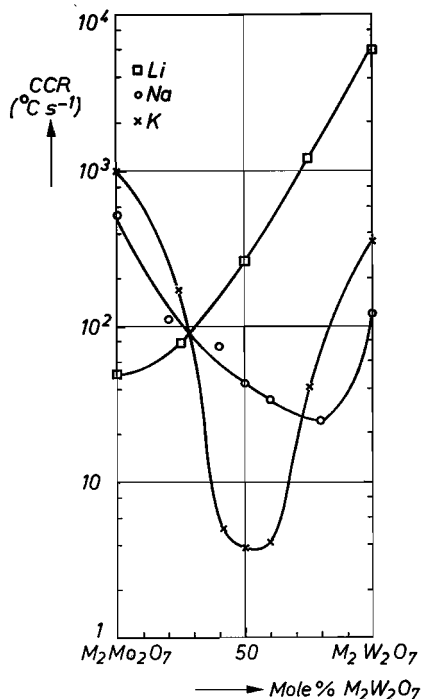
Fig. 2.4. Critical cooling rate CCR ($^{\circ}\mathrm{C\ s^{-1}}$) in the systems $M_2Mo_2O_7$–$M_2W_2O_7$ (M = Li, Na, K).

W atoms has on the value of CCR in the systems $Li_2Mo_2O_7-Li_2W_2O_7$, $Na_2Mo_2O_7-Na_2W_2O_7$ and $K_2Mo_2O_7-K_2W_2O_7$. In all three cases partial replacement of Mo by W gives a CCR value showing a negative departure from linearity. The extent of this glass-formation-favouring effect, however, strongly depends on the nature of the alkali ion present, and decreases in the order $K \rightarrow Na \rightarrow Li$. In the system $Li_2Mo_2O_7-Li_2W_2O_7$ the effect found is particularly small, probably because the effect raising the glass-formation tendency is crossed by the glass-formation-counteracting effect of the presence of Li^+ ions in a tungstate melt (cf. sec. 1.2).

When dimolybdate and ditungstate are mixed, crystallisation may be hampered if one of the following mechanisms occurs:

(a) Molybdate and tungstate polyhedra form common complex anions. This possibility seems to be most likely if the structure of molten dimolybdate is (nearly) identical to that of the molten distungstate.

(b) Molybdate and tungstate polyhedra do not form common anions, but molybdate and tungstate anions are mutually mixed. This possibility seems to be most likely if an essential difference exists between the structures of molten dimolybdate and ditungstate.

(c) A combination of (a) and (b), possibly depending on the alkali species present.

At this stage, the question of which of the proposed possibilities occurs, cannot be answered. Nevertheless, as the glass-formation-favouring effect increases in the order $Li \rightarrow Na \rightarrow K$, the conclusion seems to be justified that the stability of mixing increases in the same order.

Figure 2.5 shows the effect of the presence of two different alkali species in a dimolybdate melt.

In all three cases examined, mixing of two alkali species strongly reduces the value of CCR. This glass-formation-favouring effect increases, as the difference in field strength between the two alkali ions is raised. In the system $Li_2Mo_2O_7-K_2Mo_2O_7$ considerably lower CCR values are reached than in the system $Li_2Mo_2O_7-Na_2Mo_2O_7$. Likewise, the system $Li_2Mo_2O_7-K_2Mo_2O_7$ shows easier glass formation than the system $Na_2Mo_2O_7-K_2Mo_2O_7$.

In order to examine whether this trend is also found when Li^+ and Rb^+ ions, and Li^+ and Cs^+ ions are mixed, the CCR values of the following compositions were measured:

$$LiRbMo_2O_7: \quad CCR = 2 \cdot 6 \, °C \, s^{-1}$$
$$LiCsMo_2O_7: \quad CCR = 1 \cdot 5 \, °C \, s^{-1}.$$

These values possess the same order of magnitude as the minimum CCR value occurring in the system $Li_2Mo_2O_7-K_2Mo_2O_7$, in spite of the glass-formation tendencies of $Rb_2Mo_2O_7$ and $Cs_2Mo_2O_7$ being considerably lower than that of $K_2Mo_2O_7$ (see fig. 1.1).
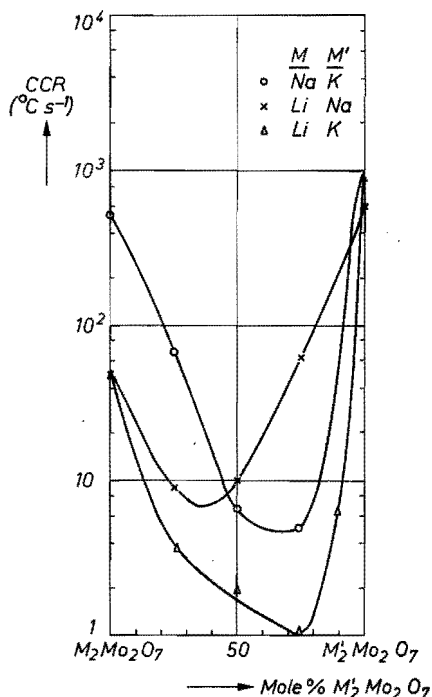
Fig. 2.5. Critical cooling rate CCR (°C s^{-1}) in mixed-alkali dimolybdate systems.

Figure 2.6 shows the effect of the simultaneous presence of two different alkali species in a ditungstate melt.

Again, a marked increase of glass-formation tendency is observed in all three systems examined. The decrease of CCR found in the systems $Li_2W_2O_7-K_2W_2O_7$ and $Li_2W_2O_7-Na_2W_2O_7$, however, is less than that found in the corresponding molybdate systems.

In the system $Li_2W_2O_7-K_2W_2O_7$, glass formation is easier than in the system $Li_2W_2O_7-Na_2W_2O_7$. Nevertheless, supplementary experiments showed that $LiRbW_2O_7$ and $LiCsW_2O_7$ only form glass if cooling rates higher than 10^3 °C s^{-1} are applied.

Considerable increase of the glass-formation tendency when two or more alkali species are mixed is a well-known phenomenon in glass technology. In addition to the tendency to glass formation, other properties as well may be non-additive in such a system. This is known as the mixed-alkali effect.

Striking examples are formed by the nitrate glasses, where the simultaneous presence of alkali ions and alkaline-earth ions of sufficiently different field strength is a necessary condition for glass formation. Thilo et al.[2-9] point out that for electrostatic reasons the ions of highest field strength will be coordinated preferably by ions having the lowest field strength. The stability of mixing will

increase with the difference in field strength. The positions of the ions in the melt will no longer correspond then to the positions which these ions should occupy in the crystal lattice. Therefore, crystallisation is hampered.

A similar mechanism may explain the increase of the glass-formation tendency observed in mixed alkali dimolybdates and ditungstates, provided that in the case of the tungstates the counteracting effect of the Li^+ ions is taken into account.

Finally, fig. 2.7 shows that mixing of two different alkali species in a mixed dimolybdate/ditungstate still gives an appreciable improvement of glass formation. The lowest CCR value attained is $1\ °C\ s^{-1}$. As the systems examined only form a small selection of the numerous compositions possible when alkali molybdates and tungstates are mixed, it seems likely that a composition can be prepared having a CCR value considerably lower than $1\ °C\ s^{-1}$.
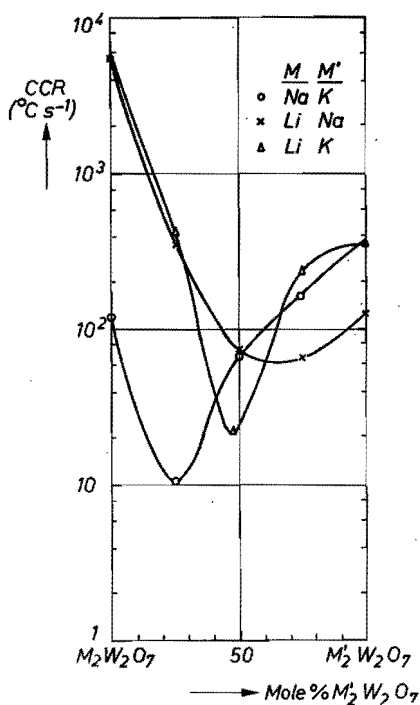
Fig. 2.6. Critical cooling rate CCR ($°C\ s^{-1}$) in mixed-alkali ditungstate systems.
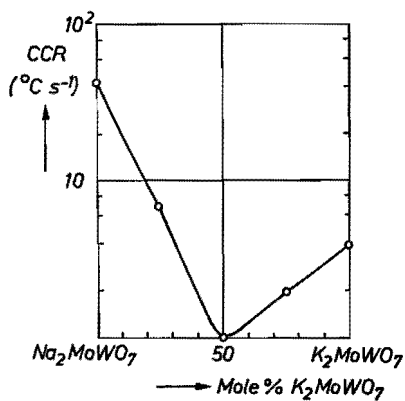
Fig. 2.7. Critical cooling rate CCR ($°C\ s^{-1}$) in the system Na_2MoWO_7–K_2MoWO_7.

2.3. Crystallisation phenomena

2.3.1. *Experimental method*

Section 1.5 discussed Dietzel's theory, which relates glass formation to a low value of the maximum linear crystal-growth rate. In the systems under consideration, the composition of highest glass-formation tendency is frequently found near compositions corresponding to congruently or incongruently melting compounds. Therefore, it seemed of interest to determine crystal-growth rates in these systems, the more so as the Welch apparatus described in sec. 2.2.1 is excellently suited for the purpose [2-10]).

Preliminary experiments, however, demonstrated that the determination of crystal-growth rates presented the following difficulties:

(a) In most cases considerable undercooling was necessary to start crystallisation.

(b) Once a nucleus was formed, growing proceeded so rapidly that it could not be measured.

(c) This instantaneous crystallisation was accompanied by such a heat effect that, though the thermocouple material guarantees good heat conducting, the temperature was strongly raised (50–100 °C).

The minimum degree of undercooling necessary for nucleation, however, was found to be satisfactorily reproducible and relatively independent of cooling rate.

This is illustrated by fig. 2.8, which shows the relations between the temperature of crystallisation from the melt (t_{CM}) and cooling rate for a non-glass-forming sample (Na_2WO_4) and a relatively easily glass-forming sample ($0.55 \, Na_2WO_4 . 0.45 \, WO_3$). Both samples were cooled 5 times at each cooling
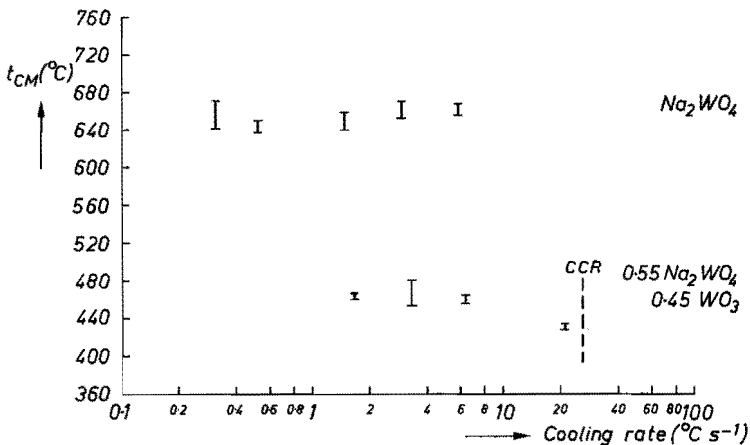
Fig. 2.8. Influence of cooling rate on crystallisation temperature t_{CM} for the compositions Na_2WO_4 and $0.55 \, Na_2WO_4 . 0.45 \, WO_3$.

Fig.2.9a.
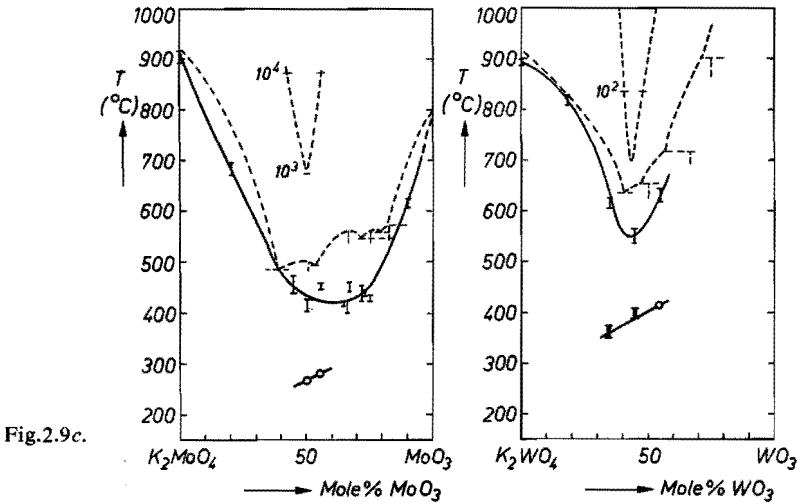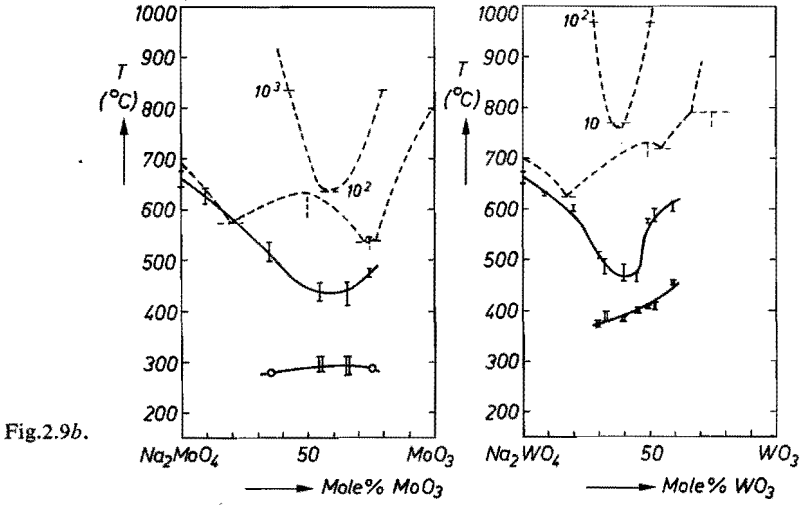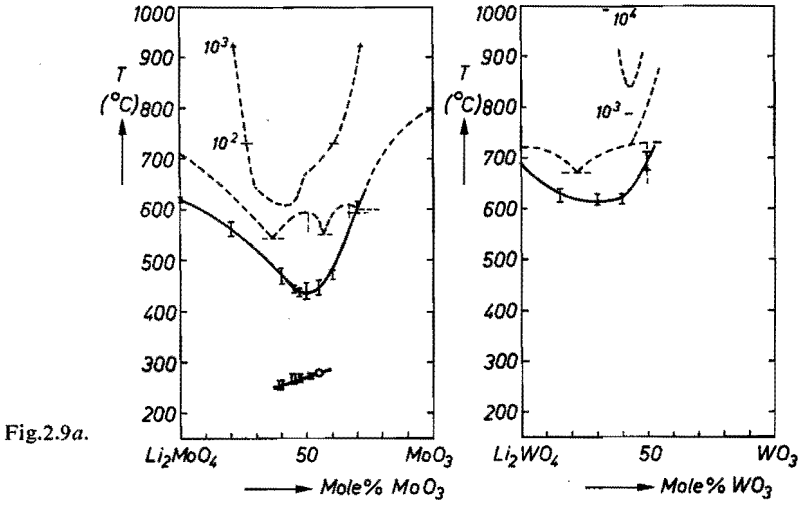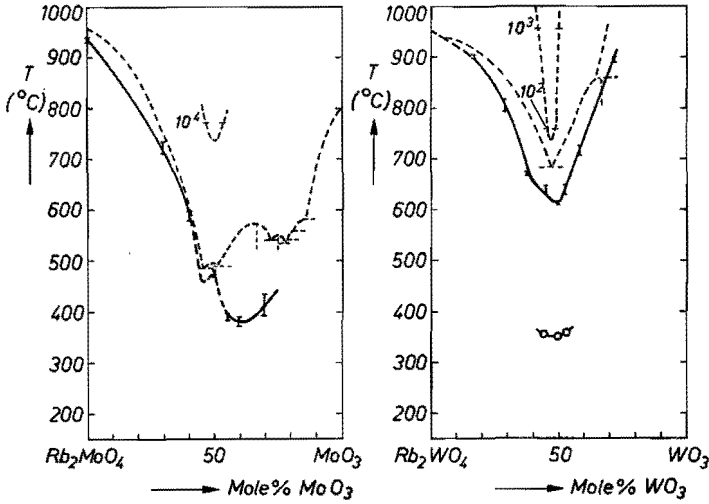
Fig.2.9b.
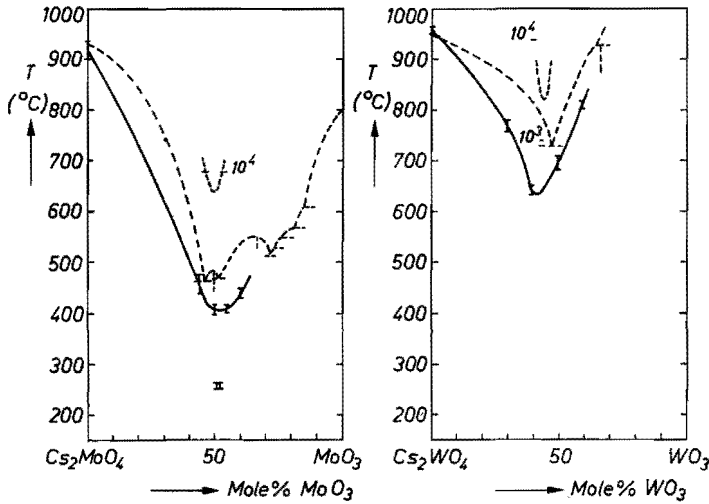
Fig.2.9c.

Fig.2.9d.

Fig.2.9e.

Fig. 2.9. Relationship between crystallisation temperatures t_{CM} and t_{CG} and composition, projected on phase diagram and critical-cooling-rate curve.
(a) System Li_2MoO_4–MoO_3; system Li_2WO_4–WO_3.
(b) System Na_2MoO_4–MoO_3; system Na_2WO_4–WO_3.
(c) System K_2MoO_4–MoO_3; system K_2WO_4–WO_3.
(d) System Rb_2MoO_4–MoO_3; system Rb_2WO_4–WO_3.
(e) System Cs_2MoO_4–MoO_3; system Cs_2WO_4–WO_3.

rate. In the figure the temperature ranges are indicated between highest and lowest t_{CM} found. The value of t_{CM} proves to be satisfactorily reproducible, provided that no cooling rates lying near CCR are applied.

The t_{CM} values for al arge number of binary alkali-molybdate and -tungstate samples were determined. In all cases the cooling rate was maintained at approximately $1 \,°C\, s^{-1}$. Again, t_{CM} of each sample was measured 5 times.

Thanks to the extent of the heat effect, crystallisation temperatures were registered easily by means of a recorder (Kipp type BD1). At the same time, samples were observed through the measuring microscope referred to in sec. 2.2.1.

Samples which could be made completely vitreous on the thermocouple were slowly reheated. It was visually established at which temperature devitrification set in. The crystal-growth rate in the glass was considerably lower than that in the supercooled melt. Therefore, a heating rate of $0·1 \,°C\, s^{-1}$ was chosen.

The temperature of crystallisation from the glass (t_{CG}) also proved to be satisfactorily reproducible. Again, t_{CG} of each sample was determined 5 times.

2.3.2. *Results and discussion*

Figures 2.9 $a - e$ show the relations between t_{CM}, t_{CG} and composition for the systems M_2MoO_4–MoO_3 and M_2WO_4–WO_3 (M $=$ Li, Na, K, Rb, Cs) projected on phase diagrams and glass-formation regions.

From these figures it is seen that the values of t_{CM} and the phase diagram show little correlation, at least in the glass-formation regions. On the other hand, a clear correlation can be observed between t_{CM} and CCR. Generally, at a low trioxide content, t_{CM} follows the course of the liquidus temperature. Whereas, however, in all systems the liquidus temperature shows a eutectic, and increases beyond this point as a result of the occurrence of higher molybdates and tungstates, t_{CM} continues to decrease beyond the eutectic composition.

From the high degree of undercooling necessary for nucleation found in this region, and the extremely rapid crystallisation once a nucleus has been formed, it can be concluded that in this case not crystal growth, but nucleation is the limiting step for crystallisation.

At the monomolybdate and monotungstate compositions, monomolybdate and monotungstate nuclei start crystallisation. The same holds when, for instance, 10 mole % trioxide is added. The continuing decrease of t_{CM} even beyond eutectic composition suggests that in this composition region crystallisation still depends on monomolybdate or monotungstate nuclei.

This implies that the melt must contain a considerable amount of MoO_4^{2-} *and* WO_4^{2-} *ions.*

When a melt is cooled, the temperature region between t_{CM} and t_{CG} forms the region where crystallisation can occur. All other things being equal, the

chance of by-passing crystallisation increases as the extent of the region $t_{CM}-t_{CG}$ decreases. As mentioned above, a clear correlation exists between t_{CM} and CCR, on the understanding that the composition of minimum t_{CM} generally corresponds with that of minimum CCR. The temperature t_{CG} is not independent of composition and shows a tendency to increase with increasing trioxide content. Nevertheless, the variation of t_{CG} with composition does not appear to be as strong as the corresponding variation of t_{CM}. Therefore, the composition of minimum t_{CM} (and consequently of minimum CCR) generally will be approximately equal to that of minimum $t_{CM} - t_{CG}$, and the correlation between the extent of the region $t_{CM} - t_{CG}$ and the glass-formation tendency, outlined above, is indeed found to exist.

However, when the various systems are compared, the value of $t_{CM} - t_{CG}$ proves to be no quantitative indication of the tendency to glass formation. For instance, the minimum $t_{CM} - t_{CG}$ values in the systems Li_2MoO_4–MoO_3, Na_2MoO_4–MoO_3, K_2MoO_4–MoO_3, Cs_2MoO_4–MoO_3 and K_2WO_4–WO_3 all lie in the range 145–170 °C, whereas the minimum CCR values in these systems vary widely.

The rapid crystal growth observed in the systems once a nucleus has been created may be an indication of a low melt viscosity. This is supported by Van der Wielen's statement that the viscosity of an alkali-molybdate melt has an order of magnitude of 1 cP (ref. 2-3).

REFERENCES

2-1) R. J. Gelsing, H. N. Stein and J. M. Stevels, Phys. Chem. Glasses **7**, 185-190, 1966.
2-2) R. J. Gelsing, Klei en Keramiek **17**, 183-189, 1967.
2-3) J. C. Th. G. M. van der Wielen, H. N. Stein and J. M. Stevels, J. non-cryst. Solids **1**, 18-28, 1968.
2-4) G. Tammann and A. Elbrächter, Z. anorg. allgem. Chem. **207**, 268-272, 1932.
2-5) P. T. Sarjeant, Thesis, Pennsylvania, 1967, pp. 8-12.
2-6) P. T. Sarjeant and R. Roy, Mat. Res. Bull. **3**, 265-280, 1968.
2-7) P. T. Sarjeant and R. Roy, J. Am. ceram. Soc. **50**, 500-503, 1967.
2-8) J. H. Welch, J. sci. Instr. **31**, 458-462, 1954.
2-9) E. Thilo, C. Wiecker and W. Wiecker, Silikattechnik **15**, 109-111, 1964.
2-10) H. Scholze and K. A. Kumm, Tonind.-Ztg. **90**, 559-561, 1966.
2-11) A. C. J. Havermans, H. N. Stein and J. M. Stevels, J. non-cryst. Solids **5**, 66-69, 1970.
2-12) M. H. C. Baeten and J. M. Stevels, to be published in Silic. Ind.

3. INFRARED SPECTROSCOPY

3.1. Introduction

In sec. 1.4 the infrared-spectrocopic studies of vitreous alkali tungstates and molybdates, carried out by Gelsing et al.[3-1,2]) and Van der Wielen et al.[3-3]) respectively, were discussed.

It was seen that these studies, which form the basis of the glass structure proposed by these authors, were rather limited with respect to the composition and frequency ranges covered.

The splat-cooling technique described in sec. 1.2, allowed a considerable extension of the regions of glass formation, especially in the case of the molybdate systems. Extension of the frequency range is merely a question of instrumentation.

Apart from those reported by the above authors, no other spectra of alkali-tungstate or -molybdate glasses are known. The majority of the crystalline compounds in the systems under consideration, however, have been studied by infrared spectroscopy.

By far the most attention has been paid to the spectra of monomolybdates and monotungstates. The spectra of the monotungstates were studied in detail by Clark and Doyle [3-4]) (4000–250 cm^{-1}), and Caillet and Saumagne [3-5]) (2000–70 cm^{-1}). Extensive reports on alkali-monomolybdate spectra were published by Clark and Doyle [3-4]), Caillet and Saumagne [3-5]), and Van der Wielen et al.[3-3]) (1700–650 cm^{-1}). Caillet and Saumagne have given a band assignment for the spectra of the alkali monocompounds examined.

Spectra of crystalline tungstates and molybdates having a higher trioxide content have been reported by Dupuis [3-6]) ($Na_2W_2O_7$, $Na_2W_4O_{13}$; 1670–670 cm^{-1}), Dupuis and Viltange [3-7]) ($Na_2W_2O_7$, $Na_2Mo_2O_7$; 1670–300 cm^{-1}), Gelsing [3-2]) (ditungstates; 1700–650 cm^{-1}), Van der Wielen et al.[3-3]) (dimolybdates; 1700–650 cm^{-1}), and Caillet and cooperators [3-8,9,10]) (di-, tri- and tetratungstates and -molybdates of Na, K, Rb, Cs, as well as a few Rb and Cs tungstates and molybdates of particularly high trioxide content; 4000–200 cm^{-1}).

Dupuis and Viltange [3-7]) have given a band assignment for $Na_2W_2O_7$ and $Na_2Mo_2O_7$. This, however, is of little value, as it is based on the incorrect concept of a crystal structure containing only double tetrahedra.

Caillet and Saumagne [3-10]) have given a partial band assignment for a large number of compounds, this band assignment, however, being founded on a comparison with the spectra of the arbitrarily chosen compounds WO_3 and Ag_2MoO_4.

The infrared spectrum of WO_3 has been studied inter alia by Caillet and Saumagne [3-10]) (4000–200 cm^{-1}). Barraclough et al.[3-11]) (1100–800 cm^{-1}) and Lipsch [3-12]) (1100–400 cm^{-1}) have reported on the spectrum of MoO_3.

Barraclough et al. have proposed a band assignment for the absorption maxima of MoO_3 appearing in the frequency region 1000–800 cm^{-1}.

From the spectra of the crystalline alkali tungstates and molybdates as published by the authors mentioned above, it is apparent that in the systems under study, considerable absorption is found only at wavenumbers lower than 1100 cm^{-1}. Important absorption maxima are certainly found in the frequency region under 650 cm^{-1}. It is expected that this region will be of similar interest in the case of vitreous tungstates and molybdates.

3.2. Experimental method

Crystalline alkali-tungstate and -molybdate samples were prepared by the method of melting together alkali carbonate and WO_3 or MoO_3, described in sec. 2.1.2. In regions of relatively easy glass formation, vitreous samples were made on the thermocouple of the Welch apparatus (see sec. 2.2.1). Vitreous samples having high CCR values were prepared with the aid of the splat-cooling technique.

A quantity of 1–2 mg of the sample to be studied was mixed and ground thoroughly with less than 100 mg dry KBr, and subsequently pressed into a thin disc (thickness not more than 0·5 mm).

All spectra were measured by the double-beam technique. The frequency region 1200–700 cm^{-1} was covered with a Hilger and Watts H 800 spectro-photometer, and the frequency region 700–300 cm^{-1} with a Hitachi Mode EPI-Li grating spectrometer.

KBr is excellently infrared-transmissive at wavenumbers higher than 400 cm^{-1}. It can, however, be used down to 300 cm^{-1}, if sufficiently thin discs are employed [3-13]).

3.3. Infrared spectra of alkali tungstates

3.3.1. *Crystalline alkali tungstates*

Before discussion of infrared spectra of crystalline alkali tungstates is under-taken, a few remarks, which will also apply to the spectra discussed in sub-sequent sections, must be made. Not all spectra measured are shown in the various figures. These figures, however, give a good impression of the results obtained. The spectra not included would not introduce new elements into the discussion.

In each case a number of spectra is shown at constant alkali species but varying trioxide content. For this purpose, the systems having the highest glass-formation tendencies (Na_2WO_4–WO_3 and Li_2MoO_4–MoO_3) were selected.

In addition to this, spectra are given at approximately constant trioxide content, but with varying alkali species. In the case of the tungstates the com-

position of 70 mole% WO_3 was selected, whereas in that of the molybdates 60 and 90 mole% MoO_3 were chosen.

The figures are arranged in such a way that comparisons are possible between the spectra of crystalline and vitreous samples of equal composition. It should be noted that the actual absorption spectra in the figures are shifted over arbitrary distances for the sake of clarity.

A number of infrared spectra of crystalline alkali tungstates is shown in figs 3.1 and 3.2.

Where comparison is possible, good agreement is generally found between the spectra obtained in this work and those measured by previous authors.

In fig. 3.1 the spectrum of Na_2WO_4 shows strong absorption maxima at 840 and 307 cm^{-1}, this being in excellent agreement with the spectra previously published [3-1,2,4,5]. Caillet and Saumagne [3-5] attribute these bands to the ν_3 and ν_4 vibrations of the tetrahedral WO_4 group. The absorption maximum of medium intensity observed at 870 cm^{-1} was also reported by Gelsing et al.[3-1,2].

The spectrum of $0.42 Na_2WO_4 . 0.58 WO_3$ is almost identical to that published by Gelsing [3-2] and Dupuis [3-6] for $Na_2W_2O_7$ in the region
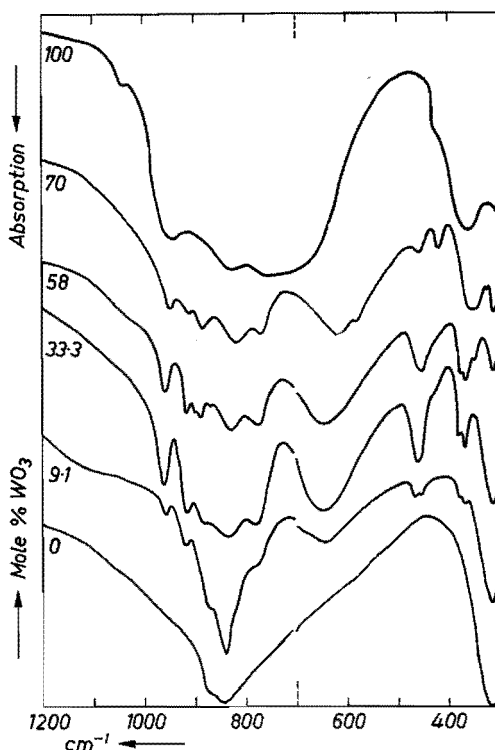
Fig. 3.1. Infrared spectra of crystalline sodium tungstates (system Na_2WO_4–WO_3).

1200–650 cm^{-1}, and, over the complete frequency range measured, shows good agreement with the $Na_2W_2O_7$ spectrum reported by Caillet and Saumagne [3–10]). The spectrum of 0·30 Na_2WO_4 . 0·70 WO_3 is in excellent correspondence with the $Na_2W_4O_{13}$ spectrum published by the latter authors. Likewise, the WO_3 spectrum of these is confirmed by our results, with the exception of a few bands of minor importance.

The spectra shown in fig. 3.1 are found to be highly dependent on WO_3 content. Addition of 9·1 mole% WO_3 to Na_2WO_4 already raises considerably the number of bands which can be observed in the spectrum. Special attention should be paid to the absorption maximum occurring at 640–610 cm^{-1}, as this is neither shown by Na_2WO_4 nor by WO_3.

The same holds for the band found in the frequency region 460–410 cm^{-1}. All compositions except Na_2WO_4 have, furthermore, an absorption band at 960–940 cm^{-1}. And finally strong absorption is shown by all compositions in the 840–820 and 400–300 cm^{-1} regions.

The main absorptions found in the spectra of crystalline sodium tungstates and WO_3 are summarised in table 3-I.

Turning to fig. 3.2, the spectrum of 0·30 K_2WO_4 . 0·70 WO_3 is found to show good agreement with the $K_2W_4O_{13}$ spectrum measured by Caillet and Saumagne [3–10]). Agreement with the spectrum of the latter compound which contains 75 mole% WO_3 is far better than with the spectrum of $K_2W_3O_{10}$, containing 67 mole% WO_3. Figure 3.2 shows that the infrared spectrum of crystalline alkali tungstates clearly depends on the alkali species present, at

TABLE 3-I

Main infrared absorption regions of crystalline sodium tungstates and WO_3;
$\times$ denotes the presence of strong absorption;
— denotes the absence of strong absorption.
"Intermediate compositions" relates to sodium tungstates included in fig. 3.1 having a WO_3 content of 9·1, 33·3, 58 and 70 mole% respectively

composition	frequency region (cm^{-1})					
	960–940	840–820	780–760	640–610	460–410	400–300
Na_2WO_4	—	$\times$	—	—	—	$\times$
intermediate compositions	$\times$	$\times$	$\times$	$\times$	$\times$	$\times$
WO_3	$\times$	$\times$	$\times$	—	$\times$	$\times$
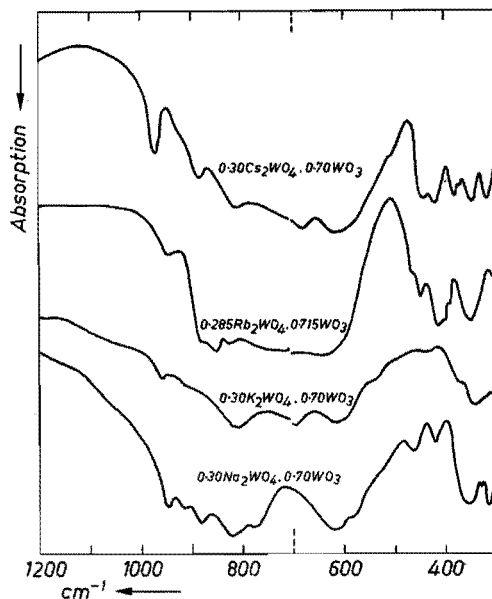
Fig. 3.2. Infrared spectra of crystalline alkali tungstates at 70 mole% WO_3.

least at the composition 70 mole% WO_3. All four spectra presented in the figure show a great number of absorption bands without having much in common.

Our spectroscopic study of crystalline alkali tungstates confirms, therefore, the conclusions drawn by Gelsing et al.[3-1,2] on the basis of more limited information, viz. that the infrared spectra of these systems are strongly affected by variation either of WO_3 content or of alkali species present. These conclusions, for that matter, will not come as a surprise, since it can be derived from the data given in sec. 1.3 that the structures and stabilities of the compounds found in alkali-tungstate systems vary widely with composition.

3.3.2. *Vitreous alkali tungstates*

Figures 3.3 and 3.4 show the spectra of a number of vitreous alkali tungstates. These spectra are in excellent agreement with those reported by Gelsing et al.[3-1,2] in the frequency region 1200–650 cm^{-1}. The tungstate glasses exhibit strong absorption at 880–850 cm^{-1}, whilst a band of medium intensity is found at 950–930 cm^{-1}. Gelsing's conclusion that spectra of vitreous tungstates hardly depend on WO_3 content and nature of the alkali ions, is confirmed. (It should, however, be pointed out that in fig. 3.4 the absorption maximum observed at 945 cm^{-1} is more pronounced in the order Na $\rightarrow$ K $\rightarrow$ Rb $\rightarrow$ Cs The same applies to the spectra of the corresponding crystalline tungstates.)

In the frequency region 650–300 cm^{-1}, not measured by Gelsing et al., the
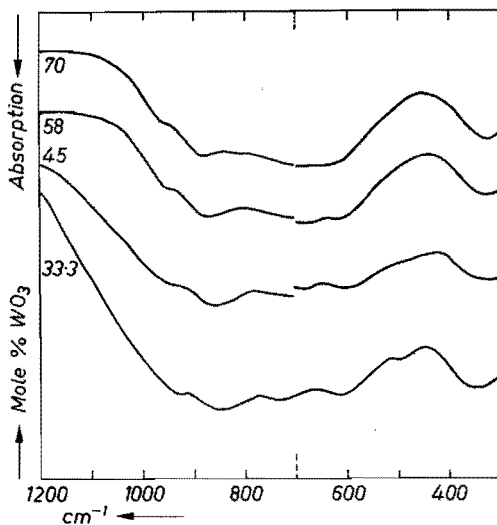
Fig. 3.3. Infrared spectra of vitreous sodium tungstates (system Na_2WO_4–WO_3).
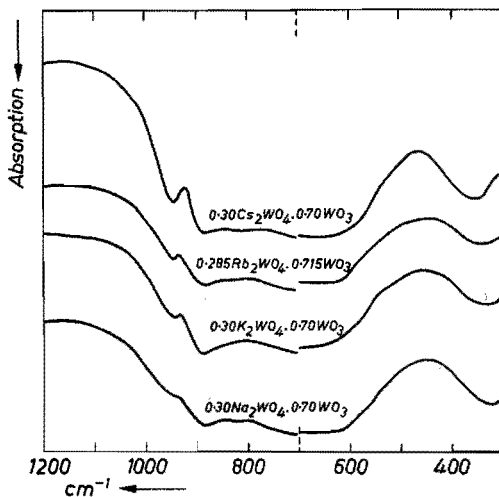
Fig. 3.4. Infrared spectra of vitreous alkali tungstates at 70 mole% WO_3.

spectra show two additional absorption bands, viz. at 650–600 cm^{-1} and at 355–320 cm^{-1}. The composition 0·67 Na_2WO_4 . 0·33 WO_3 shows an extra absorption maximum at 485 cm^{-1}. From comparison of the spectra of tungstate glasses with the Na_2WO_4 spectrum (other monotungstates having nearly identical spectra [3–1,2,3,4])), it is seen that, in the glass spectra, the two most important bands of the monotungstate spectrum are observed, though displaced to some extent. At the same time, however, it is obvious that strong

absorption is also found in frequency regions where absorption in the mono-tungstate spectrum is absent.

Therefore, the similarity between the spectra of vitreous tungstates and mono-tungstates forms too small a basis for the conclusion that the coordination of the W atom is identical in both cases, i.e. tetrahedral (as was assumed by Gelsing et al., cf. sec. 1.4).

This does not mean, however, that the structure proposed by Gelsing et al. cannot be correct. According to this structure the glass contains a mixture of chains of WO_4 tetrahedra, which implies that in the glass a bond is found which is not present in the monotungstate structure, viz. the W–O–W bond. Obviously, this bond will give rise to additional absorption maxima.

In the analogous case of the crystalline potassium chromates the infrared spectrum is essentially changed by the creation of double tetrahedra. K_2CrO_4 (containing isolated $CrO_4{}^{2-}$ tetrahedra) shows only one region of strong absorption in the frequency range 1200–300 cm^{-1}, viz. at 885–855 cm^{-1}. The dichromate $K_2Cr_2O_7$ (containing double tetrahedra) absorbs strongly at 966–885 cm^{-1} and at 796–764 cm^{-1}, whilst a few bands of lower intensity are found at lower wavenumbers [3-14,15]). Stammreich et al.[3-14]) attribute the band at 796–764 cm^{-1} and those at lower frequencies to vibrations of the Cr–O–Cr bond. Therefore, if a structure consisting exclusively of WO_4 tetrahedra existed, then, in addition to the monotungstate bands, new absorptions, the number and character of which would depend on the symmetry properties of the polytungstate chains, would arise.

The aspect of the spectra of vitreous tungstates might also be accounted for by a dissociation according to the views of Kordes and Nolte [3-16,17]) (cf. sec. 1.4), who assume $Na_2W_2O_7$ to undergo dissociation by the reaction

$$Na_2W_2O_7 \rightarrow 2\,Na^+ + WO_4{}^{2-} + WO_3.$$
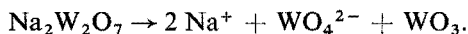
The spectrum of a tungstate glass should then correspond to that of a mixture of monotungstate, WO_3 and (when the dissociation is not complete) poly-tungstate, accompanied by a band-broadening effect caused by the absence of long-range order.

To examine this possibility, we will "synthesize" the spectrum of vitreous $Na_2W_2O_7$ from the spectra of crystalline Na_2WO_4 (I), $Na_2W_2O_7$ (II) and WO_3 (III).

For convenience the spectrum of crystalline $Na_2W_2O_7$ is assumed to be identical with that of 0·42 Na_2WO_4 . 0·58 WO_3 (cf. sec.3.3.1, where it was pointed out that the spectrum of the latter composition shows excellent agreement with that of $Na_2W_2O_7$ as published by previous authors).

In order to obtain "mixed spectra" the spectra of crystalline I, II and III were shifted with respect to each other to the extent that the maximum absorptions observed in these spectra were caused to lie at the same value. After this

the average spectrum was calculated for the degrees of dissociation $\alpha = 0$, $\frac{1}{2}$, $\frac{2}{3}$, and 1. For example, at $\alpha = \frac{2}{3}$ the spectrum was obtained by taking the arithmetic mean of the absorptions of $2 \times I$, $1 \times II$ and $2 \times III$ at a great number of frequencies.

This method has an admittedly arbitrary character, which, however, does not negate its usefulness.

When comparing the calculated spectra with the spectrum of vitreous $0.42 \, Na_2WO_4 \cdot 0.58 \, WO_3$ (see fig. 3.5), it is seen that the glass structure and the structure of a dissociated polytungstate cannot be related satisfactorily by this method.

Even in the "mixed" spectrum at $\alpha = 1$, which approaches best the spectrum of the glass, the strong absorption band at $600 \, cm^{-1}$ observed in the glass spectrum is absent.

It should, however, be stressed that the absence of long-range order may account for a strong distortion of the absorption bands.

The main conclusion of the infrared-spectroscopic study of vitreous alkali tungstates is that this study cannot provide a basis for definite conclusions.
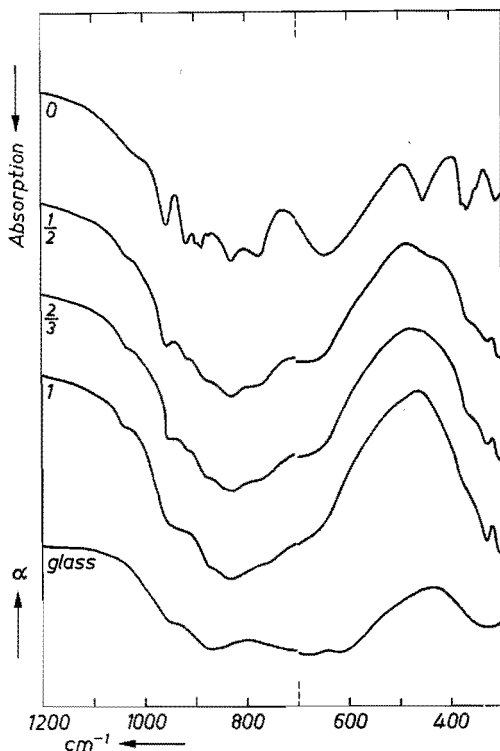
Fig. 3.5. Theoretical infrared spectra of crystalline $Na_2W_2O_7$ as a function of the degree of dissociation α (dissociation scheme: $Na_2W_2O_7 \rightarrow Na_2WO_4 + WO_3$).

However, the great similarity observed between the spectra may be an indication of a great similarity between the structures of tungstate glasses of varying composition. For this, both a structure according to the ideas of Gelsing et al.[3-1,2]), and a structure according to those of Kordes and Nolte [3-16,17]) can be responsible.

3.4. Infrared spectra of alkali molybdates

3.4.1. *Crystalline alkali molybdates*

Infrared spectra of a number of crystalline molybdates are shown in figs 3.6, 3.7 and 3.8.

In the frequency region 1200–650 cm^{-1} the spectrum of Li_2MoO_4 (fig. 3.6) shows good agreement with the Li_2MoO_4 spectra reported before [3-3,4]). In the region 650–300 cm^{-1} a few differences with respect to Clark and Doyle's spectrum are observed, presumably as a result of higher resolution demonstrated by our spectrum.

The spectrum of 0·60 Li_2MoO_4 . 0·40 MoO_3 is similar to that of $Li_2Mo_2O_7$ measured by Van der Wielen et al. in the region 1200–650 cm^{-1}. And, finally,
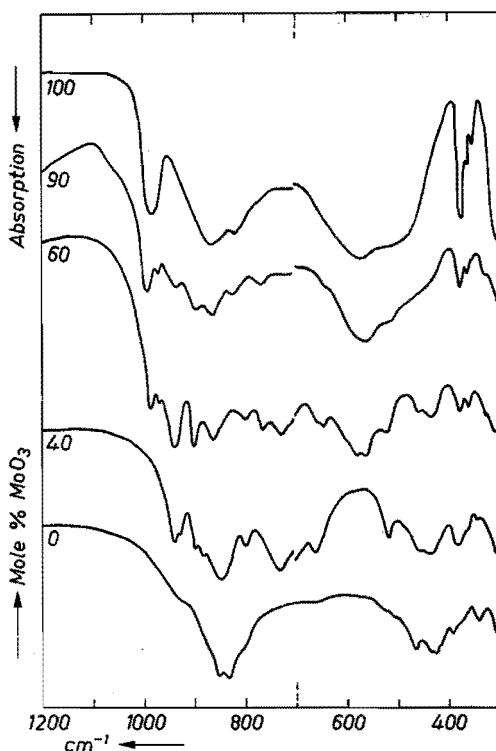
Fig. 3.6. Infrared spectra of crystalline lithium molybdates (system Li_2MoO_4–MoO_3).
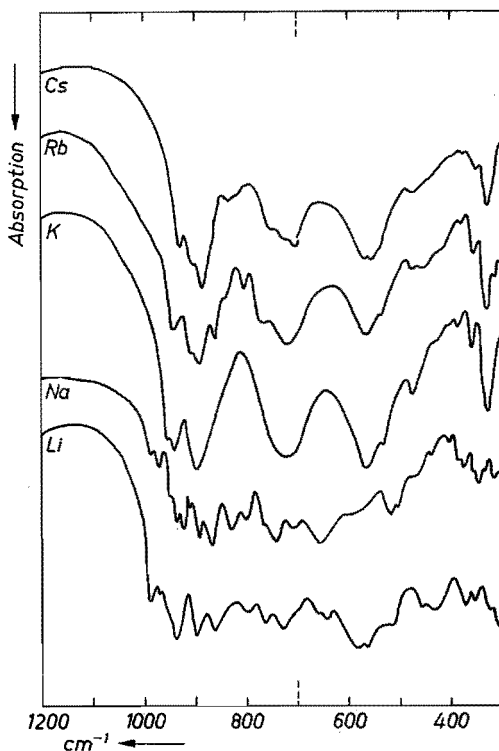
Fig. 3.7. Infrared spectra of crystalline alkali molybdates at 60 mole% MoO_3 (potassium molybdate at 65 mole% MoO_3).

the MoO_3 spectrum in fig. 3.6 is identical to that reported by Lipsch [3-12]) for the frequency region 1200–400 cm^{-1}.

It is seen from fig. 3.6 that crystalline alkali molybdates, like the corresponding tungstates, possess infrared spectra which are strongly dependent on trioxide content.

In fig. 3.7 the spectrum of 0·35 K_2MoO_4 . 0·65 MoO_3 shows excellent agreement with that of $K_2Mo_3O_{10}$ (containing 67 mole% MoO_3) as published by Caillet and Saumagne [3-10]). Likewise, our spectra of 0·40 Rb_2MoO_4 . . 0·60 MoO_3 and 0·40 Cs_2MoO_4 . 0·60 MoO_3 strongly resemble those of the trimolybdates.

A striking mutual similarity is observed in the spectra of K, Rb and Cs molybdates. This may be explained by the fact that K, Rb and Cs trimolybdates exist and are isomorphous (see sec. 1.3), whereas in the Na-molybdate system no trimolybdate is formed.

The congruently melting phase $Li_2Mo_3O_{10}$, reported by Van der Wielen et al. (see fig. 1.2a) either is not formed during crystallisation from the melt, or has a structure essentially different from that of $K_2Mo_3O_{10}$.
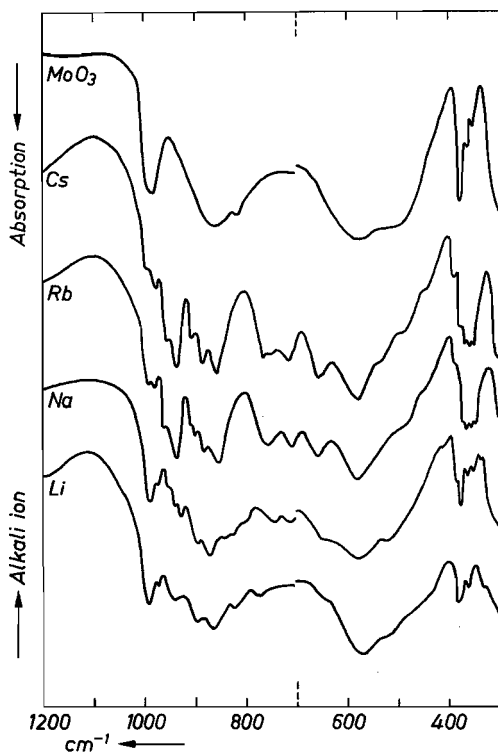
Fig. 3.8. Infrared spectra of crystalline alkali molybdates at 90 mole% MoO_3.

The spectra of 0.10 Rb_2MoO_4 . 0.90 MoO_3 and 0.10 Cs_2MoO_4 . 0.90 MoO_3 (fig. 3.8) show excellent agreement with the spectra of $Rb_2Mo_9O_{28}$ and $Cs_2Mo_9O_{28}$ (89 mole% MoO_3) respectively, measured by Salmon and Caillet [3-9]). Again, Rb- and Cs-molybdate spectra show a strong similarity, whereas equally strong dissimilarities are observed with respect to the spectra of 0.10 Na_2MoO_4 . 0.90 MoO_3 and 0.10 Li_2MoO_4 . 0.90 MoO_3. The latter two spectra already resemble the spectrum of pure MoO_3, due to the fact that no compounds $Na_2Mo_9O_{28}$ and $Li_2Mo_9O_{28}$ exist (see figs 1.2a and 1.2b). The molybdates of highest MoO_3 content formed in the Na_2MoO_4–MoO_3 and Li_2MoO_4–MoO_3 systems are the tetramolybdates, containing 75 mol% MoO_3.

3.4.2. Vitreous alkali molybdates

Spectra of a number of vitreous alkali molybdates are presented in figs 3.9, 3.10 and 3.11.

Comparing our spectra with those of the 6 vitreous molybdates published by Van der Wielen et al. [3-3]), we observe good agreement in the frequency region 1200–650 cm^{-1} between our spectrum of 0.60 Li_2MoO_4 . 0.40 MoO_3
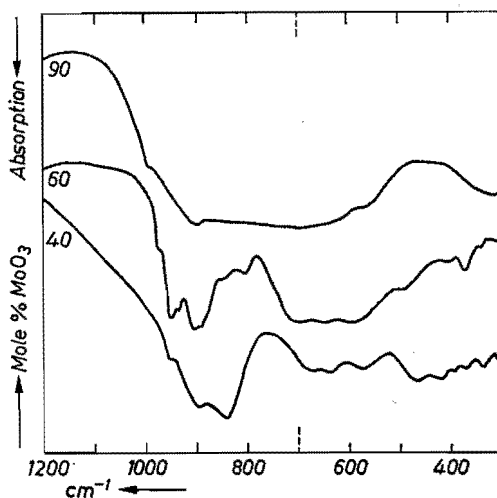
Fig. 3.9. Infrared spectra of vitreous lithium molybdates (system Li_2MoO_4–MoO_3).

and Van der Wielen's spectra of lithium-molybdate glasses containing 30 and 47 mole% MoO_3. In all three cases absorption bands can be found at approximately 950, 895 and 840 cm^{-1}, the intensities, however, showing mutual differences.

In fig. 3.9 it is seen that the spectra of vitreous lithium molybdates, at least at 40 and 60 mole% MoO_3, show a great number of absorption bands, contrary to the spectra of the corresponding tungstate glasses. At 90 mole% MoO_3 this abundance has disappeared.

Comparison of the spectra of vitreous and crystalline lithium molybdates (figs 3.9 and 3.6 respectively) prompts the following remarks.

In the spectrum of vitreous $0.60\ Li_2MoO_4 \cdot 0.40\ MoO_3$ all important bands of crystalline Li_2MoO_4 are still found (840, 465, 420, 390, 335 and 305 cm^{-1}). On the other hand, similarities can be observed with the spectrum of the crystalline molybdate of equal composition (which will also contain Li_2MoO_4, in accordance with the phase diagram of Li_2MoO_4–MoO_3: cf. fig. 1.2a). In addition to these bands, which are similar to those found in the spectra of crystalline compounds, strong absorption can be observed where none of the crystalline lithium molybdates shows strong absorption, viz. at 675–625 cm^{-1}.

An analogous consideration applies to the spectrum of vitreous $0.40\ Li_2MoO_4 \cdot 0.60\ MoO_3$. A number of absorption bands can be observed in the spectrum of the crystalline compound of equal composition, whereas the spectrum of the glass shows additional bands lying in the same frequency region as those of vitreous $0.60\ Li_2MoO_4 \cdot 0.40\ MoO_3$. Finally, the spectrum of vitreous $0.10\ Li_2MoO_4 \cdot 0.90\ MoO_3$ shows strong absorption over the whole frequency region 1000–500 cm^{-1}. The position of the three bands which

can be distinguished in this region, corresponds approximately to that of the absorption maxima displayed by crystalline MoO_3.

Figure 3.10 demonstrates that vitreous alkali molybdates having an MoO_3 content of approximately 60 mole %, possess spectra which are clearly dependent on the nature of the alkali ions present, with, however, the K-, Rb- and Cs-molybdate glasses showing strong mutual similarities.

As was observed above, these glasses generally present a multitude of absorption bands, contrary to the analogous tungstate glasses. Comparison with the spectra of the corresponding crystalline molybdates (fig. 3.7) shows first of all that a distinct similarity exists between the spectra of vitreous and crystalline K, Rb and Cs molybdates. (It should be remembered that crystalline K, Rb and Cs molybdates have spectra which show excellent mutual agreement.)

The strong absorptions exhibited by the crystalline molybdates at approximately 720 and 560 cm^{-1} seem to be merged together in the glass spectra.
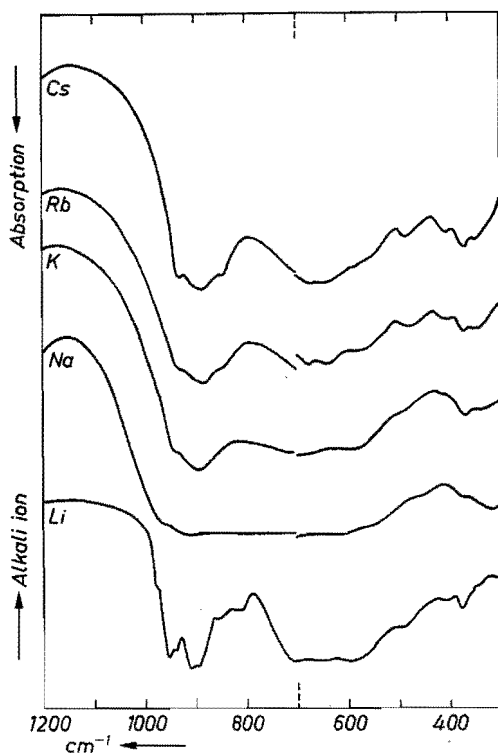
Fig. 3.10. Infrared spectra of vitreous alkali molybdates at 60 mole% MoO_3 (potassium molybdate at 65 mole% MoO_3).

The resemblance between the spectra of vitreous 0·40 Na_2MoO_4 . 0·60 MoO_3 and 0·40 Li_2MoO_4 . 0·60 MoO_3 and those of the corresponding crystalline molybdate is less easily seen, although the spectrum of the sodium-molybdates glass may be considered to have originated from a rigorous broadening of the many bands observed in the spectrum of the crystalline molybdate.

Figure 3.11 demonstrates that the spectrum of molybdate glasses at 90 mole % MoO_3 hardly depends on the nature of the alkali ions, contrary to the spectra of the corresponding crystalline molybdates (see fig. 3.8). This suggests that the structures of the alkali-molybdate glasses at high MoO_3 content are similar.

An explanation for this may be the structure proposed in sec. 2.1.3: addition of alkali oxide to pure MoO_3 raises the number of non-bridging oxygens by the breaking of bridges between two octahedra; the number of bonds involving three octahedra remains constant; by this mechanism the MoO_3 layers are "cleft".

From the above discussion of infrared spectra of vitreous alkali molybdates it is seen that these spectra

(a) are dependent on MoO_3 content;

(b) are dependent on the nature of the alkali ions present, provided that the MoO_3 content is not very high;

(c) show similarities with the spectra of the corresponding crystalline molybdates;
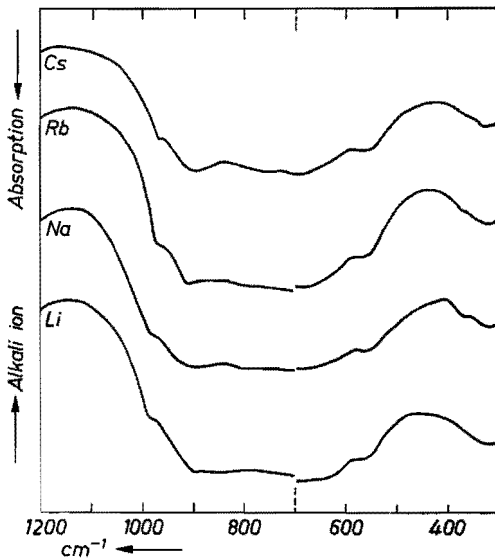
Fig. 3.11. Infrared spectra of vitreous alkali molybdates at 90 mole% MoO_3.

(d) show, however, additional absorption bands not observed in the latter spectra.

It appears to be impossible to account for these phenomena by a glass structure consisting exclusively of chains of tetrahedra, even if these are assumed to be strongly distorted [3-3] (see sec. 1.4). In that case, the mutual similarities between the spectra of the vitreous molybdates would undoubtedly be greater than they are now. The similarities between the spectra of the glasses and those of the corresponding crystalline molybdates, however, suggest that even in the vitreous state, complex anions are found built up by tetrahedra as well as octahedra, probably forming chains, as is the case with the crystalline polymolybdates.

Naturally, within the limits of this structure some variation is possible. For example, the average chain length of the polymolybdate anion may decrease on melting. In association therewith, the average coordination number of the Mo atoms may change, as for reasons of stoichiometry there is a correlation between the average coordination number and the dimensions of the complex anions.

Again, it should be stressed that definite conclusions cannot easily be drawn on the basis of an infrared-spectroscopic study.

RFFERENCES

[3-1]) R. J. H. Gelsing, H. N. Stein and J. M. Stevels, Phys. chem. Glasses 7, 185-190, 1966.

[3-2]) R. J. H. Gelsing, Klei en Keramiek 17, 183-189, 1967.

[3-3]) J. C. Th. G. M. van der Wielen, H. N. Stein and J. M. Stevels, J. non-cryst. Solids 1, 18-28, 1968.

[3-4]) G. M. Clark and W. P. Doyle, Spectrochim. Acta 22, 1441-1447, 1966.

[3-5]) P. Caillet and P. Saumagne, J. mol. Struct. 4, 191-201, 1969.

[3-6]) T. Dupuis, Mikrochim. Acta 214-222, 1963.

[3-7]) T. Dupuis and M. Viltange, Mikrochim. Acta 232-238, 1963.

[3-8]) P. Caillet, C.R. Acad. Sci. Paris 256, 1968-1989, 1963.

[3-9]) R. Salmon and P. Caillet, Bull. Soc. chim. 1569-1573, 1969.

[3-10]) P. Caillet and P. Saumagne, J. mol. Struct. 4, 351-359, 1969.

[3-11]) C. G. Barraclough, J. Lewis and R. S. Nyholm, J. chem. Soc. 3552-3555, 1959.

[3-12]) J. M. J. G. Lipsch, Thesis, Eindhoven, 1968, p. 29.

[3-13]) J. Derkosch, Absorptionsspektralanalyse, Akademische Verlagsgesellschaft, Frankfurt, 1967, p. 60.

[3-14]) H. Stammreich, D. Bassi, O. Sala and H. Siebert, Spectrochim. Acta 13, 192-196, 1958.

[3-15]) J. A. Campbell, Spectrochim. Acta 21, 1333-1343, 1965.

[3-16]) G. Nolte, Thesis, Bonn, 1967.

[3-17]) E. Kordes and G. Nolte, Z. anorg. allgem. Chem. 371, 156-171, 1969.

4. DENSITY OF MOLTEN ALKALI TUNGSTATES AND MOLYBDATES *)

4.1. Introduction

In the preceding chapter it was seen that from infrared-spectroscopic measurements few indications could be derived with regard to the structures of tungstate and molybdate glasses. Therefore, the structures of these glasses have to be approached from a different angle.

In chapter 1 the method of determining property/composition relationships was mentioned, from which it may be possible to derive new indications regarding structure and coordination. Because of the narrow composition regions, in which vitreous samples of reasonable quantity can be prepared, this method is not feasible in the case of tungstate and molybdate systems. This difficulty, however, can be avoided if the same property/composition relations are measured for the systems in the molten state, on the basis of the concept that there will not be an essential difference between the structure of a glass and that of its melt.

When a melt is cooled without crystallisation taking place, its properties change continually. The structure variations occurring above and below the liquidus temperature are completely analogous. At the transformation temperature T_g an abrupt structural transition is absent; melt and glass structures at this temperature are identical. Once T_g has been passed, the structure is "rigid" and no further essential changes are found.

It seems, therefore, permissible to extrapolate information on the structure of the melt to that of the glass.

This qualitative way of discussing the similarities of glass and melt is supported by the work of Riebling [4-1], which shows that the densities of most glasses can even be calculated from the density of a high-temperature melt (or vice versa) to within several per cent.

Some data on physical properties of molten alkali-tungstate and -molybdate systems have already been reported by previous authors.

Jaeger [4-2] measured the densities of K_2WO_4 and K_2MoO_4, as well as the surface tensions of Na_2WO_4, K_2WO_4 and K_2MoO_4.

Jaeger and Kapma [4-3] reported the densities and electrical conductivities of Na_2WO_4 and Na_2MoO_4.

Spitzin and Tscherepneff [4-4] determined the electrical-conductivity values of six compositions in the system Na_2WO_4–WO_3.

Kvist and Lundén [4-5] measured the electrical conductivity of molten Li_2MoO_4.

---

*) Part of the contents of chapters 4 and 5 have been published previously by R. G. Gossink, H. N. Stein and J. M. Stevels, Silic. ind. **35**, 245-252, 1970; R. G. Gossink and J. M. Stevels, J. non-cryst. Solids **5**, 217-236, 1971.

An extensive study of density and electrical conductivity in molten alkali-molybdate and alkali-tungstate systems, the alkali metal being Li, Na or K, has been published by Morris and cooperators [4–6,7,8]. However, on the basis of their data it is not always possible to obtain reliable isotherms, as the individual temperature ranges valid for the compositions measured in many cases do not sufficiently overlap. Their only thorough discussion of results concerns the electrical-conductivity values of Li- and K-molybdate systems [4–7], and is based on conductivity/composition relationships at 100 °C above the liquidus. It will not come as a surprise that maxima and minima observed in these conductivity/composition graphs correspond to melting points and eutectics in the phase diagrams. It is, however, doubtful whether conclusions drawn from this kind of relationship have any real significance with regard to the structure of the melt.

The density measurements on Li, Na and K molybdates carried out by Van der Wielen et al. have already been mentioned in sec. 1.4. It should be noted that the results of Van der Wielen's measurements have been published only in part [4–9,10]. From their results, Van der Wielen et al. calculated the departures between ideal and actual density values at 920 °C. It was concluded that actual density values were relatively low in regions of optimal glass formation, involving a relatively spacious structure in the vitreous state. Van der Wielen et al. considered this to be an indication of a structure comprising chains of tetrahedra which have undergone disproportionation, as in their opinion this structure would require more space than a structure consisting of large groups also containing octahedra.

Our own investigations concern the determination of density, surface-tension and viscosity values. Like Morris and cooperators and Van der Wielen et al., we have restricted ourselves to systems containing Li, Na or K.

In addition to those of the binary alkali-tungstate and -molybdate systems, we have measured the properties of a few mixed-alkali and mixed-molybdate–tungstate systems, viz. the systems

$$Na_2W_2O_7–K_2W_2O_7; \qquad Na_2Mo_2O_7–K_2Mo_2O_7;$$
$$Na_2W_2O_7–Na_2Mo_2O_7; \qquad K_2W_2O_7–K_2Mo_2O_7.$$
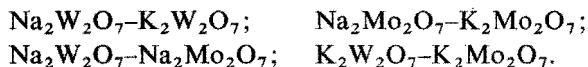
In the present chapter density measurements on molten alkali-tungstate systems will be described, and the results will be compared with Van der Wielen's data on the corresponding molybdate systems.

Surface-tension measurements will be described in chapter 5, and the determination of viscosities in chapter 6.

4.2. Experimental method

Alkali tungstates were prepared from alkali carbonates and WO_3 by the method described in sec. 2.1.2.

Densities were measured by Mackenzie's method [4-11]) using the apparatus of Van der Wielen et al.[4-9]) (see fig. 4.1). This method involves the determination of the buoyancy exerted on a platinum bob on submersion in the melt.

The melt was contained in a cylindrical Pt/Rh-alloy crucible having a diameter of 3 cm and a height of 5 cm. This crucible was placed in an electric furnace.

The volume of the cylindrical Pt bob at 0 °C was $V_0 = 1.4607$ cm^3. It was corrected for thermal expansion by the formula

$$V_t = V_0 (1 + 0.269631 . 10^{-4} t + 0.34379 . 10^{-8} t^2 + 0.4062 . 10^{-12} t^3),$$

where V_t is the volume (cm^3) of the bob at t and t is the temperature (°C), which was calculated from the linear-expansion formula of Esser and Eusterbrock [4-12]).

Density measurements with the aid of the above method may be influenced by the effect of surface tension exerted by the melt on the suspension wire (Pt/Rh-alloy wire; diameter 0.2 mm). To eliminate this difficulty completely, either the surface-tension effect has to be calculated by means of a formula derived by Shartsis and Spinner [4-13]), or two bobs of different sizes must be used.
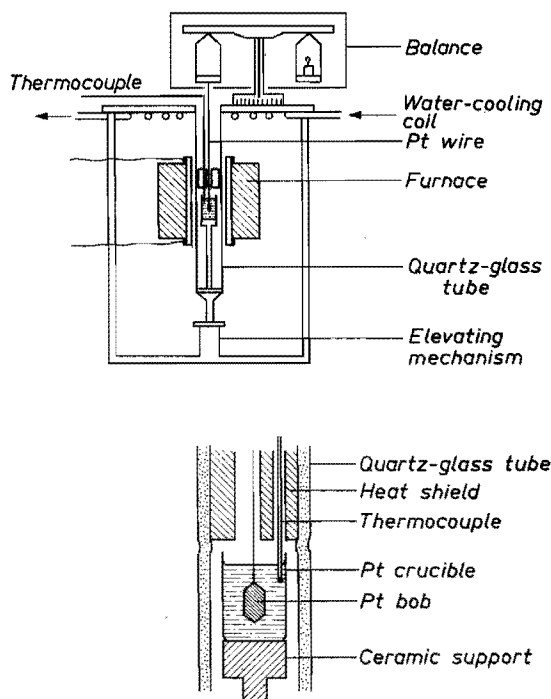
Fig. 4.1. Apparatus for the determination of melt densities.

In employing the latter approach, Van der Wielen et al.[4-9] found that significant surface-tension effects were absent for the apparatus used and the systems investigated. Further, Riebling [4-11] observed little difference between densities calculated by the method of two bobs, and uncorrected single-bob data using a bob of 1·6 cm^3. And, finally, calculation of the surface-tension effect for an "average" case (the density of 0·70 Na$_2$WO$_4$. 0·30 WO$_3$ at 950 °C) using the formula of Shartsis and Spinner [4-13], showed that an error of 0·07% was made when the effect of surface tension was not taken into account.

Putting all this together, it was decided to neglect the effect of surface tension on the suspension wire.

Temperatures were measured in the melt with a calibrated thermocouple (Pt–Pt/10%Rh).

The density of each sample was determined at 5–10 different temperatures, the temperature range covered being at least 150 °C.

The accuracy of the measurements is estimated to be $\pm$ 0·5%.

4.3. Binary alkali tungstates; a comparison with alkali molybdates

4.3.1. *Results*

For all compositions measured the relation between density and temperature can be represented satisfactorily by the linear equation

$$\varrho = a - b\,t,$$

where ϱ is the density (g cm^{-3}), a and b are constants (> 0), and t is the temperature (°C).

Values of a and b obtained by the method of least-squares minimising $\Sigma\,(\varDelta\varrho)^2$, as well as the standard deviations of estimate of the least-squares lines *) are included in table 4-I. This table also contains the values of the density at 950 °C (ϱ_{950}), the molar volume at 950 °C (v_{950}), the thermal-expansion coefficient at 950 °C ($\alpha_{950} = [(1/v)\,\mathrm{d}v/\mathrm{d}t]_{950}$), as well as the temperature ranges for which the equations are valid.

Comparison of our values of ϱ_{950} for the monotungstates with those obtained by Jaeger [4-2], Jaeger and Kapma [4-3], and Morris and Robinson [4-7]

---

*) The standard deviation of estimate $s(\hat{\varrho})$ is the square root of the variance of estimate as defined by Volk [4-15]:

$$s(\hat{\varrho}) = \sqrt{\frac{(\varrho - \hat{\varrho})^2}{n - 2}},$$

where $\hat{\varrho}$ is the density according to least-squares line, ϱ the density measured, and n the number of measuring points.

TABLE 4-1

Density of alkali tungstates

mole % WO_3	a (g cm^3)	$b \cdot 10^3$ (g cm^{-3} °C^{-1})	$s(\hat{\varrho})$ (g cm^{-3})	ϱ_{950} (g cm^{-3})	v_{950} (cm^3 mole^{-1})	$\alpha_{950} \cdot 10^3$ (°C^{-1})	temp. range (°C)
lithium tungstates							
0	4·893	0·863	0·005	4·073	64·26	0·212	825– 992
15	5·168	0·919	0·002	4·295	59·89	0·214	803–1000
30	5·465	1·040	0·005	4·477	56·46	0·232	875–1031
40	5·538	0·942	0·006	4·643	53·80	0·203	860–1010
50	6·079	1·339	0·004	4·807	51·34	0·279	890–1005
sodium tungstates							
0	4·507	0·919	0·005	3·634	80·86	0·253	716– 957
20	4·896	1·056	0·002	3·893	72·29	0·271	748– 964
30	5·192	1·217	0·002	4·036	68·20	0·302	800– 965
45	5·738	1·473	0·001	4·339	61·29	0·339	785–1016
50	5·701	1·364	0·007	4·405	59·67	0·310	846– 998
60	5·812	1·279	0·017	4·597	55·83	0·278	792–1020
70	6·075	1·339	0·006	4·803	52·14	0·279	882–1028
potassium tungstates							
0	3·648	0·517	0·006	3·157	103·28	0·164	943–1055
20	4·219	0·893	0·003	3·371	91·13	0·265	834–1015
35	4·849	1·303	0·005	3·611	81·16	0·361	754– 989
45	5·129	1·443	0·003	3·758	75·48	0·384	703– 960
50	5·299	1·574	0·005	3·804	73·33	0·414	783– 985
55	5·242	1·333	0·008	3·976	68·97	0·335	813–1003
70	5·934	1·637	0·002	4·379	59·40	0·374	923–1053

TABLE 4-II

Comparison of density values at 950 °C (g cm^{-3}) obtained by previous authors and those in the present work

	present work	Jaeger [4-2]), Jaeger and Kapma [4-3])	Morris and Robinson [4-8])
K_2WO_4	3·157	3·153	3·154
Na_2WO_4	3·634	3·654	3·659
Li_2WO_4	4·073	—	4·140 (extrapolated)

shows that the mutual departures are small (see table 4-II).

The results of Van der Wielen's measurements on the analogous molybdate systems, obtained by the same method and only published in part [4-9]), have been treated in the same way and are represented in table 4-III. Comparison of Van der Wielen's values of ϱ_{950} for the monomolybdates with those obtained by Jaeger [4-2]), Jaeger and Kapma [4-3]) and Morris and cooperators [4-6,7]) shows that for these compounds the mutual departures are larger (in the order of a few %); Van der Wielen's values are lower than those of the other authors (see table 4-IV).

Density isotherms at 950 °C for tungstates and molybdates are shown in figs 4.2 and 4.3. In these figures isotherms are also represented for the thermal-expansion coefficient α and the molar volume v. The temperature of 950 °C has been selected, because this temperature lies near the upper limit of the temperature ranges over which the density was measured, the systems thus being liquid over large composition regions, whilst the density can still be determined satisfactorily accurately. It should, however, be remarked that the aspect of the isotherms does not change essentially by selecting a temperature of 100 or 200 °C lower.

The molar volume v has been calculated by the formula

$$v = \frac{M}{\varrho},$$

where ϱ is the density measured, M the value obtained by linear interpolation between the formula weight of the monocompound and that of the trioxide; e.g. for the tungstate systems

$$M = x_{M_2WO_4} \cdot M_{M_2WO_4} + x_{WO_3} \cdot M_{WO_3},$$

where M is the formula weight and x the molar fraction.

The physical meaning of v can be understood as follows: both $M_{M_2WO_4}$ grammes of M_2WO_4 and M_{WO_3} grammes of WO_3 contain 1 gramatom W.

TABLE 4-III

Density of alkali molybdates, calculated from unpublished results of Van der Wielen [4-10])

mole% MoO_3	a (g cm^{-3})	$b \cdot 10^3$ (g cm^{-3} °C^{-1})	$s(\hat{\varrho})$ (g cm^{-3})	ϱ_{950} (g cm^{-3})	v_{950} (cm^3 mole^{-1})	$\alpha_{950} \cdot 10^3$ (°C^{-1})	temp. range (°C)
lithium molybdates							
0	2·886	0·2380	0·003	2·660	63·35	0·0895	842–1012
10	3·268	0·5693	0·001	2·727	62·64	0·2088	773– 991
20	3·381	0·6636	0·003	2·751	61·01	0·2413	754– 972
30	3·407	0·6422	0·002	2·797	58·94	0·2296	717–1028
40	3·488	0·6895	0·002	2·833	57·14	0·2434	710– 955
50	3·656	0·8331	0·006	2·865	55·46	0·2908	644– 953
60	3·703	0·8231	0·002	2·921	53·37	0·2818	701– 960
70	3·883	0·9970	0·003	2·936	52·08	0·3396	686– 950
sodium molybdates							
0	3·168	0·6542	0·002	2·547	80·85	0·2569	815– 990
10	3·224	0·6844	0·006	2·574	77·59	0·2659	705– 955
30	3·454	0·8506	0·009	2·646	70·80	0·3215	712– 955
40	3·462	0·8324	0·003	2·671	67·81	0·3116	706– 955
50	3·524	0·8705	0·009	2·697	64·86	0·3228	696– 961
60	3·706	1·0246	0·003	2·733	61·74	0·3750	696– 965
70	3·885	1·1300	0·003	2·812	57·80	0·4019	698– 955
80	3·786	0·8963	0·007	2·935	53·27	0·3054	680– 970
potassium molybdates							
0	2·699	0·4044	0·003	2·315	102·87	0·1747	920– 975
12	3·007	0·6771	0·025	2·364	95·95	0·2865	896– 964
19	2·998	0·6703	0·009	2·361	93·28	0·2839	884–1040
31·5	3·193	0·8541	0·008	2·382	87·52	0·3586	645– 954
39	3·200	0·8563	0·019	2·387	84·37	0·3588	542– 954
50	3·309	0·9198	0·007	2·435	78·46	0·3777	592– 944
58	3·355	0·9347	0·006	2·467	74·38	0·3789	648– 958
70	3·664	1·0072	0·001	2·707	63·61	0·3720	738– 951

TABLE 4-IV

Comparison between density values at 950 °C (g cm^{-3}) calculated from the results of previous authors and from unpublished data of Van der Wielen [4-10])

	Van der Wielen [4-10])	Jaeger [4-2]), Jaeger and Kapma [4-3])	Morris et al.[4-6], Morris and Robinson [4-7])
K_2MoO_4	2·315	2·350	2·471
	2·547	2·638	—
Na_2MoO_4	$\varrho_{825} = 2\cdot628$	$\varrho_{825} = 2\cdot716$	$\varrho_{825} = 2\cdot68$ (only 1 determination)
Li_2MoO_4	2·660	—	2·806

The same holds for M grammes of an intermediate composition. Therefore, v is the volume occupied by an amount of material containing 1 gramatom W, irrespective of trioxide content.

As is seen from figs 4.2 and 4.3 the molar volumes of two corresponding
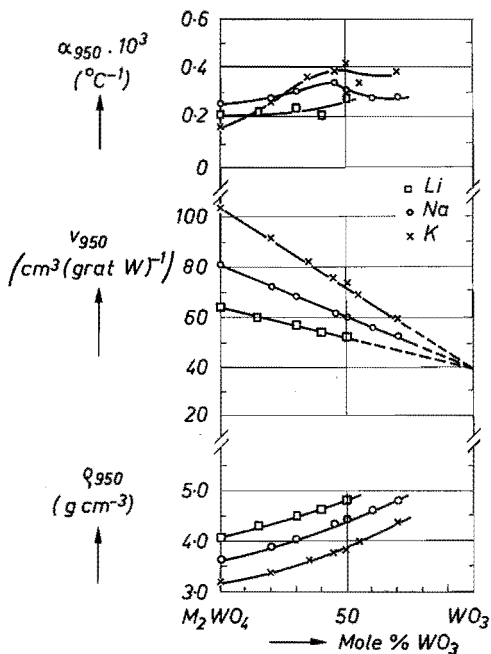
Fig. 4.2. Isotherms of density (ϱ), molar volume (v) and thermal-expansion coefficient (α) at 950 °C for molten alkali tungstates.
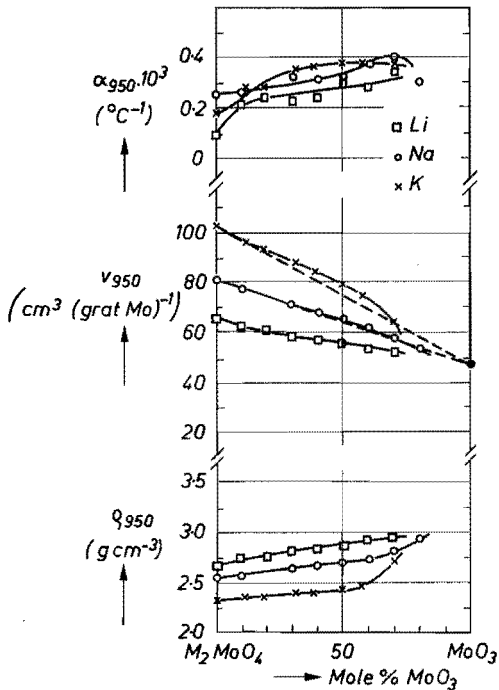
Fig. 4.3. Isotherms of density (ϱ), molar volume (v) and thermal-expansion coefficient (α) at 950 °C for molten alkali molybdates (calculated from the data of Van der Wielen et al.[4–9,10]).

monocompounds (e.g. Li_2WO_4 and Li_2MoO_4) are approximately equal, which is not surprising, as corresponding monocompounds are isomorphous and have approximately equal unit-cell dimensions when crystalline (cf. sec. 1.3). The molar-volume isotherms appear to be linear in the case of the tungstate systems, whereas for the molybdate systems departures from linearity are found, especially in the case of the sodium and potassium molybdates (it should be remarked that the accuracy of v is equal to that of ϱ, viz. $\pm 0.5\%$). These departures from linearity can be shown objectively in the following way: when by the method of least squares the linear coefficient is calculated that represents best the relation between v_{950} and trioxide content, each individual measuring point shows a departure Δv_{950} from the linear relation.

In fig. 4.4 this particular departure Δv_{950} is plotted vs composition for all compositions measured. The value of Δv_{950} is small and non-systematic for the tungstate systems. The same applies to the lithium-molybdate system. However, for the sodium and potassium molybdates larger departures are seen. Clearly, there is a maximum, and at higher MoO_3 content large negative departures are found.

The same effect is shown by fig. 4.3. The dashed lines represent the linear
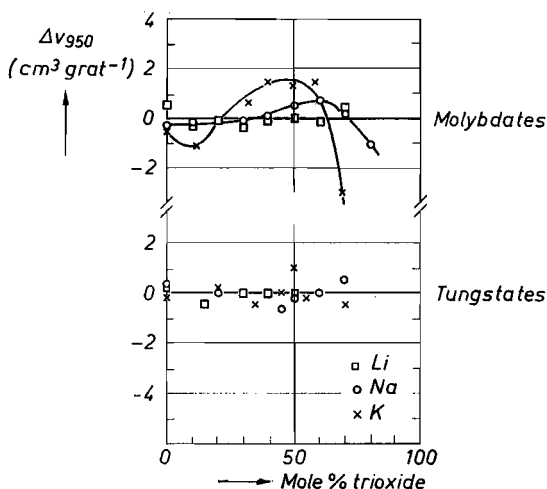
Fig. 4.4. Departure from linearity (Δv) of molar-volume isotherms for molten alkali molybdates and tungstates at 950 °C.

interpolation lines between $v_{M_2MoO_4}$ and v_{MoO_3} (v_{MoO_3}, based on the data of Morris et al.[4–6]), $= 47.53$ cm^3/grat Mo).

Little can be said regarding the isotherms of the thermal-expansion coefficient (see figs 4.2 and 4.3). The values of α_{950} for both tungstates and molybdates are found in the same range, viz. 0.1–$0.4 \cdot 10^{-3}$ (°C^{-1}).

4.3.2. Discussion

When trioxide is added to alkali monotungstate or monomolybdate, in the crystalline state compounds are formed in which various types of polyhedra — tetrahedra, units having 5-coordination, octahedra — build up large anionic groups of the infinite-chain type (cf. the crystal structures of $Na_2W_2O_7$, $Na_2Mo_2O_7$, $K_2Mo_3O_{10}$, discussed in sec. 1.3).

In the previous chapters indications were found for the fact that these large anionic groups dissociate on melting. According to the ideas of Gelsing et al. (cf. sec. 1.4) the dissociation in tungstate systems is so strong that the melt contains a mixture of on the average short chains of WO_4 tetrahedra. Navrotsky and Kleppa (cf. sec. 1.4), on the other hand, assume that alkali dimolybdates ($M_2Mo_2O_7$) do not undergo complete dissociation on melting, the degree of dissociation being dependent on the alkali species present.

Generally, on the addition of trioxide to molten alkali monotungstate or monomolybdate, a melt will be formed, the structure of which is situated between two extreme possibilities:

A. When the degree of dissociation of the large anionic groups is very low, the melt will contain large groups in which Mo or W atoms, having coordination numbers higher than 4, occur.

B. When the degree of dissociation of the large anionic groups is very high, the melt will contain exclusively small groups built up by tetrahedra.

(It should be emphasized that for stoichiometric reasons the formation of large groups *implies* the occurrence of polyhedra with coordination numbers higher than 4, and vice versa; on the other hand, the occurrence of exclusively small groups *implies* that only 4-coordination is found, and vice versa.)

In the following an attempt will be made to predict what the effects will be of possibilities A and B on the molar-volume/composition relationships. After that, a comparison will be made of the relationships predicted with those experimentally found for molten alkali-tungstate and -molybdate systems.

Possibility A implies that large anionic groups are formed containing polyhedra with coordination numbers higher than 4, when trioxide is added to monotungstate or monomolybdate. Obviously, the structures of crystalline alkali tungstates and molybdates obey possibility A. Therefore, the structural transitions occurring on the addition of trioxide to M_2WO_4 or M_2MoO_4 can be summarised as follows:

M_2MoO_4 and M_2WO_4	isolated tetrahedra
$M_2Mo_2O_7$ and $M_2W_2O_7$	infinite chains of distorted polyhedra (tetrahedra and octahedra)
$M_2Mo_3O_{10}$	infinite chains of distorted polyhedra (square pyramids and octahedra)
MoO_3 or WO_3	two- or three-dimensional network of octahedra.

In view of the complicated character of this transition it seems unlikely that a linear relation will be found between the molar volume and the composition of the melt. The monotungstates and monomolybdates have a regular and compact structure. So have the trioxides. In the regions in between, however, irregular groups are found containing various types of distorted polyhedra. It is not unthinkable that this will give rise to a relatively high molar volume.

The hypothesis of a non-linear relationship between molar volume and composition becomes even more plausible when the molar volumes of the crystalline alkali molybdates and tungstates at room temperature are considered, as can be calculated from the dimensions of the unit cell and the number of formula units it contains. The values obtained represent "ideal" molar volumes, i.e. without lattice imperfections and without the even higher lack of long-range order introduced upon melting. The results, therefore, unambiguously show the effect of coordinational transition.

The results of the calculations are included in table 4-V. It is seen that the molar volumes calculated for $Na_2W_2O_7$, $Na_2Mo_2O_7$, as well as $K_2Mo_3O_{10}$, are distinctly higher than those obtained by linear interpolation between the molar volumes of monotungstate or monomolybdate, and trioxide.

These results support the above assumption that the transition from tetra-

TABLE 4-V

Molar volumes of alkali molybdates, tungstates and chromates at room temperature, calculated from crystal-structure data [4-16,17,18,19]; $v_{interpolated}$ = value obtained by linear interpolation between the molar volumes of mono-compound and trioxide

	$v_{calculated}$ (cm^3/mole)	$v_{interpolated}$ (cm^3/mole)	$v_{calc.} - v_{interp.}$ (cm^3/mole)
molybdates			
Na_2MoO_4	56·9		
K_2MoO_4	76·8		
$Na_2Mo_2O_7$	46·9	43·8	+3·1
$K_2Mo_3O_{10}$	48·2	46·0	+2·2
MoO_3	30·6		
tungstates			
Na_2WO_4	57·3		
$Na_2W_2O_7$	46·9	44·4	+2·5
WO_3	31·6		
chromates			
K_2CrO_4	70·5		
$K_2Cr_2O_7$	53·8	53·0	+0·8
CrO_3	35·4		

hedral to higher coordination gives rise to a relatively high molar volume in the region of "mixed coordination".

Possibility B implies that on the addition of trioxide to alkali monotungstate or monomolybdate, separate tetrahedra are combined into chains of tetrahedra.

In view of our definition of the molar volume v as the volume containing 1 gramatom W or Mo, the addition of trioxide may better be represented by a removal of alkali oxide (M_2O), during which the amount of W or Mo remains constant; e.g.

$$4\,M^+ + 2\,WO_4{}^{2-} - M_2O \rightarrow 2\,M^+ + (WO_3–O–WO_3)^{2-}.$$
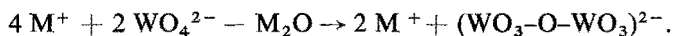
The removal of 1 unit M_2O accompanied by the creation of 1 oxygen bridge between two tetrahedra, will cause a volume decrease $-dv$. If the coordination remains tetrahedral and if $-dv$ is independent of composition, the total decrease of v is directly proportional to the number of units M_2O removed, and as a

consequence to the trioxide content expressed in mole % *). A linear relation between v and mole % trioxide will then be found.

To make it acceptable that $-dv$ is only slightly dependent on the trioxide content, we will again consider suitable crystal structures, viz. those in the K_2CrO_4–CrO_3 system. In sec. 3.3.2 it was observed that in the K_2CrO_4 as well as in the $K_2Cr_2O_7$ structure all Cr atoms are tetrahedrally coordinated by oxygens. The same holds for the structure of CrO_3 in which the tetrahedra form infinite chains [4-19].

The molar volumes of these three compounds, calculated from unit-cell dimensions, are shown in table 4-V. It is seen from this table that the molar volume of crystalline $K_2Cr_2O_7$ hardly differs from the value obtained by linear interpolation between the molar volumes of K_2CrO_4 and CrO_3.

On consideration of the molar-volume isotherms at 950 °C for molten alkali-tungstate and alkali-molybdate systems (figs 4.2 and 4.3) it is seen that *the tungstate melts show a behaviour corresponding to possibility* B, *whereas the behaviour of the molybdate melts complies with possibility* A.

This strongly suggests that in molten molybdates dissociation has not proceeded as far as in molten tungstates. In molybdate melts a structure will probably still be found resembling that of the crystalline molybdates, involving polyhedra of various coordination numbers which form large groups.

From fig. 4.3 it is seen that the extent of the departure from linearity shown by the molar-volume isotherms for the molybdate systems, is dependent on the nature of the alkali ion. This may be attributed to the fact that the alkali ions may influence the position of the dissociation equilibrium.

Navrotsky and Kleppa [4-20] (cf. sec. 1.4) have suggested that alkali-dimolybdate melts might undergo stronger dissociation in the order $K_2Mo_2O_7 \rightarrow$ $\rightarrow Na_2Mo_2O_7 \rightarrow Li_2Mo_2O_7$. The increase of dissociation in this order may counteract the molar-volume-raising effect described above.

Tungstate melts appear to be strongly dissociated and show the behaviour expected for a melt containing exclusively WO_4 tetrahedra, in accordance with the structure proposed by Gelsing et al. (see sec. 1.4). This being the case, the value obtained by extrapolation of v_{950} to pure WO_3 (see fig. 4.2), approxi-

---

*) The equivalency of the expressions "number of units M_2O removed" and "mole % trioxide" can be shown as follows. The number of units M_2O removed is proportional to the fraction of M_2O removed. Let this fraction be x. When the tungstate systems are taken as an example, the composition obtained can be represented by $M_{2(1-x)}WO_{4-x}$. This is equivalent to

$$M_{2(1-x)}W_{(1-x)}O_{4(1-x)} \cdot W_xO_{3x} \text{ or } (1-x) M_2WO_4 \cdot x \, WO_3.$$

The mole percentage of WO_3 is

$$\frac{x}{x + (1-x)} \cdot 100\% = x \cdot 100\%.$$

mately 40 cm³ mole⁻¹, represents the molar volume of WO_3, if it were molten at 950 °C and if the melt consisted of infinite chains of tetrahedra.

Essentially, it is still possible to account for the linear molar-volume isotherms of molten-tungstate systems by a complete dissociation into monotungstate and WO_3, as assumed by Kordes and Nolte for $Na_2W_2O_7$ (cf. sec. 1.4). Both components must then form an ideal mixture in terms of molar volume. In this case the v_{950} value extrapolated to pure WO_3 represents the molar volume of octahedral WO_3, if this were molten at 950 °C.

4.4. Mixed alkali molybdates and tungstates

4.4.1. *Results*

For all compositions measured the relation between density and temperature can again be represented satisfactorily by a linear equation. The results are shown in table 4-VI. In this table the same symbols are used as in the analogous tables 4-I and 4-III.

Isotherms of density, molar volume and thermal-expansion coefficient at 950 °C are shown in figs 4.5 and 4.6. From fig. 4.5 it is seen that the molar-volume isotherms for the systems $Na_2W_2O_7$–$K_2W_2O_7$ and $Na_2Mo_2O_7$–$K_2Mo_2O_7$ appear to be linear, indicating that the mixing of two different alkali species is ideal in terms of molar volume.

The mixing of ditungstate and dimolybdate containing identical alkali species, however, is non-linear, as can be concluded from the molar-volume isotherms of the systems $Na_2W_2O_7$–$Na_2Mo_2O_7$ and $K_2W_2O_7$–$K_2Mo_2O_7$ (see fig. 4.6).

The above observations can be shown objectively by the method applied in sec. 4.3.1, i.e. by calculating the departures Δv_{950} from the least-squares straight lines (see fig. 4.7). For the systems $Na_2W_2O_7$–$K_2W_2O_7$ and $Na_2Mo_2O_7$–$K_2Mo_2O_7$ these departures from linearity do not exceed the experimental accuracy of $\pm 0.5\%$ (± 0.3–0.4 cm³ mole⁻¹ for a molar volume of 60–80 cm³ mole⁻¹). The $Na_2W_2O_7$–$Na_2Mo_2O_7$ and $K_2W_2O_7$–$K_2Mo_2O_7$ systems, however, show larger, though unsystematic departures from linearity. Some are positive, some negative.

The isotherms of the expansion coefficient α show positive departures from linearity for all four systems examined.

4.4.2. *Discussion*

In sec. 2.2.2 it was observed that the mixing of either two different alkali species, or of dimolybdate and ditungstate often has a strong glass-formation-favouring effect. The results of the density measurements on binary alkali-tungstate and -molybdate systems, however, show that a strong variation of glass-formation tendency does not imply a strong variation of density. From

TABLE 4-VI
Density of mixed alkali-tungstate and -molybdate systems

composition (mole % of component II)	a (g cm^{-3})	$b \cdot 10^3$ (g cm^{-3} °C^{-1})	$s(\hat{\varrho})$ (g cm^{-3})	ϱ_{950} (g cm^{-3})	v_{950} (cm^3 mole^{-1})	$\alpha_{950} \cdot 10^3$ (°C^{-1})	temp. range (°C)
system Na$_2$W$_2$O$_7$(I)–K$_2$W$_2$O$_7$(II)							
0	5·701	1·3642	0·007	4·405	59·67	0·3097	846– 998
20	5·720	1·5376	0·005	4·259	62·47	0·3610	787–1012
35	5·607	1·5083	0·005	4·174	64·32	0·3614	735– 990
50	5·512	1·4846	0·003	4·102	66·05	0·3619	680– 979
65	5·456	1·5393	0·003	3·994	68·44	0·3854	716– 977
80	5·424	1·5805	0·004	3·923	70·29	0·4029	758–1017
100	5·299	1·5735	0·005	3·804	73·33	0·4136	783– 985
system Na$_2$Mo$_2$O$_7$(I)–K$_2$Mo$_2$O$_7$(II)							
0	3·475	0·7803	0·010	2·734	63·99	0·2854	765– 985
20	3·536	0·9156	0·005	2·666	66·82	0·3434	760– 953
35	3·425	0·8650	0·003	2·603	69·36	0·3323	700– 982
50	3·379	0·8591	0·005	2·563	71·40	0·3352	708–1004
80	3·241	0·7851	0·020	2·495	75·27	0·3147	691– 991
100	3·175	0·7600	0·011	2·453	77·88	0·3098	675– 996
system Na$_2$W$_2$O$_7$(I)–Na$_2$Mo$_2$O$_7$(II)							
20	5·264	1·3559	0·010	3·976	61·69	0·3410	746– 983
35	5·021	1·3172	0·004	3·770	61·56	0·3494	765– 997
50	4·687	1·2048	0·010	3·542	61·79	0·3401	744–1006
65	3·136	1·1023	0·002	3·269	62·93	0·3372	730– 967
80	3·721	0·7529	0·005	3·006	64·05	0·2505	768– 970
system K$_2$W$_2$O$_7$(I)–K$_2$Mo$_2$O$_7$(II)							
20	4·985	1·5525	0·008	3·510	74·46	0·4423	727– 978
35	4·595	1·3256	0·004	3·336	74·40	0·3974	672– 996
50	4·268	1·2360	0·005	3·094	75·96	0·3995	730–1004
65	3·966	1·1475	0·002	2·876	77·13	0·3990	756– 992
80	3·603	0·9390	0·006	2·711	76·96	0·3464	741– 999

Fig. 4.5. Isotherms of density (ϱ), molar volume (v) and thermal-expansion coefficient (α) at 950 °C for the molten systems

$$Na_2W_2O_7(I)-K_2W_2O_7(II) \qquad (\times)$$
and $\qquad Na_2Mo_2O_7(I)-K_2Mo_2O_7(II) \qquad (O)$

figs 4.5 and 4.6 it is seen that this conclusion also applies to the four "mixed" systems examined.

We will discuss the effects provoked by the mixing of alkali and those provoked by the mixing of tungstate and molybdate separately.

(a) Mixed-alkali systems

From the previous chapters and from the discussion of density values of binary molten alkali-tungstate and -molybdate systems it can be concluded that the structure of these systems is probably not changed essentially by the substitution of one alkali species for another, although such a substitution may certainly influence the degree of dissociation or disproportionation. In a mixed-alkali system the different alkali ions will be distributed throughout the melt, but this distribution is not liable to affect the molar volume to the extent that a distinct departure from linearity is observed. This is supported by the review article by Isard on the mixed-alkali effect in glasses [4-21]. The molar volume appears to be the property which is affected least by a partial substitution of one alkali species for another.

A property which is generally affected to a greater extent is the thermal-expansion coefficient. The value of α normally shows a positive departure

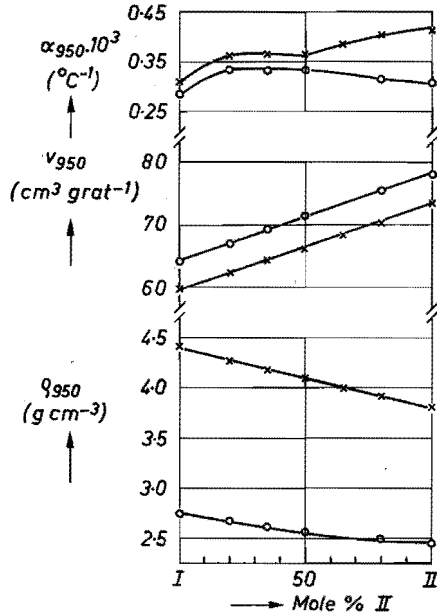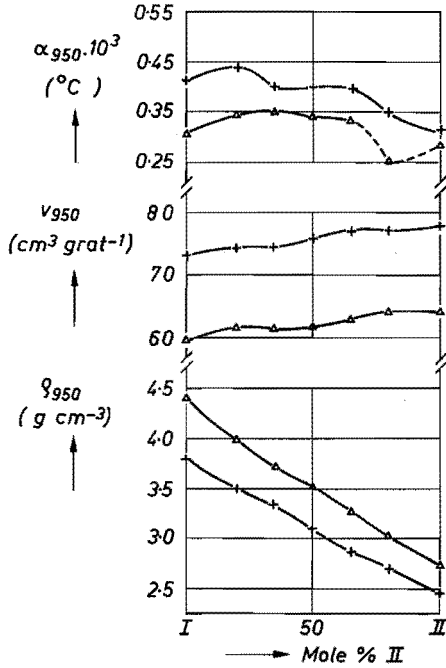Fig. 4.6. Isotherms of density (ϱ), molar volume (v) and thermal-expansion coefficient (α) at 950 °C for the molten systems

$$\mathrm{Na_2W_2O_7(I)-Na_2Mo_2O_7(II)} \qquad (\triangle)$$
and $\qquad\qquad \mathrm{K_2W_2O_7(I)-K_2Mo_2O_7(II)} \qquad (+)$
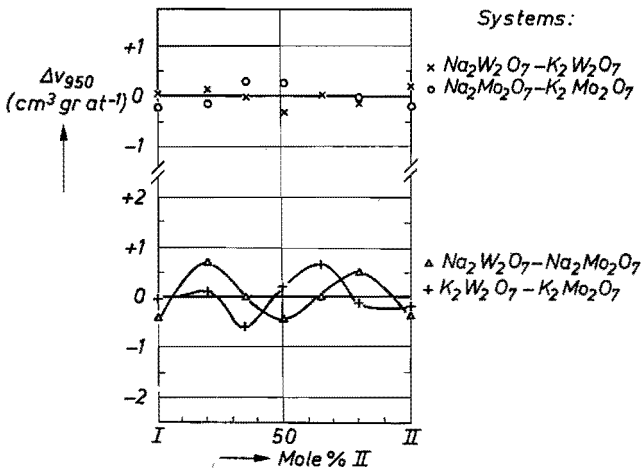
Fig. 4.7. Departure from linearity ($\varDelta v$) of molar-volume isotherms for molten mixed alkali-dimolybdate/alkali-ditungstate systems at 950 °C.

from linearity [4-21]). In figs 4.5 and 4.6 it is seen that this positive departure is indeed found in the systems under consideration.

(b) Mixed ditungstate/dimolybdate systems

If the structure of corresponding ditungstate and dimolybdate melts were similar, the molar-volume isotherms of the mixed systems would probably be linear.

However, if the structures of corresponding ditungstate and dimolybdate melts are essentially different, as was suggested in the previous chapters and in sec. 4.3.2, the mixing may affect the value of the molar volume in many different ways, and a non-linear behaviour is to be expected.

For instance, the smaller tungstate anions may occupy large interstices in the molybdate structure, thus reducing the molar volume. On the other hand, on the addition of dimolybdate to a ditungstate melt, part of the W atoms may assume higher coordinations and form common complex anions with the dimolybdate. This would raise the molar volume. The opposite effect is observed if part of the Mo atoms assumes a strictly tetrahedral coordination. Further, one effect may dominate in one composition region, while another effect may dominate in another composition region.

It appears to be impossible to discuss the results of these effects in terms of molar volume. Nevertheless, a non-linear behaviour of the molar-volume isotherms in mixed ditungstate/dimolybdate systems appears to be connected with differences between the structures of the components, rather than with similarities between these structures.

REFERENCES

[4-1] E. F. Riebling, J. Am. ceram. Soc. **51**, 143-149, 1968.

[4-2] F. M. Jaeger, Z. anorg. allgem. Chem. **101**, 1-214, 1917.

[4-3] F. M. Jaeger and B. Kapma, Z. anorg. allgem. Chem. **113**, 27-58, 1920.

[4-4] V. Spitzin and A. Tscherepneff, Z. anorg. allgem. Chem. **198**, 276-286, 1931.

[4-5] A. Kvist and A. Lundén, Z. Naturforsch. **20a**, 102-104, 1965.

[4-6] K. B. Morris, M. I. Cook, C. Z. Sykes and M. B. Templeman, J. Am. chem. Soc. **77**, 851-854, 1955.

[4-7] K. B. Morris and P. L. Robinson, J. phys. Chem. **68**, 1195-1205, 1964.

[4-8] K. B. Morris and P. L. Robinson, J. chem. eng. Data **9**, 444-445, 1964.

[4-9] J. C. Th. G. M. van der Wielen, H. N. Stein and J. M. Stevels, J. non-cryst. Solids **1**, 18-28, 1968.

[4-10] J. C. Th. G. M. van der Wielen, unpublished results. H. N. Stein, personal communication.

[4-11] J. D. Mackenzie, Rev. sci. Instr. **27**, 297-299, 1956.

[4-12] H. Esser and H. Eusterbrock, Arch. Eisenhüttenw. **14**, 341-355, 1941.

[4-13] L. Shartsis and S. Spinner, J. Res. nat. Bur. Stand. **46**, 176-194, 1951.

[4-14] E. F. Riebling, Rev. sci. Instr. **34**, 568-572, 1963.

[4-15] W. Volk, Applied statistics for engineers, McGraw-Hill, New York, 1958, p. 237.

[4-16] I. Lindqvist, Acta chem. Scand. **4**, 1066-1074, 1950.

[4-17] B. M. Gatehouse and P. Leverett, J. chem. Soc. (A) 1398-1405, 1968.

[4-18] B. M. Gatehouse and P. Leverett, J. chem. Soc. (A) 849-854, 1969.

[4-19] R. W. G. Wyckoff, Crystal structures, Interscience Publishers, New York, 2nd ed., 1964/1965, Vols. 2 and 3.

[4-20] A. Navrotsky and O. J. Kleppa, Inorg. Chem. **6**, 2119-2121, 1967.

[4-21] J. O. Isard, J. non-cryst. Solids **1**, 235-261, 1969.

5. SURFACE TENSION OF MOLTEN ALKALI TUNGSTATES AND MOLYBDATES *)

5.1. Introduction

Whilst the density of a melt is related to the arrangement of atoms and complexes, the surface tension may give useful information on the strength of the interparticle bonds in the surface layer of the melt. The surface tension being a property related to a certain unit surface area, its value is not only determined by the strength of the interparticle bonds but also by the number of particles per unit area, and therefore by the dimensions of the particles.

The restriction should be made that the surface tension is a property of a very thin layer, the composition of which may differ considerably from that inside the melt. For instance, in a binary system of components which neither form complexes on mixing nor undergo constitutional changes, the component which in the pure state has the lower surface tension, will be preferentially adsorbed in the surface layer. Likewise, when complex ions of various types are present in the liquid, those having the highest surface activity will accumulate in the surface layer. As will be seen in sec. 5.3.2, the occurrence or absence of adsorption may be used as evidence for the presence or absence of surface-active complex ions in the liquid.

Surface-tension values of molten alkali tungstates and molybdates have been reported only by Jaeger [5-1]), who determined the surface tensions of molten Na_2WO_4, Na_2MoO_4, K_2WO_4 and K_2MoO_4, using the maximum-bubble-pressure method.

In the present chapter the determination will be described of the surface tensions of molten Li-, Na- and K-tungstate and -molybdate systems as well as the surface tensions of four molten mixed alkali-tungstate/molybdate systems, the density measurements of which were described in chapter 4.

5.2. Experimental method

Alkali-tungstate and -molybdate samples were prepared from alkali carbonates, WO_3 and MoO_3, by the method described in sec. 2.1.2.

Surface tensions were measured by the ring method, involving determination of the pull necessary to detach a platinum ring from the surface of the melt.

The melt was held in a platinum dish (diameter 8·5 cm, height 3·5 cm), which was placed in an electric furnace.

The maximum pull was measured by means of a torsion balance, which

allowed continuous variation of the pull exerted on the ring. The apparatus is shown in fig. 5.1. Surface tensions were calculated by the equation

$$\sigma = \frac{M\,g}{4\,\pi\,R}\,F,$$

where σ is the surface tension (dyne cm^{-1}), M the pull at the moment of detachment (g) (pull measured with the torsion balance, reduced by the weights of ring and suspension wire), g the acceleration of gravity (cm s^{-2}), R the radius of the ring (cm), and F a dimensionless factor.

Essentially, the ring method is an absolute method, as was shown by Freud and Zollman Freud [5-2]). We derived the values for the correction factor F, however, from the experimentally determined tables of Harkins and Jordan [5-3]). In these tables the value of F can easily be found when the values of R/r and R^3/V are known (r = radius of the wire from which the ring was made; V = volume of the liquid raised above the free liquid surface = M/ϱ, where ϱ = density of the liquid). For ϱ Van der Wielen's and our own data were used, in some cases after interpolation (see chapter 4).

The dimensions of the ring at 0 °C were:
— ring used for binary tungstates and for mixed systems: $2\,R_0 = 1\cdot29$ cm, $2\,r_0 = 0\cdot0308$ cm;
— ring used for binary molybdates: $2\,R_0 = 1\cdot43$ cm, $2\,r_0 = 0\cdot0358$ cm.
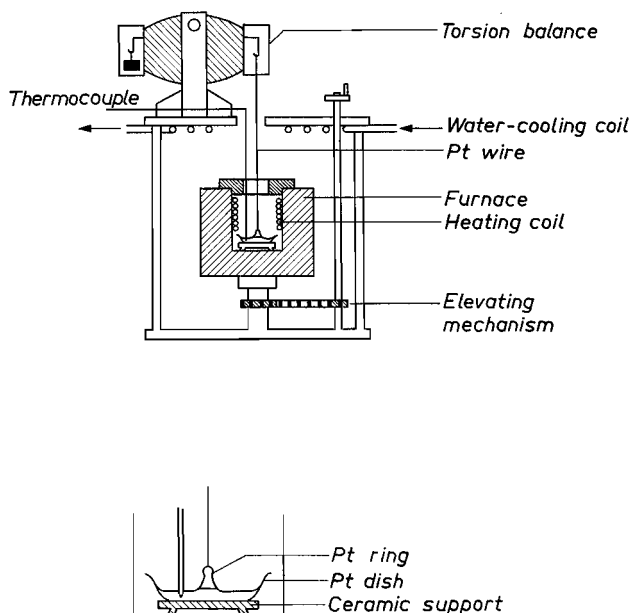
Fig. 5.1. Apparatus for the determination of melt surface tensions.

The values of R and r were corrected for thermal expansion by the formula of Esser and Eusterbrock [5-4]) for the linear expansion of Pt:

$$l_t = l_0 (1 + 898 \cdot 77 \cdot 10^{-4} t + 0 \cdot 10652 \cdot 10^{-8} t^2 + 0 \cdot 1256 \cdot 10^{-12} t^3).$$

Temperatures were measured in the melt by means of a calibrated thermocouple (Pt/5%Rh–Pt/20%Rh).

By far the most important error may be introduced when the plane of the ring is not horizontal [5-3]). According to Harkins and Jordan a deviation of 1° from horizontal position reduces the value of σ by 0·45%, and a deviation of 2·1° reduces σ by 1·57%.

As the angle between horizontal and plane of the ring could not be determined, the shape and correct position of the ring were verified between measurements on two successive samples by determining the surface tensions of pure water and benzene at ambient temperature. When the departure from literature values [5-5]) remained within ± 0·5%, we assumed that the plane of the ring was sufficiently horizontal.

As a further verification of the accuracy of the method the surface tension of an NaCl melt was determined (850–1050 °C). The maximum departure from literature values [5-1,6]) observed was +0·5%.

Temperature ranges throughout were at least 150 °C, while for each sample at least 5 different temperatures were chosen.

5.3. Binary alkali tungstates and molybdates

5.3.1. *Results*

For all compositions measured the relation between surface tension and temperature can be represented satisfactorily by the linear equation

$$\sigma = p - q\, t,$$

where σ is the surface tension (dyne cm^{-1}), p and q are constants (> 0), $q = d\sigma/dt$, and t is the temperature (°C).

The values of p and q for each composition measured, calculated by the method of least squares, as well as the standard deviations of estimate of the least-squares lines ($s(\hat{\sigma})$) are included in tables 5-I and 5-II. These tables also contain the values of the surface tension at 950 °C (σ_{950}), and the molar free surface energy at 950 °C (Σ_{950}), as well as the temperature ranges for which the equations are valid. A comparison of our results for the sodium and potassium monomolybdates and monotungstates with those obtained by Jaeger [5-1]), is shown in table 5-III. Our results are considerably lower than Jaeger's values. This is in accordance with the conclusion of Janz et al.[5-6]) that most of Jaeger's surface-tension values are 2–8 % (and even more) higher than those obtained by more recent determinations.

TABLE 5-I

Surface-tension values of alkali tungstates. For an explanation of the symbols used, see text

mole % WO_3	p (dyne cm^{-1})	$q \cdot 10^3$ (dyne cm^{-1} °C^{-1})	$s(\hat{\sigma})$ (dyne cm^{-1})	σ_{950} (dyne cm^{-1})	$\Sigma_{950} \cdot 10^{-3}$ (erg (grat W)$^{-2/3}$)	temp. range (°C)
lithium tungstates						
0	264·42	55·67	0·33	211·5	3·39	800–1010
30	263·46	76·42	0·67	190·9	2·81	728–1004
50	263·54	91·04	0·12	177·1	2·45	827– 960
sodium tungstates						
0	244·94	66·03	0·25	182·2	3·41	769–1002
20	260·75	93·12	0·57	172·3	2·99	766–1001
30	274·07	115·35	0·59	164·5	2·75	803– 978
40	250·06	94·66	0·54	160·1	2·55	815– 953
45	249·74	98·80	0·47	155·9	2·42	822–1004
60	232·75	87·73	0·23	149·4	2·18	858–1010
potassium tungstates						
0	197·28	59·43	0·27	140·8	3·10	966–1067
20	208·66	79·71	0·18	132·9	2·69	849–1015
35	210·66	88·02	0·28	127·0	2·38	759– 972
45	215·76	95·32	0·28	125·2	2·24	782–1004
55	206·72	89·31	0·19	121·9	2·05	740– 966

TABLE 5-II

Surface-tension values of alkali molybdates. For an explanation of the symbols used, see text

mole % MoO_3	p (dyne cm^{-1})	$q \cdot 10^3$ (dyne cm^{-1} °C^{-1})	$s(\widehat{\sigma})$ (dyne cm^{-1})	σ_{950} (dyne cm^{-1})	$\Sigma_{950} \cdot 10^{-3}$ (erg (grat Mo)$^{-2/3}$)	temp. range (°C)
lithium molybdates						
0	260·28	57·87	0·32	205·3	3·33	830–1035
20	218·87	53·42	0·06	168·1	2·61	746– 992
40	201·40	58·76	0·45	145·6	2·16	698–1030
60	186·04	64·88	0·64	124·4	1·76	648– 995
70	164·97	58·48	0·24	109·4	1·53	801– 971
sodium molybdates						
0	241·54	66·59	0·55	178·3	3·33	828–1021
20	218·13	68·27	0·67	153·3	2·71	709– 970
40	201·34	69·51	0·32	135·3	2·25	658– 969
60	194·64	82·02	0·62	116·7	1·82	672– 965
60	185·02	73·82	1·04	114·9	1·79	721– 964
70	169·42	67·28	0·92	105·5	1·58	756– 983
80	154·55	65·89	0·53	92·0	1·30	756–1009
potassium molybdates						
0	199·83	64·26	0·13	138·8	3·05	963–1100
19	174·30	56·54	0·27	120·6	2·48	900–1110
39	174·15	68·90	0·40	108·7	2·09	900–1106
50	164·31	65·55	0·27	102·0	1·86	800– 981
58	164·69	69·83	0·39	98·4	1·74	818–1113
75	155·23	66·64	0·32	91·9	—	854–1088

TABLE 5-III

Comparison of the surface-tension values at 950 °C (in dyne cm^{-1}) of mono-molybdates and monotungstates obtained by Jaeger [5-1]) with those in the present work

	present work	Jaeger [5-1])	departure (%) from Jaeger's values
Na_2MoO_4	178·3	191·0	− 6·6
K_2MoO_4	138·8	149·4	− 7·1
Na_2WO_4	182·2	187·2	− 2·7
K_2WO_4	140·8	157·2	−10·4

Figures 5.2 and 5.3 show the isotherms of the surface tension and molar free surface energy at 950 °C, as well as the relations between $-d\sigma/dt$ and
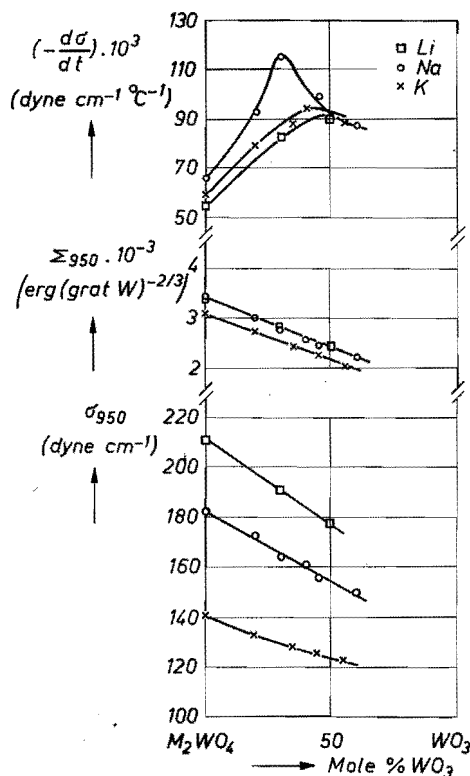
Fig. 5.2. Isotherms of surface tension (σ) and molar free surface energy (Σ) at 950 °C, as well as the relations between negative temperature coefficient of surface tension ($-d\sigma/dt$) and composition for molten alkali tungstates.
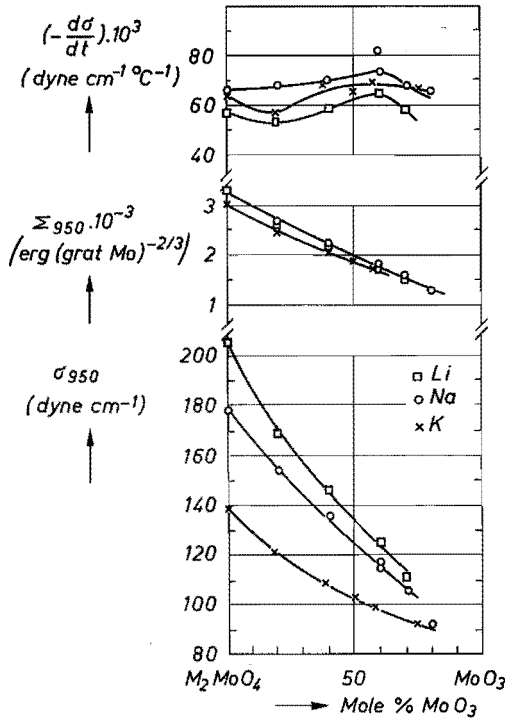
Fig. 5.3. Isotherms of surface tension (σ) and molar free surface energy (Σ) at 950 °C, as well as the relations between negative temperature coefficient of surface tension ($-d\sigma/dt$) and composition for molten alkali molybdates.

composition. As was the case for the density isotherms (cf. sec. 4.3.1), the aspect of the surface-tension isotherms is not essentially changed by selecting a temperature 100 or 200 °C lower; however, the composition range covered is then considerably reduced.

The surface-tension isotherms are smooth curves. The surface tensions of the monomolybdates are approximately equal to those of the corresponding mono-tungstates. As the trioxide content is increased, the surface tension is reduced, more rapidly in the case of the molybdate systems than in that of the corresponding tungstate systems.

The above-mentioned molar free surface energy is defined as

$$\Sigma = \sigma \, v^{2/3},$$

where v is the molar volume, and Σ represents the free surface energy of one side of a cube with volume v. Taking our definition of v into account (cf. sec. 4.3.1) this means that such a cube will always contain 1 gramatom W or Mo.

Figure 5.2 shows that the relation between Σ_{950} and the trioxide content is a linear one in the case of the tungstate systems.

For the molybdate systems (see fig. 5.3) this relation is non-linear. (It should be noted that the accuracy estimated for Σ is $\pm 1\cdot3\%$.) Moreover, it is surprising that, whereas both surface tension and molar volume strongly depend on the alkali species present, this dependence is practically absent in the case of the molar free surface energy.

The value of $-d\sigma/dt$ for the molybdate systems hardly depends on the composition, whereas for the tungstate systems $-d\sigma/dt$ shows a maximum. For both groups of systems $-d\sigma/dt$ increases at constant trioxide content in the direction $Li \rightarrow K \rightarrow Na$.

5.3.2. Discussion

In the preceding section it was observed that the surface-tension values of a monotungstate and its corresponding monomolybdate (e.g. Li_2WO_4 and Li_2MoO_4) are approximately equal. The same applies to the values of the molar free surface energy. However, when trioxide is added the values of σ and Σ show a stronger decrease for the molybdate melts than for the tungstate melts.

Especially in the case of surface tensions, a pronounced difference is seen. As comparison on a molar basis, however, appears to be more correct, we will restrict ourselves to the discussion of the Σ isotherms.

The decrease of Σ occurring on the addition of trioxide can be explained by the fact that the sizes of the complex ions increase while their valencies remain constant. Taking the tungstate systems as an example and comparing the monotungstate and ditungstate compositions, in the former case WO_4^{2-} units are found, and in the latter case $W_2O_7^{2-}$ units (irrespective of whether these units are part of larger groups or are separate ions). It is apparent that in the monotungstate structure the electrostatic attraction between alkali ions and complex ions will be stronger than in the ditungstate structure.

The structures of a molten monotungstate and its corresponding monomolybdate are identical; these structures contain both alkali ions and isolated tetrahedra (WO_4^{2-} and MoO_4^{2-} respectively). From the fact that the Σ values of a monotungstate and its corresponding monomolybdate are equal, it is seen that substitution of a molybdate polyhedron for a tungstate polyhedron, and vice versa, does not in itself influence the value of Σ.

Therefore, the differences occurring between the Σ values of corresponding tungstate and molybdate melts at higher trioxide content, are probably caused by differences between the structures of the surface layers, i.e. the presence of different types of complex ions in the surface layers.

In chapter 4 the structures of molten alkali tungstates and molybdates were assumed to be situated between two extreme possibilities, viz.

A. a structure corresponding with that of the crystalline compounds; the addition of trioxide to a monotungstate or monomolybdate gives rise to the

formation of large groups containing polyhedra with coordination numbers higher than 4;

B. a structure containing exclusively WO_4 or MoO_4 tetrahedra which form averagely short chains.

The question to be answered is: What is the effect of possibilities A and B on the value of Σ?

To answer this question the analogous case of the surface tension of certain molten metasilicates containing bivalent cations (Mn^{2+}, Mg^{2+}, Ca^{2+}) [5-7]) will be considered. In metasilicates the SiO_4 tetrahedra share two corners with adjacent tetrahedra. The silicate anion, therefore, either is of the infinite-chain type, or it forms rings.

Contrary to most other liquids the surface tension of these silicates *increases* when the temperature is raised. This abnormal behaviour is attributed by King [5-7]) to a breakdown mechanism by which at high temperatures larger ions break down to a large number of smaller ions.

According to this conception a large number of smaller ions gives rise to a higher surface-tension value than a small number of larger ions. *Thus, the small groups existing in the case of possibility B will cause a higher value of Σ than the large groups existing in the case of possibility* A. As the addition of trioxide reduces Σ in the molybdate systems to a higher extent than in the tungstate systems, it may be expected that the structure of the surface layer of a molybdate melt is closer to A, involving the occurrence of more large groups, than is the structure of the surface layer of the corresponding tungstate melt. This is in accordance with the conclusions derived from the density measurements (cf. sec. 4.3.2).

The fact that the surface layer of a molybdate melt contains a relatively high proportion of large groups does not necessarily mean that inside the melt small groups are absent. When large and small groups are simultaneously present in the melt, an adsorption mechanism will give rise to a comparatively high concentration of large groups in the surface layer.

The fact that the surface layer of a tungstate melt contains a relatively low proportion of large groups, however, does imply that inside the melt likewise relatively few large groups are found.

In the previous chapters the question whether $Na_2W_2O_7$ dissociates on melting either into Na^+, WO_4^{2-} and WO_3^0 (as assumed by Kordes and Nolte, cf. sec. 1.4) or into a mixture of short chains of WO_4 tetrahedra (as assumed by Gelsing et al.[5-8])) could not be answered definitely. It seems likely, however, that these two types of dissociation would have quite different effects on the value of Σ. If both bivalent tetrahedra and neutral trioxide particles were present in the melt, the latter would undoubtedly accumulate in the surface layer, thus reducing the value of Σ. In this case a linear relation between Σ and composition (as found for the tungstate systems, cf. fig. 5.2) would be

highly improbable. If, on the contrary, the melt contained exclusively short chains of tetrahedra, an adsorption mechanism would only slightly affect the value of Σ, and a linear relationship between Σ and composition would certainly be possible.

In sec. 5.3.1 it was seen that the value of $-d\sigma/dt$ in tungstate systems attains a maximum, which in the molybdate systems is absent (cf. figs 5.2 and 5.3). The structure of the tungstate melt, outlined above, can be used to give a tentative explanation for this phenomenon.

When WO_3 is added to molten monotungstate, chains of WO_4 tetrahedra are formed according to the reaction

$$WO_4{}^{2-} + WO_3 \rightarrow W_2O_7{}^{2-}.$$

Gelsing et al.[5−8] (cf. sec. 1.4) assumed the chain length, e.g. at the composition $M_2W_2O_7$, to be non-uniform, since disproportionation reactions may occur of the type

$$2\,W_2O_7{}^{2-} \rightleftarrows WO_4{}^{2-} + W_3O_{10}{}^{2-}.$$
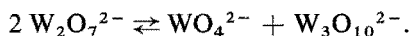
On the basis of thermodynamic considerations it was thought likely that the degree of disproportionation increases with temperature, i.e. that at high temperatures a relatively high proportion of longer chains occurs [5−8].

In the surface layer the concentration of longer chains will be relatively high, giving rise to a lower Σ value. When at high temperatures the proportion of longer chains increases, the Σ value will show an additional decrease, superimposed on the decrease brought about by thermal expansion, and, therefore, $-d\sigma/dt$ will show an additional increase.

In molybdate melts an analogous effect is absent, as in these melts even at lower temperatures larger groups will be present in the surface layer.

5.4. Mixed alkali tungstates and molybdates

For all compositions measured the relation between surface tension and temperature can again be represented satisfactorily by a linear equation. The results are represented in table 5-V. In this table the symbols used are the same as those in the analogous tables 5-I and 5-II.

Isotherms of surface tension and molar free surface energy at 950 °C as well as the relations between $-d\sigma/dt$ and composition are shown in figs 5.4 and 5.5.

From fig. 5.4 it is seen that the σ and Σ isotherms for the system $Na_2W_2O_7$–$K_2W_2O_7$ are non-linear and suggest the occurrence of an adsorption mechanism. Possible explanations for these phenomena appear to be the following:
(a) In the surface layer a relatively high concentration of K^+ ions and consequently a relatively low concentration of Na^+ ions is found.

TABLE 5-V

Surface-tension values of mixed alkali-ditungstate/alkali-dimolybdate systems. For an explanation of the symbols used, see text; * = interpolated value

composition (mole % II)	p (dyne cm^{-1})	$q \cdot 10^3$ (dyne cm^{-1} °C^{-1})	$s(\hat{\sigma})$ (dyne cm^{-1})	σ_{950} (dyne cm^{-1})	$\Sigma_{950} \cdot 10^{-3}$ (erg grat$^{-2/3}$)	temp. range (°C)
system $Na_2W_2O_7(I)-K_2W_2O_7(II)$						
0	—	92·0 *	—	154·4*	2·36*	—
20	229·15	91·52	0·52	142·2	2·23	734– 970
50	224·16	98·01	0·49	131·1	2·14	712–1011
80	205·42	84·99	0·70	124·7	2·12	708–1004
100	—	92·0 *	—	123·0*	2·16	—
system $Na_2Mo_2O_7(I)-K_2Mo_2O_7(II)$						
0	—	72·0 *	—	122·5*	1·96*	—
20	183·39	68·65	0·24	118·2	1·95	729–1032
50	176·70	69·65	0·44	110·5	1·90	786–1012
80	167·91	66·19	0·34	105·0	1·87	765–1020
100	164·31	65·55	0·27	102·0	1·86	800– 981
system $Na_2W_2O_7(I)-Na_2Mo_2O_7(II)$						
0	—	92·0 *	—	154·4*	2·36*	—
20	226·65	85·75	0·79	145·2	2·27	724–1015
35	220·30	83·90	0·21	140·6	2·19	753–1026
50	208·18	77·05	0·22	135·0	2·11	773– 962
65	203·88	75·74	0·63	131·9	2·09	752– 987
80	200·56	75·95	0·55	128·4	2·06	738–1027
100	—	72·0 *	—	122·5*	1·96*	—
system $K_2W_2O_7(I)-K_2Mo_2O_7(II)$						
0	—	92·0 *	—	123·0*	2·16*	—
20	199·83	88·11	0·50	116·1	2·06	732– 953
50	186·67	80·60	0·71	110·1	1·98	662–1021
65	175·97	72·13	0·53	107·4	1·95	776–1059
80	170·94	67·56	0·54	106·8	1·93	740–1018
80	177·38	76·75	0·98	104·5	1·89	770–1000
100	164·31	65·55	0·27	102·0	1·86	800– 981
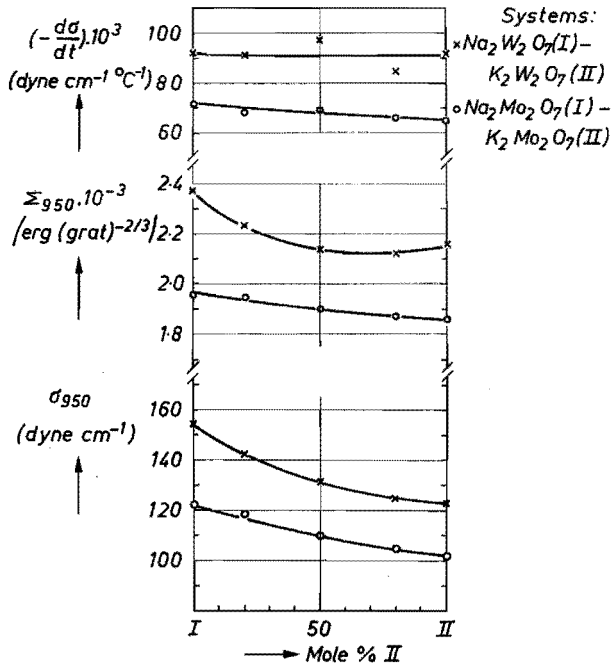
Fig. 5.4. Isotherms of surface tension (σ) and molar free surface energy (Σ) at 950 °C, as well as the relations between negative temperature coefficient of surface tension ($-d\sigma/dt$) and composition for the molten systems

$$Na_2W_2O_7(I)-K_2W_2O_7(II) \qquad (\times)$$
and $$Na_2Mo_7O_2(I)-K_2Mo_2O_7(II) \qquad (O)$$

(b) Molten $K_2W_2O_7$ contains a higher proportion of large anionic groups than molten $Na_2W_2O_7$. These groups accumulate in the surface layer.

For the mixed-alkali system $Na_2Mo_2O_7-K_2Mo_2O_7$ (fig. 5.4) the values of surface tension and molar free surface energy of the two components show only small differences. Therefore, the drawing of conclusions from the isotherms is difficult.

For the mixed ditungstate/dimolybdate systems $Na_2W_2O_7-Na_2Mo_2O_7$ and $K_2W_2O_7-K_2Mo_2O_7$ (fig. 5.5) both surface-tension and molar-free-surface-energy isotherms show negative departures from linearity. These departures are to be expected, as the larger molybdate groups will accumulate in the surface layer.

The results, however, do not allow any further conclusions regarding the structures of the melts involved.
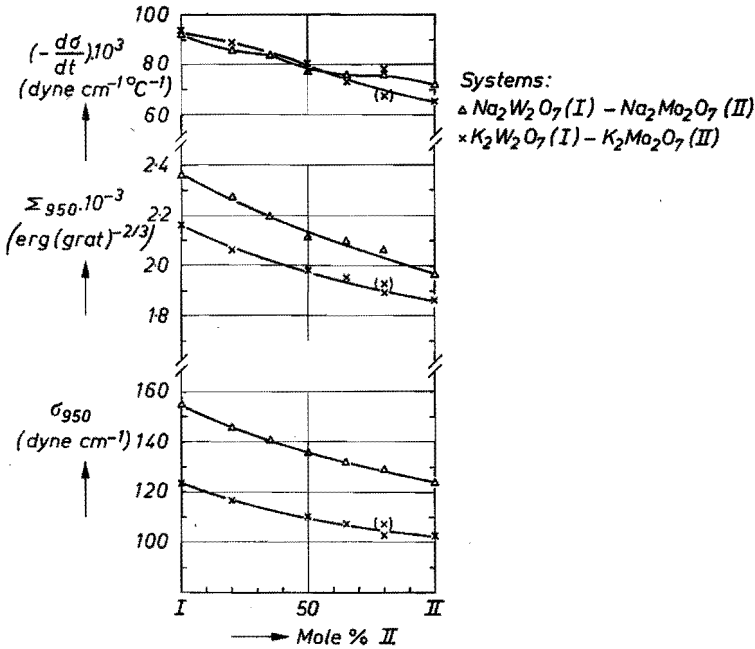
Fig. 5.5. Isotherms of surface tension (σ) and molar free surface energy (Σ) at 950 °C, as well as the relations between negative temperature coefficient of surface tension ($-d\sigma/dt$) and composition for the molten systems

$$Na_2W_2O_7(I)-Na_2Mo_2O_7(II) \qquad (\triangle)$$

and $\qquad K_2W_2O_7(I)-K_2Mo_2O_7(II) \qquad (\times)$

REFERENCES

5-1) F. M. Jaeger, Z. anorg. allgem. Chem. **101**, 1-214, 1917.

5-2) B. B. Freud and H. Zollman Freud, J. Am. chem. Soc. **52**, 1772-1782, 1930.

5-3) W. D. Harkins and H. F. Jordan, J. Am. chem. Soc. **52**, 1751-1771, 1930.

5-4) H. Esser and H. Eusterbrock, Arch. Eisenhüttenw. **14**, 341-355, 1941.

5-5) International critical tables, Vol. IV, pp. 447, 454.

5-6) G. Janz et al., Molten salts, Vol. 2, Section 2, Surface tension data, NBS, Washington, 1969, p. 73.

5-7) T. B. King, J. Soc. Glass Technol. **35**, 241-259, 1951.

5-8) R. J. H. Gelsing, H. N. Stein and J. M. Stevels, Phys. Chem. Glasses **7**, 185-190, 1966.

6. VISCOSITY OF MOLTEN ALKALI TUNGSTATES AND MOLYBDATES

6.1. Introduction

The value of viscosity is related to the strength of the interparticle bonds and the dimensions of the flow units in the liquid. As required by electrical neutrality viscous flow involves the migration of both anions and cations. According to Frenkel [6-1]) this migration is limited by the ions with smaller mobility. In molten alkali tungstates and molybdates these ions will be the relatively large anions. In many cases it is useful to compare the values of viscosity with those of electrical conductivity, as the latter property also involves the migration of ions. However, electrical conductance only requires the transport of electrically charged particles of one sign, viz. those for which the activation energy of migration has the smallest value. These are usually the cations.

No viscosity values of alkali tungstates and molybdates have been reported in the literature. The only indication has been given by Van der Wielen et al.[6-2]), this stating that alkali-molybdate melts have viscosities of the order of 1 cP, which lies below the range of the falling-sphere method.

More attention has been paid to electrical-conductivity measurements of molten tungstates and molybdates. Jaeger and Kapma [6-3]) determined the electrical conductivities of Na_2WO_4 and Na_2MoO_4. Spitzin and Tscherepneff[6-4]) reported the electrical conductivities of several compositions in the system Na_2WO_4–WO_3. Morris et al.[6-5]) measured the electrical conductivity in the system Na_2MoO_4–MoO_3, while Morris and Robinson [6-6,7]) worked on the systems Li_2MoO_4–MoO_3 and K_2MoO_4–MoO_3 as well as the Li-, Na- and K-tungstate systems. Finally, Kvist and Lundén [6-8]) reported the electrical conductivity of Li_2MoO_4, at the same time criticizing the accuracy of Morris and Robinson's measurements on this compound.

In the present chapter viscosity measurements will be described of the binary tungstate and molybdate systems, the density and surface-tension values of which have been reported in chapters 4 and 5 respectively. Furthermore, a comparison will be made of the viscosity values obtained and the electrical-conductivity values evaluated from the literature data mentioned above.

In addition to this, the viscosity values of the systems $Na_2W_2O_7$–$Na_2Mo_2O_7$ and $Na_2W_2O_7$–$K_2W_2O_7$ will be reported.

6.2. Experimental method

Alkali-tungstate and -molybdate samples were prepared from alkali carbonates, WO_3 and MoO_3 by the method described in sec. 2.1.2. The method used for the determination of viscosity values was that of the oscillating hollow cylinder. The melt is contained in a cylindrical crucible, which is suspended by

a torsion wire. When the crucible is oscillating, the logarithmic decrement of the oscillations is a measure of the viscosity of the melt.

The apparatus used was almost identical to that of Janz and Saegusa [6–9,10], the most important difference being that the adjustable inertia pieces were omitted in order to enlarge the viscosity range (see fig. 6.1).
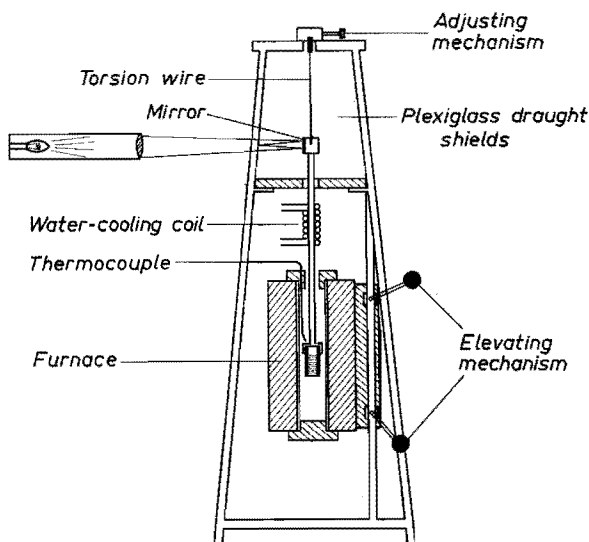
Fig. 6.1. Apparatus for the determination of melt viscosities.

The crucible containing the melt consisted of an 80% Au–20% Pd alloy, the height being 6 cm and the diameter 2·5 cm. It was inserted in a closely fitting inconel cradle. In the course of the experiments three different crucibles and three corresponding cradles were used. The cradle was rigidly connected to a nickel rod, which was suspended by a tungsten torsion wire (diameter 0·4 mm).

The crucible was suspended in a long electric furnace. A cooling coil served to prevent the torsion wire from getting hot.

The oscillating part of the apparatus was protected against air currents by plexiglass shields.

Amplitudes of oscillation were determined visually. Light from a lamp situated 1 m from a mirror cemented to the oscillating part of the apparatus, passed through a hole in one of the plexiglass shields and was reflected by the mirror. Amplitudes were read on a non-transparent scale fixed on the same plexiglass shield at a distance of 15·35 cm from the mirror.

The maximum distance D between the centre of the hole and the spot on the scale for each individual oscillation was observed visually, and the torsion angle α was calculated by

$$\alpha = \arctan (D/15{\cdot}35) \quad (D \text{ in cm}).$$

The logarithmic decrement δ followed from

$$\delta = \frac{1}{n} \ln \frac{\alpha_0}{\alpha_n},$$

where n is the number of oscillations measured.

The decrement δ only increases with viscosity up to a certain value. When the viscosity is still further increased, δ drops and the liquid behaves itself more and more as a rigid body [6-11,12]. In order to get an impression of the position of the viscosity of maximum decrement, the relation between viscosity and decrement was determined for a number of water–glycerol mixtures at 22·5 °C. Viscosity values for these mixtures were derived from Landolt–Börnstein's tables [6-13]. For the system water–glycerol the maximum decrement was found at a viscosity of about 150 cP (see fig. 6.2). From the work of Reeves and Janz [6-12] it is seen that the viscosity of maximum decrement is directly proportional to the density of the liquid, provided that the oscillation time, diameter of the cylinder and height of the liquid remain constant. Therefore, for densities of the order of magnitude of those of the molten tungstates and molybdates (see chapter 4) the maximum decrement is attained at even higher values than 150 cP. This means that no ambiguity arises in the measurements of the viscosities of molten tungstates and molybdates.

Equations for calculating viscosity values from logarithmic decrements have been proposed by several authors [6-11]. These equations can be divided into empirically and mathematically derived equations.

To the first group belongs the formula of Yao [6-12], which was also used by Janz and Saegusa [6-9]:

$$(\delta - \delta_0) \frac{\varrho_t}{\varrho_{t_m}} = K \sqrt{(\eta \, \varrho_t \, \tau)},$$

where δ_0 is the logarithmic decrement of the empty system, ϱ_t the density of
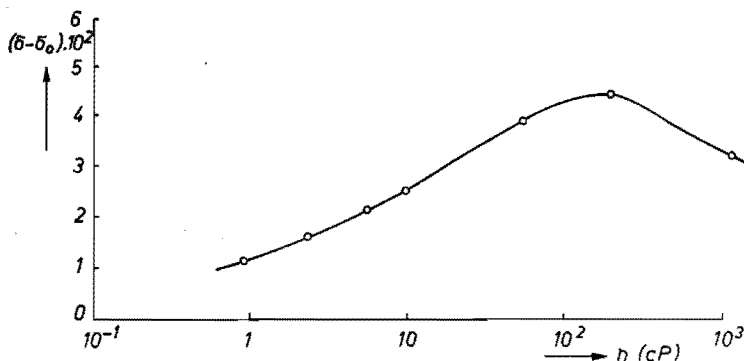
Fig. 6.2. Relationship between viscosity (η) and logarithmic decrement ($\delta - \delta_0$) for water–glycerol mixtures.

the liquid at temperature t, ϱ_{t_m} the density of the liquid at melting temperature t_m, K an apparatus constant, and τ the oscillation time.

Hopkins and Toye's formula [6-14] was based on a mathematical analysis of the motion of the system:

$$(\delta - \delta_0)\left(\frac{\tau^2}{\tau_0{}^2} + 1\right) = A \eta \tau + B \sqrt{(\eta \varrho \tau)} + C \sqrt{\frac{(\eta \tau)^3}{\varrho}},$$

where τ_0 is the oscillation time of the empty system, and A, B and C are apparatus constants.

Reeves and Janz's objection [6-11] to this formula is that the apparatus "constants" A, B and C are actually functions of the diameter of the crucible and the height of the liquid, both of which may vary appreciably with temperature. Reeves and Janz propose

$$I(\delta - \delta_0)\left(\frac{\tau^2}{\tau_0{}^2} + 1\right) = 2 \pi^{3/2} a^3 (c + 0{\cdot}2246\, a) \sqrt{(\eta \varrho \tau)} +$$

$$- \pi a^2 (3 c + 1{\cdot}844\, a) \eta \tau + \frac{3 \sqrt{\pi}}{8} a c \sqrt{\frac{(\eta \tau)^3}{\varrho}},$$

where a is the radius of the cylinder, c the height of the liquid, and I the moment of inertia of the oscillating part of the system.
They point out that Yao's empirical equation is only valid for liquids of viscosities of less than about 1 cP.

In our case the logarithmic decrement δ and the oscillation time τ_0 of the empty system were about $0{\cdot}6 \cdot 10^{-2}$ and 2·5 s respectively; both values remained unchanged when the temperature in the furnace was raised to 900 °C, but showed some variation with the crucible and corresponding cradle used. Application of Reeves and Janz's equation to the systems and samples used demonstrated that the third term of the right-hand side of the equation was less than 0·1 % of the second term, this again being about 10 % of the first. Therefore, the third term could be neglected. The resulting equation is a quadratic expression in $\sqrt{\eta}$.

To calculate viscosity values, the moment of inertia I must be known. Although the equation permits an absolute determination of viscosity, I was evaluated from measurements of the logarithmic decrements of liquids of known viscosity. The liquids used were water (distilled $2\times$), toluene (Merck p.a.) and chloroform (Merck p.a.) at ambient temperatures, and KNO_3 (Merck p.a.) and $LiNO_3$ at elevated temperatures (the latter compound was obtained by adding Li_2CO_3 to HNO_3 (1 : 1), after which the water and excess of HNO_3 were evaporated; m.p. 255 °C). Viscosity and density values used, were derived from International Critical Tables, Janz and Saegusa [6-9], and Murgulescu and Zuca [6-15]. The resulting values for the moment of inertia I varied with

the three Au–Pd crucibles and corresponding inconel cradles used, being 498, 524 and 547 g cm² respectively. Temperatures were measured by a calibrated (Pt–5%Rh/Pt–20%Rh) thermocouple placed directly above the crucible.

6.3. Binary alkali tungstates and molybdates; a comparison with electrical-conductivity data

6.3.1. *Results*

In tables 6-I and 6-II the viscosity values of the alkali-tungstate and -molybdate samples measured are given. These tables also contain the values for the activation energies E_η, calculated by the Arrhenius equation

$$\eta = A \exp \frac{E_\eta}{RT},$$

where A is a pre-exponential factor, R the gas constant, and T the temperature (K).

Figures 6.3 and 6.4 show the relations between $\log \eta$ and $1/T$ for tungstates and molybdates. For most compositions examined the Arrhenius equation proves to be obeyed satisfactorily. In cases where considerable departures from linear relationship are observed, these departures should be attributed to experimental errors rather than to properties of the melt. In the latter case a systematic behaviour of the departures would appear likely, which is in fact absent.

Figures 6.5 and 6.6 give viscosity isotherms for the six systems examined. Consideration of the results summarised in these figures leads to the following conclusions:

(a) The value of the viscosity is dependent on the alkali species present. For both tungstate and molybdate systems the viscosity increases in the direction K → Na → Li.

(b) Viscosity values of tungstate systems are higher than those of the corresponding molybdate systems.

(c) On first addition of WO_3 to a monotungstate melt the viscosity value remains constant. However, the addition of more than 30 mole% WO_3 raises the viscosity; the increase observed is stronger in the order K → Na → Li.

(d) On the addition of MoO_3 to a monomolybdate melt the value of the viscosity is somewhat decreased. At very high MoO_3 contents the opposite effect is observed.

(e) The conclusion of Van der Wielen et al.[6-2] that the viscosity of molybdate melts is of the order of 1 cP is confirmed by our experiments. The viscosities of the tungstate melts, though higher, are of the same order of magnitude, being surprisingly low for glass-forming systems.

TABLE 6-I

Viscosity values of alkali tungstates

mole% WO_3	act. en. E_η (kcal mole^{-1})	temp. (°C)	viscosity (cP)
system Li_2WO_4–WO_3			
0	12·0	843	8·13
		891	6·42
		942	5·27
15	10·5	725	13·25
		783	9·42
		824	7·49
		880	6·63
30	11·5	752	13·52
		787	10·15
		849	8·11
		894	6·51
		948	5·39
		982	4·56
40	14·7	800	14·48
		846	11·71
		888	8·80
		929	7·39
		958	5·91
50	14·4	915	10·22
		944	8·67
		982	7·25
		1024	6·11
system Na_2WO_4–WO_3			
0	9·2	772	6·80
		808	5·71
		850	5·13
		890	4·44
		940	3·64
		985	3·20

TABLE 6-I (continued)

mole% WO_3	act. en. E_η (kcal mole^{-1})	temp. (°C)	viscosity (cP)
20	7·9	728	7·90
		760	6·43
		805	5·34
		846	4·66
		898	4·32
		944	3·81
30	10·4	773	7·12
		810	5·69
		857	4·77
		904	3·92
		946	3·50
45	11·8	764	10·74
		824	8·56
		861	6·16
		920	5·05
		969	4·34
60	13·8	795	11·87
		839	9·23
		856	8·21
		894	7·40
		948	5·23
		988	4·39
system K_2WO_4–WO_3			
0	8·6	962	2·57
		982	2·43
20	7·9	830	3·02
		872	2·74
		952	2·13
		992	1·93
35	10·9	727	8·03
		773	6·38
		812	4·93
		854	4·03
		910	3·56

mole % WO_3	act. en E_n (kcal mole^{-1})	temp. (°C)	viscosity (cP)
45	12·0	656	15·83
		700	10·77
		741	8·04
		810	5·92
		868	4·46
		917	3·66
55	12·3	762	9·07
		808	6·77
		870	4·85
		930	3·98
65	7·8	902	5·63
		937	5·09
		965	4·76

The viscosity values in the regions of easiest glass formation (cf. sec. 1.2) are in the case of the molybdates lower than those of the non-glass-forming mono-compounds. In the tungstate systems the regions of maximum glass-formation tendency do not show relatively high viscosities. Furthermore, the system of lowest glass-formation tendency, Li_2WO_4–WO_3 (cf. sec. 1.2) has the highest viscosity values of the systems examined. *In short, no correlation between high viscosity and easy glass formation appears to exist in the systems under consideration.*

Figures 6.7 and 6.8 show the relations between the activation energy of viscous flow E_n and composition for the same six systems. Again, marked similarities and dissimilarities are observed between tungstate and molybdate systems.

(a) Although the differences are only small, E_n for both tungstate and molybdate systems increases in the order K → Na → Li.

(b) E_n in tungstate systems is higher than E_n in the corresponding molybdate systems.

(c) In the tungstate systems the first addition of trioxide to a monotungstate melt produces a slight decrease of E_n. On further addition of WO_3, E_n is increased beyond the value of the monotungstate.

(d) In the molybdate systems the addition of trioxide to a monomolybdate melt gives a gradual increase of E_n.

From literature data [6–3.8]) isotherms for the specific conductivity $\varkappa$ and relations between the activation energy of specific conductivity $E_\varkappa$ and composition were calculated. In calculating, difficulties arose from the fact that reliable

TABLE 6-II

Viscosity values of alkali molybdates

mole % MoO_3	act. en. E_η (kcal mole^{-1})	temp. (°C)	viscosity (cP)
system Li_2MoO_4–MoO_3			
0	7·0	723	7·48
		804	6·01
		846	5·23
		886	4·70
		936	3·98
20	7·9	758	5·45
		880	3·46
		937	3·11
40	9·6	662	7·80
		742	4·96
		792	4·79
		848	3·53
		911	2·46
60	9·1	674	7·52
		761	4·71
		852	3·51
		934	2·62
70	10·2	686	7·77
		745	5·38
		802	4·33
		856	3·44
system Na_2MoO_4–MoO_3			
0	6·8	756	4·95
		786	4·40
		832	3·76
		882	3·29
		926	3·13
20	8·3	674	5·90
		709	4·80
		764	3·70
		816	3·08
		903	2·51

mole% MoO_3	act. en. E_η (kcal mole^{-1})	temp. (°C)	viscosity (cP)
40	7·0	645	4·99
		722	3·54
		782	2·76
		854	2·15
		913	2·01
		959	1·93
60	6·3	730	3·39
		790	2·54
		845	2·24
		903	2·01
		949	1·90
80	9·6	652	7·90
		754	4·44
		830	3·30
		895	2·62
		943	2·23

system K_2MoO_4–MoO_3

mole% MoO_3	act. en. E_η (kcal mole^{-1})	temp. (°C)	viscosity (cP)
0	5·1	938	2·36
		958	2·38
		983	2·25
		1014	2·10
19	6·5	861	2·41
		907	2·15
		956	1·93
39	6·8	650	4·18
		718	3·22
		800	2·58
		902	1·84
		940	1·74
58	8·2	640	4·96
		726	3·05
		808	2·22
		894	1·80
		939	1·60

TABLE 6-II (continued)

mole% MoO_3	act. en E_η (kcal mole^{-1})	temp. (°C)	viscosity (cP)
70	8·9	650	5·55
		731	3·74
		832	2·50
		928	1·82

isotherms could not be obtained for all systems, this because the temperature ranges valid for the various compositions measured do not always overlap sufficiently. Further, large departures were observed between the results obtained by different authors. For the molten system $Na_2WO_4–WO_3$ the electrical-conductivity values of Spitzin and Tscherepneff [6-4]) are considerably higher than those of Morris and Robinson [6-7]) in the regions of high WO_3 contents. In this case Morris and Robinson's data were used, as these better correspond to the results found for the systems $Li_2WO_4–WO_3$ and $K_2WO_4–WO_3$. In the case of Li_2MoO_4, however, Morris and Robinson report improbably high
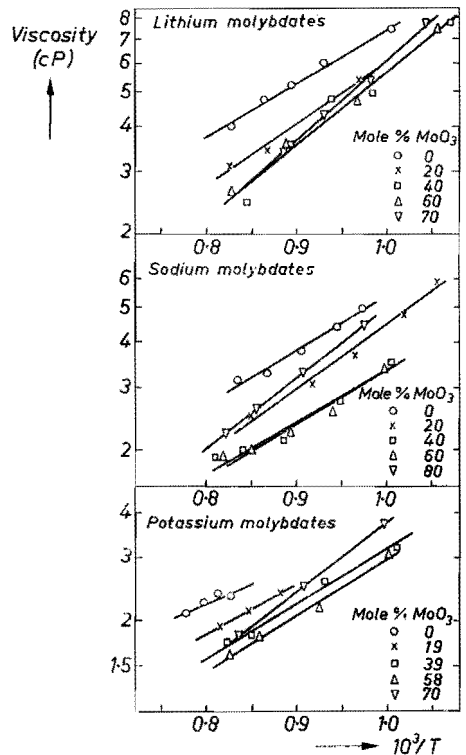
Fig. 6.3. Viscosities of molten alkali tungstates (systems $M_2WO_4–WO_3$).
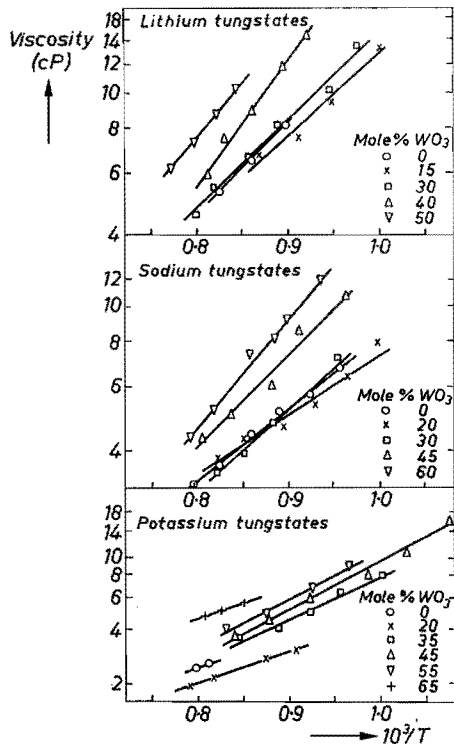
Fig. 6.4. Viscosities of molten alkali molybdates (systems M_2MoO_4–MoO_3).

conductivity values compared with the rest of the system Li_2MoO_4–MoO_3. Here we have used the results of Kvist and Lundén [6-8]).

Specific-conductivity isotherms and E_x-composition relationships are summarized in figs 6.9–6.12.

In figs 6.9 and 6.10 large departures from the isotherms drawn are observed in some cases. In our opinion there is no reason to attribute these departures to compound formation in the melt, as was suggested by Morris and Robinson [6-6]). It is likely that they merely illustrate the inaccuracy of the measurements.

Electrical conductivity in alkali-tungstate and -molybdate systems shows in part a behaviour similar to that of viscosity. In fig. 6.9 it is seen that the electrical conductivity decreases when the trioxide content is raised. Figure 6.10, however, shows that in the case of the molybdate systems this is not so pronounced, with the exception of the system Li_2MoO_4–MoO_3.

Figure 6.11 shows that the activation energy for specific conductivity E_x in the tungstate systems increases with increasing trioxide content. In the corresponding molybdate systems (see fig. 6.12) this increase is only small.

It should, however, be noted that electrical transport shows the reversed dependence on alkali species as viscous transport: electrical transport is easier
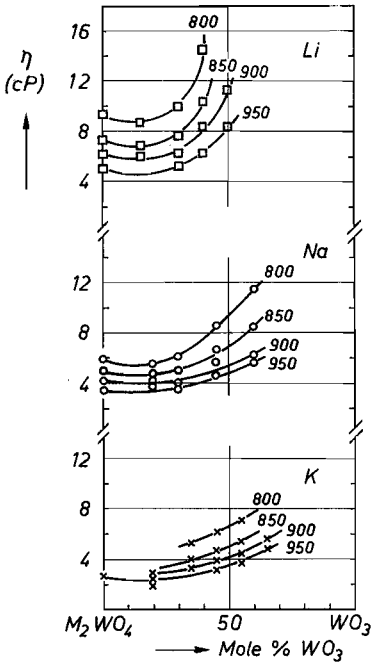
Fig. 6.5. Viscosity isotherms of alkali tungstates.
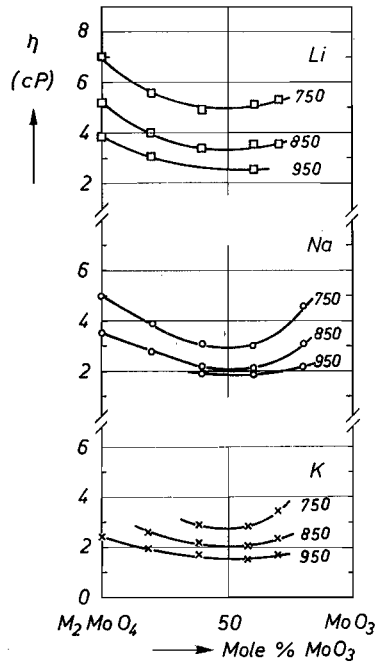
Fig. 6.6. Viscosity isotherms of alkali molybdates.
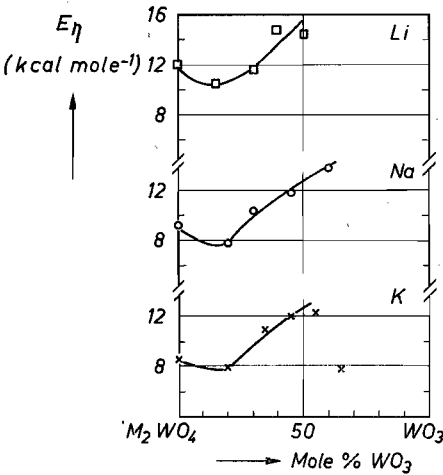
Fig. 6.7. Activation energies for viscous flow (E_η) of alkali tungstates.
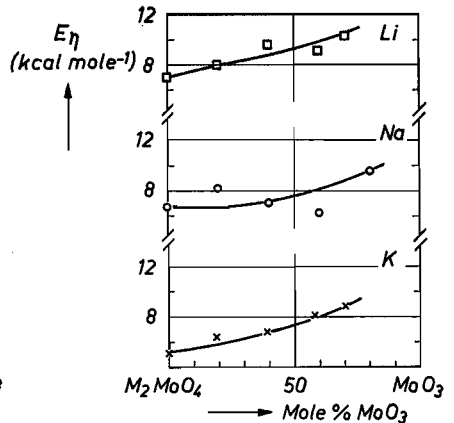
Fig. 6.8. Activation energies for viscous flow (E_η) of alkali molybdates.
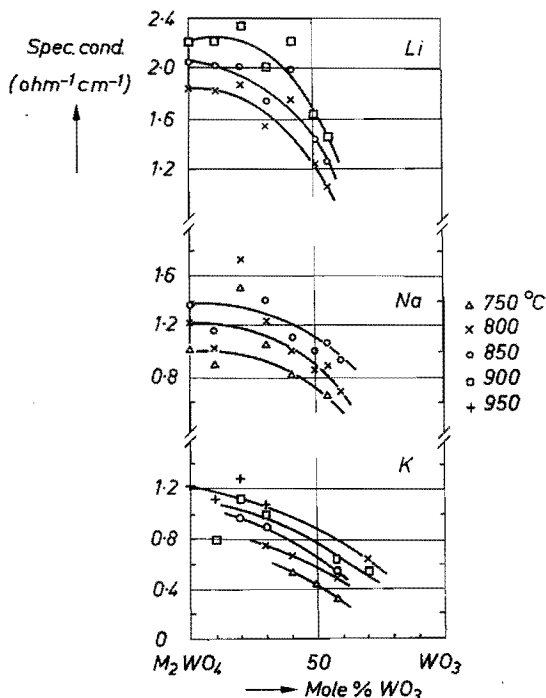
Fig. 6.9. Electrical-conductivity isotherms of alkali tungstates (calculated from ref. 6–7).

(specific conductivity increases) in the order $K \rightarrow Na \rightarrow Li$, whereas viscous transport is easier (viscosity decreases) in the order $Li \rightarrow Na \rightarrow K$.

6.3.2. Discussion

In the preceding section it was seen that all viscosity values determined, though showing some variation with composition, are of the order of 1–15 cP. Viscosity values having the same order of magnitude have been reported for molten alkali chlorides, nitrates, carbonates, and other liquids for which the presence of relatively small groups is assumed [6–16]. Similar values were also found for molten $K_2Cr_2O_7$, which — as we have seen — contains anionic groups consisting of two tetrahedra.

These low viscosity values indicate that the units involved in viscous flow cannot be large, proving the occurrence of dissociation in both alkali-tungstate and -molybdate melts. If the infinite-chain-type anions, present in the crystal structures of $Na_2W_2O_7$, $Na_2Mo_2O_7$ and $K_2Mo_3O_{10}$ (cf. sec. 1.4) continued to exist in the molten state, no doubt considerably higher viscosities would have been measured.

Not only in the case of molten tungstates, but also in that of molten molybdates, which in the glass-formation regions even show lower viscosity values than the corresponding tungstates, small groups must be present. This was
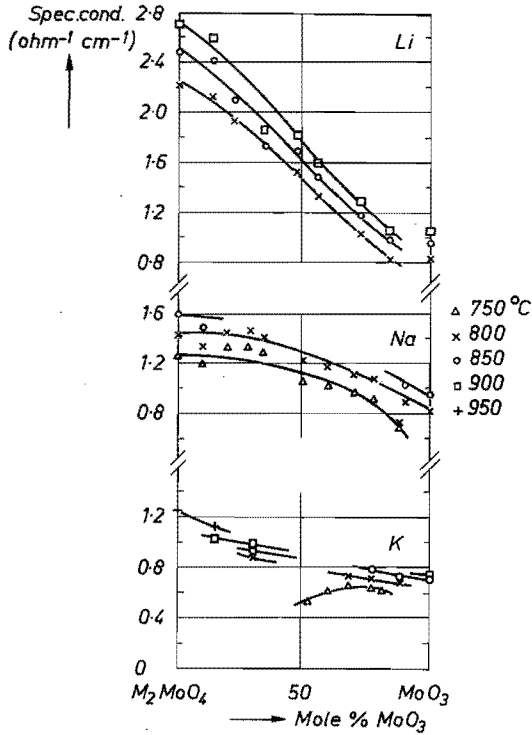
Fig. 6.10. Electrical-conductivity isotherms of alkali molybdates (calculated from lit. 6–5, 6–6 and 6–8).
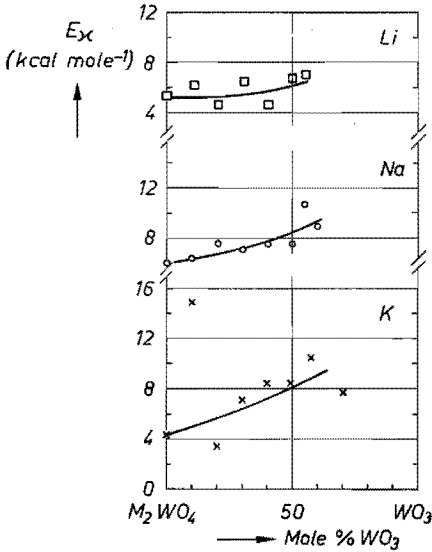
Fig. 6.11. Activation energies for specific conductivity (E_x) of alkali tungstates (calculated from lit. 6–7).
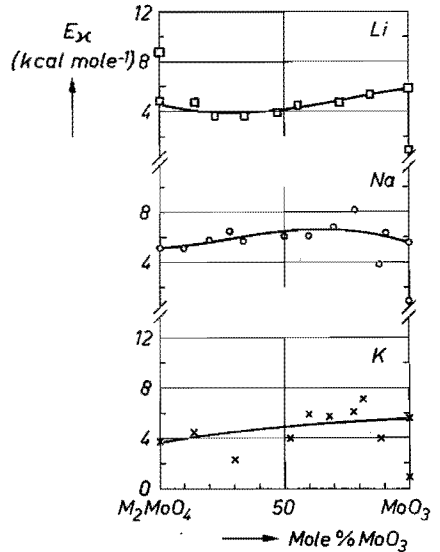
Fig. 6.12. Activation energies for specific conductivity (E_x) of alkali molybdates (calculated from lit. 6–5, 6–6 and 6–8).

already assumed in the discussion of undercooling phenomena (see sec. 2.3.2).

The fact that, although in both cases viscous transport depends on the migration of relatively small anionic groups, the viscosities of molten molybdates are lower than those of molten tungstates may perhaps be attributed to higher deformability of the molybdate polyhedra. This higher deformability was already assumed by Van der Wielen et al.[6-2]) in discussing glass formation in alkali-molybdate systems. The low viscosity values of molten alkali molybdates in the glass regions do not appear to contradict our previous assumption of the simultaneous presence of larger groups comprising polyhedra with coordination numbers higher than 4. For viscous flow it appears to be sufficient that alkali ions together with anionic groups for which the activation energy of migration is smallest take part in the transport mechanism.

In the preceding section it was observed that electrical conductivity increases in the order $K \rightarrow Na \rightarrow Li$. In this order the radius of the alkali ion decreases and as a consequence its field strength is raised. A small radius as such gives rise to a higher electrical conductivity, whereas it also involves a higher field strength, giving rise to stronger cation–anion attractions. The fact that electrical conductivity is increased by the presence of small cations indicates that the effect favouring electrical transport (smaller radius) dominates the effect hampering it (higher field strength).

In chapter 1 (sec 1.5) the theories of Turnbull [6-17]) and Sarjeant and Roy [6-18]) were mentioned, which, on the basis of theoretical considerations of nucleation and crystal growth, try to predict glass formation.

Turnbull distinguishes between low- and high-viscosity liquids. The former have a viscosity of the order of 1 cP above the liquidus. Crystallisation can only be prevented in this type of liquid when nucleation is suppressed completely. This is in accordance with the phenomena observed during cooling of tungstate and molybdate melts: once a nucleus has been formed, crystal growth occurs almost instantaneously (cf. sec. 2.3.2).

In a simplified form [6-19]) the equation governing the nucleation frequency I (number of nuclei per cm^3 and per s) is

$$I = n \, \nu \exp \frac{-N \, W^*}{R \, T} \exp \frac{-\Delta G'}{R \, T} \, ,$$

where n is the number of atoms per cm^3, ν the vibrational frequency of the atoms at the nucleus–liquid interface, N Avogadro's number, R the gas constant and T the temperature (K).

Exp $(-N W^*/RT)$ gives the probability at temperature T of a nucleus larger than the critical size being formed; W^* is called by Turnbull and Cohen [6-20]) the "thermodynamic barrier to nucleation". Exp $(-\Delta G'/RT)$ governs the rate at which the structure of the material can be changed during the formation

of a nucleus. This may require a diffusion process and/or some kind of reorientation. $\Delta G'$, according to Turnbull and Cohen the "kinetic barrier to nucleation", is the activation energy associated with this rearrangement process.

To ensure that no temperature exists at which I reaches the value of 1 cm^{-3} s^{-1}, then, according to the views of Turnbull and Cohen, the condition must be fulfilled that $\Delta G' \geqslant 40\ R\ T_m$ (T_m = melting temperature). For e.g. $Na_2W_2O_7$, which has a melting temperature of approximately 1000 K (see sec. 1.3), $\Delta G'$ must have a value higher than 80 kcal mole^{-1}.

An estimate of $\Delta G'$ can only be made when the mechanism of nucleation is considered in more detail. Turnbull and Cohen discern two types of nucleation, viz. (a) nonreconstructive and (b) reconstructive nucleation.

(a) Non-reconstructive nucleation occurs when the structural units in the nucleus to be formed are identical to those in the liquid. It does not require the breaking of strong interatomic bonds. The value of $\Delta G'$ is likely to be of the same order as the activation energy for viscous flow E_η. In the case of molten tungstates and molybdates the values of E_η are considerably lower than 40 $R\ T_m$. If a non-reconstructive rearrangement process occurred during nucleation, according to the theory of Turnbull and Cohen no glass formation would be found. The fact that glass formation is found, therefore, suggests that the process of nucleation is reconstructive.

(b) Reconstructive nucleation requires the breaking of strong interatomic bonds. It occurs when the liquid has a random-network structure, or when the liquid contains structural units which differ from those in the nucleus to be formed. In this case the value of $\Delta G'$ (and for network liquids likewise the value of E_η) is likely to be of the order of bond strength of the strong interatomic bonds (for the systems under consideration these are the W–O and Mo–O bonds). When the structures of tungstate and molybdate melts, outlined in the previous chapters and the present section, are correct, the process nucleation will undoubtedly be reconstructive. When relatively small of groups, or a mixture of small and larger groups form a nucleus containing infinite-chain-type anions in which part of the polyhedra have undergone a coordinational change, the breaking of W–O and Mo–O bonds is inevitable. The bond strengths of the W–O and Mo–O bonds are 103 and 92 kcal mole^{-1} respectively [6-21], higher than 40 $R\ T_m$, which explains the glass formation found.

The value of this result, however, is doubtful, as Turnbull and Cohen's theory presupposes the occurrence of homogeneous nucleation. In fact, it is highly improbable that the liquid will be free of extraneous nuclei.

As has been observed in sec. 1.2 the value of the critical cooling rate forms a quantitative measure of the glass-formation tendency of a melt. From the point of view of glass theory it would be an ideal situation if an expression could be found by which the value of the critical cooling rate could be cal-

culated from a number of quantitative properties of the melt. Such an expression has been proposed by Sarjeant and Roy [6-18]:

$$Q = 2 \cdot 0 . 10^{-6} T_m{}^2 R/v \, \eta,$$

where Q is the critical cooling rate, T_m the melting temperature (K), R the gas constant, v the molar volume at T_m, and η the viscosity at T_m.

As can be seen, this equation is too simple, as it relates the critical cooling rate only to melting temperature and viscosity. It may be valid only for liquids in which the mechanisms of viscous flow and crystallisation are similar, i.e. both reconstructive or both non-reconstructive, so that the activation energies of rearrangement and of viscous flow are of the same order of magnitude.

Further, Sarjeant and Roy's expression cannot explain the strong dependence on composition in complex systems (cf. chapter 1 for alkali-tungstate and -molybdate systems, and Havermans et al.[6-22]) for alkali-silicate systems). As an illustration of the inaccuracy of the equation, we will take the critical cooling rate of $Na_2W_2O_7$ as an example.

For $Na_2W_2O_7$ the approximate values of T_m, v and η are 1000 K, 60 cm^3 $mole^{-1}$ and 20 cP $= 0 \cdot 2$ g cm^{-1} s^{-1} respectively. From these data it follows that the theoretical critical-cooling-rate value is $1 \cdot 4 . 10^7$ °C s^{-1}, whereas the experimental value, measured by Gelsing et al., is lower than 10^2 °C s^{-1} (see sec. 1.2).

6.4. Mixed alkali tungstates and molybdates

The results of the viscosity measurements on the systems $Na_2W_2O_7$–$K_2W_2O_7$ and $Na_2W_2O_7$–$Na_2Mo_2O_7$ are summarised in table 6-III and fig. 6.13. As can
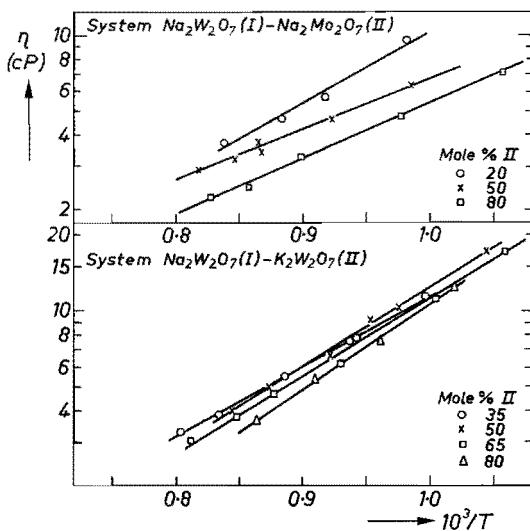
Fig. 6.13. Viscosities of mixed alkali-ditungstate/alkali-dimolybdate systems.

TABLE 6-III

Viscosity values of mixed alkali-tungstate/alkali-molybdate systems

mole % II	activation energy E_η (kcal mole^{-1})	temperature (°C)	viscosity (cP)
system $Na_2W_2O_7(I)$–$K_2W_2O_7(II)$			
35	12·8	731	11·34
		794	7·61
		790	7·66
		856	5·44
		927	3·82
		972	3·30
50	14·4	685	17·11
		752	10·22
		775	9·19
		814	6·61
		872	5·00
		912	4·01
65	13·9	672	17·34
		724	11·04
		804	6·16
		868	4·65
		908	3·77
		960	3·06
80	15·2	708	12·36
		768	7·48
		827	5·36
		885	3·69
system $Na_2W_2O_7(I)$–$Na_2Mo_2O_7(II)$			
20	13·1	746	9·44
		818	5·64
		860	4·66
		920	3·67
50	9·2	741	6·32
		809	4·65
		879	3·44
		883	3·79

mole% II	activation energy E_η (kcal mole^{-1})	temperature (°C)	viscosity (cP)
		908	3·22
		950	2·93
80	10·3	676	7·10
		751	4·74
		840	3·25
		894	2·47
		936	2·24

be seen from fig. 6.13, in which the viscosity axis is logarithmic, the viscosity values of all compositions examined obey satisfactorily the Arrhenius equation. Viscosity isotherms and relations between the activation energy for viscous flow and composition are given in fig. 6.14. For both systems investigated the viscosity isotherms show negative departures from linearity. In the case of the mixed-alkali system $Na_2W_2O_7$–$K_2W_2O_7$ this complies with the behaviour of mixed-alkali glasses [6-23]). It is pointed out by Isard [6-23]) that up till now no
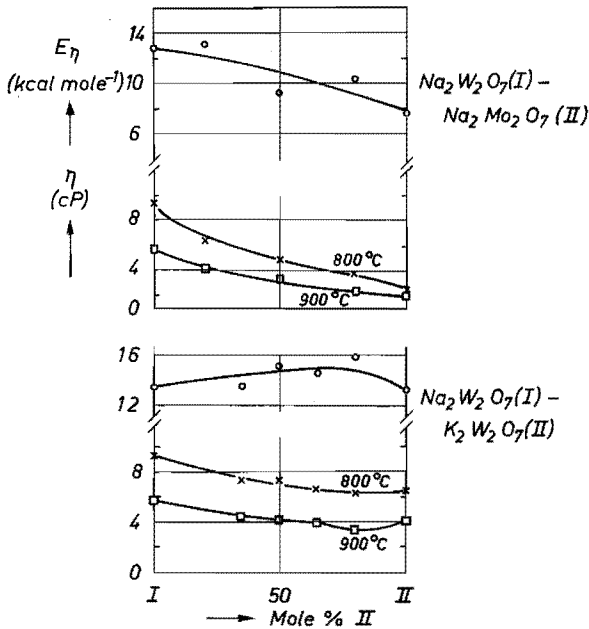
Fig. 6.14. Viscosity isotherms and activation energies for viscous flow of mixed alkali-ditungstate/alkali-dimolybdate systems.

satisfactory explanation has been given for the minimum observed in the viscosity/composition relationship for mixed-alkali systems. From the viscosity data it is clear that the considerable increase of glass formation found in NaK tungstates and Na molybdotungstates (see sec. 2.2) cannot be attributed to an increase of viscosity.

REFERENCES

[6-1] J. Frenkel, Kinetic theory of liquids, Dover Publications, New York, 1956, p. 440.

[6-2] J. C. Th. G. M. van der Wielen, H. N. Stein and J. M. Stevels, J. non-cryst. Solids 1, 18-28, 1968.

[6-3] F. M. Jaeger and B. Kapma, Z. anorg. allgem. Chem. 113, 27-58, 1920.

[6-4] V. Spitzin and A. Tscherepneff, Z. anorg. allgem. Chem. 198, 276-286, 1931.

[6-5] K. B. Morris, M. I. Cook, C. Z. Sykes and M. B. Templeman, J. Am. chem. Soc. 77, 851-854, 1955.

[6-6] K. B. Morris and P. L. Robinson, J. phys. Chem. 68, 1194-1205, 1964.

[6-7] K. B. Morris and P. L. Robinson, J. chem. eng. Data 9, 444-445, 1964.

[6-8] A. Kvist and A. Lundén, Z. Naturforsch. 20a, 102-104, 1965.

[6-9] G. J. Janz and F. Saegusa, J. electrochem. Soc. 110, 452-456, 1963.

[6-10] R. D. Reeves and G. J. Janz, Rev. sci. Instr. 36, 1124-1129, 1965.

[6-11] R. D. Reeves and G. J. Janz, Trans. Faraday Soc. 61, 2300-2304, 1965.

[6-12] T. P. Yao, Giesserei Techn. wissensch. Beihefte, Heft 16, 837-851, 1956.

[6-13] Landolt-Börnstein, Zahlenwerte und Funktionen, 6th ed., Band IV, Vol. 1, Springer, Berlin, 1955, p. 600.

[6-14] M. R. Hopkins and T. C. Toye, Proc. phys. Soc. B 63, 773-782, 1950.

[6-15] I. G. Murgulescu and S. Zuca, Electrochim. Acta 11, 1383-1389, 1966.

[6-16] G. J. Janz et al., Molten salts, Vol. 1, Electrical conductance, density and viscosity data, NBS, Washington, 1968.

[6-17] D. Turnbull, Contemp. Phys. 10, 473-488, 1969.

[6-18] P. T. Sarjeant and R. Roy, Mat. Res. Bull. 3, 265-280, 1968.

[6-19] H. Rawson, Inorganic glass-forming systems, Academic Press, London, 1967, p. 32.

[6-20] D. Turnbull and M. H. Cohen, J. chem. Phys. 29, 1049-1054, 1958.

[6-21] H. Rawson, Trav. du IVe congr. internat. du verre (Paris 1956), Imprimerie Chaix, Paris, 1957, pp. 62-69.

[6-22] A. C. J. Havermans, H. N. Stein and J. M. Stevels, J. non-cryst. Solids 5, 66-69, 1970.

[6-23] J. O. Isard, J. non-cryst. Solids 1, 235-261, 1969.

7. CONCLUSIONS AND REMARKS

7.1. The structures of vitreous and molten alkali tungstates and molybdates

In chapter 1 it was observed that the structure of a glass is seldom understood when the investigation is restricted to one method of approach. Therefore, in the preceding chapters an attempt was made to study the structure of alkali-molybdate and -tungstate glasses from a number of different angles, viz. from literature data, crystallisation phenomena, infrared spectroscopy, and the determination of densities, surface tensions and viscosities of the melts. It is the purpose of the present section to come to a synthesis of the results obtained. This synthesis will be summarised in three "main" conclusions, which the results enable us to draw. After each conclusion the evidence supporting it will be briefly discussed.

(a) *The large anionic groups in crystalline alkali tungstates and molybdates occurring in the regions of glass formation, dissociate on melting into a large number of smaller groups.*

The crystalline compounds in the region of glass formation of which the structures have been determined, contain anionic groups of the infinite-chain type (cf. the structures $Na_2W_2O_7$, $Na_2Mo_2O_7$, $K_2Mo_3O_{10}$, $Rb_2Mo_3O_{10}$ and $Cs_2Mo_3O_{10}$, which have been discussed in sec. 1.3). Evidence for the fact that these large groups are not maintained in the molten and vitreous state can be derived from the following:

— Kordes and Nolte [7-1]) (see sec. 1.4) concluded from cryometric studies that $Na_2W_2O_7$ undergoes complete dissociation into Na^+ and WO_4^{2-} ions, and WO_3^0 particles. However, in our opinion, any dissociation scheme involving the presence of considerable amounts of WO_4^{2-} ions can account for the experimental data. Such a scheme may be a dissociation according to the ideas of Gelsing et al.[7-2]) comprising a mixture of averagely short chains of WO_4 tetrahedra subject to disproportionation by reactions of the type

$$2 W_2O_7^{2-} \rightleftarrows WO_4^{2-} + W_3O_{10}^{2-}.$$

On the basis of mixing-enthalpy determinations Navrotsky and Kleppa [7-3]) (see sec. 1.4) assume alkali dimolybdates also to undergo dissociation on melting, the dissociation being incomplete and increasing in the order $K \rightarrow Na \rightarrow Li$.

— The observation of crystallisation phenomena (see sec. 2.3) showed that in the systems under study, nucleation is the limiting step in crystallisation. Once a nucleus has been formed, crystallisation occurs instantaneously

(this already suggests low melt viscosities). It was observed that the temperature at which crystallisation sets in on cooling (t_{CM}) decreases when trioxide is added to either monotungstate or monomolybdate. This decrease of t_{CM} generally continues beyond the eutectic composition, which can be explained by the assumption that even beyond eutectic composition monotungstate or monomolybdate nuclei start crystallisation. This, however, implies the presence of considerable amounts of WO_4^{2-} and MoO_4^{2-} ions respectively, which can only be expected when the large anionic groups undergo dissociation on melting.

— The infrared spectra of vitreous alkali tungstates in the frequency region 1200–300 cm^{-1} (see sec. 3.3.2) show a great mutual similarity, irrespective of trioxide content and alkali species present, a similarity which is not found in the case of the corresponding crystalline tungstates. This suggests that the structures of all alkali-tungstate glasses are essentially the same, which can be explained by the occurrence of dissociation, either according to the ideas of Kordes and Nolte [7-1]) or to those of Gelsing et al.[7-2]). The spectra which can be synthesized from those of crystalline Na_2WO_4, $Na_2W_2O_7$ and WO_3 considering several values of the degree of dissociation, do not show a satisfactory resemblance to the spectrum of vitreous $Na_2W_2O_7$. A comparison with the spectrum obtained when Gelsing's dissociation scheme is valid, is not possible, since the absorption maxima produced by the W–O–W bond cannot be predicted. (It should be noted here that the conclusions drawn from infrared-spectroscopic results are highly tentative, as the absence of long-range order in the vitreous samples strongly affects the form of the absorption maxima.)

— Both alkali-tungstate and alkali-molybdate melts are low-viscous, having viscosities of 1–20 cP and activation energies for viscous flow of 5–15 kcal $mole^{-1}$. This implies that the flow units in these melts cannot be large, and that no breaking of strong bonds (W–O and Mo–O) is involved.

(b) *In addition to isolated tetrahedra, vitreous alkali molybdates and their melts contain larger groups in which the Mo atoms have coordination numbers higher than 4; in the corresponding tungstates, these larger groups are absent.*

— From a survey of phase diagrams of alkali-molybdate and -tungstate systems (see sec. 1.3) it is seen that crystalline molybdates with compositions situated in the regions of glass formation (viz. di-, tri-, tetramolybdates, etc.) appear more frequently and have higher thermal stabilities than the corresponding tungstates. Further, crystal-structure data (see sec. 1.3) suggest that the Mo atom is more liable to assume distorted coordination than the W atom. Therefore, it is likely that molybdate melts in the regions of glass formation contain more remnants of the groups found in crystal structures than do the corresponding tungstate melts.

— The great mutual similarity shown by the infrared spectra of vitreous alkali tungstates is absent in the case of the corresponding molybdates (see sec. 3.4.2). The spectra are dependent on MoO_3 content and also on the nature of the alkali ion, provided that the MoO_3 content is not extremely high. Moreover, the infrared spectra of the molybdate glasses show certain similarities with the spectra of the crystalline molybdates of equal composition. All this suggests that in the molybdate glasses remnants of the large groups found in crystals are still present, involving Mo atoms having coordination numbers higher than 4. (Again, the restriction must be made that the absence of long-range order in the glasses strongly affects the aspects of the spectra, so that only tentative conclusions can be drawn.)

— The linearity of the molar-volume isotherms of molten alkali-tungstate systems can be correlated with a melt structure containing a mixture of averagely short chains of tetrahedra, in accordance with the views of Gelsing et al.[7-2]). The departures from linearity shown by the isotherms of the corresponding molybdate systems can be attributed to the occurrence of polyhedra with coordination numbers higher than 4 in the glass-formation regions. It should be stressed that the occurrence of these polyhedra implies the formation of larger groups.

— Surface-tension and molar-free-surface-energy values of alkali tungstates in the glass-formation regions are higher than those of the corresponding molybdates (see sec. 5.3). Comparison with the surface tensions of molten alkali metasilicates demonstrates that large anionic groups cause lower surface-tension values than do small groups. Moreover, when both large and small groups are present in the melt, the larger groups will accumulate in the surface layer as a result of the mechanism of adsorption, thus reducing the value of surface tension. Therefore, the relatively low surface-tension values shown by alkali-molybdate melts in the glass-formation regions again strongly suggest the presence of large groups in these melts. At the same time, the high surface-tension values of the corresponding tungstate melts suggest the absence of such groups.

(c) *The relatively small groups occurring in vitreous and molten alkali tungstates are subject to disproportionation*

From the evidence supporting conclusion (a) it is seen that tungstate glasses and their melts contain small anionic groups, while conclusion (b) implies that there cannot be relatively large groups present in these glasses and melts, at least not groups that are liable to raise molar volume and reduce surface tension. The absence of larger groups means that the average coordination number of the W atoms must be approximately 4. Taking the ditungstate composition as an example, glass and melt will consist, on average, of dimers $W_2O_7^{2-}$. However, as was already mentioned above, Gelsing et al.[7-2]) assume the

occurrence of disproportionation, this giving rise to a mixture of monomers, dimers, trimers, etc. (see sec. 1.4).

In the case of phosphate glasses of high alkali content a similar situation exists. Sodium-pyrophosphate glass ($Na_4P_2O_7$), for instance, consists, on average, of dimers $P_2O_7^{4-}$. However, Westman [7-4]) using a paper-chromatographic technique, demonstrated unambiguously that these dimers undergo significant disproportionation, giving rise to a mixture of monomers up to pentamers.

Evidence that considerable amounts of WO_4^{2-} are present in alkali-tungstate glasses and their melts can be derived from the following:

— The cryometric phenomena observed by Kordes and Nolte [7-1]) can only be accounted for by the assumption that an $Na_2W_2O_7$ melt contains WO_4^{2-} monomers.

— As was observed above, crystallisation-temperature determinations (see sec. 2.3) suggest that monotungstate nuclei generally start crystallisation even beyond the eutectic composition. This is only possible when the melts still contain considerable amounts of isolated WO_4^{2-} tetrahedra.

When isolated WO_4^{2-} tetrahedra occur in melts of approximately the ditungstate composition, then, for stoichiometric reasons, higher polymers such as trimers, involving the existence of a disproportionation equilibrium, must also be present.

7.2. Glass formation

Having understood to a certain degree the structures of alkali-molybdate and -tungstate glasses and their melts, we will now consider the reasons why glass formation is found and why it is dependent on the trioxide content and the nature of the alkali ion.

From the crystallisation phenomena observed it was seen that in the systems under consideration nucleation is the limiting step for crystallisation. According to Havermans et al. [7-5]) the formation of a nucleus can be separated into two successive steps:

(a) the formation of a domain of certain critical dimensions having the composition of the crystal to be formed (formation of a protonucleus);

(b) the ordering of such a domain (formation of a nucleus).

When trioxide is added to a melt of the monomolybdate or monotungstate composition, the statistical probability of the formation of a monomolybdate or monotungstate protonucleus gradually decreases. Consequently, the chance of by-passing crystallisation and thus glass formation is increased. The initial formation of ditungstate or dimolybdate nuclei is highly improbable as this is limited by step (b): formation of these nuclei requires a reconstructive process in which the breaking of strong W–O or Mo–O bonds is inevitable (see sec. 6.3.2).

However, when considerable amounts of trioxide have been added, the number of larger groups is raised more and more. Formation of larger groups implies an increase in the tendency of W and Mo atoms to assume higher coordination numbers than 4, corresponding to the situation in crystalline di-, tri- and higher tungstates and molybdates. The process of nucleation needs no longer be reconstructive and, therefore, the tendency to crystallisation is increased.

On this line of reasoning, the presence in the molybdate melts of large groups containing polyhedra with coordination numbers higher than 4 may account for the fact that the glass-formation tendency in molybdate systems generally is lower than that in tungstate systems.

The nature of the alkali ion may influence the glass-formation tendency in at least three different ways:

(a) As its radius decreases and its field strength increases, the alkali ion is likely to have a stronger distorting effect on the complex anion, thus favouring glass formation. Molybdate polyhedra are probably more sensitive to this effect than tungstate polyhedra, as Mo atoms are assumed to have more different coordination possibilities (see sec. 1.3).

(b) The relative numbers of smaller and larger groups (in molybdate melts: degree of dissociation; in tungstate melts: degree of disproportionation) are likely to be dependent on the nature of the alkali ion. Navrotsky and Kleppa [7-3] already assumed that $M_2Mo_2O_7$ on melting undergoes stronger dissociation in the order K → Na → Li. Likewise, Lindqvist [7-6] and Seleborg [7-7] assumed that smaller alkali ions, having higher field strengths, tend to reduce the size of the anionic groups in molybdate melts. In tungstate melts, which contain chains of WO_4 tetrahedra, the average chain length is determined by the trioxide content. However, the position of the disproportionation equilibrium may be dependent on the nature of the alkali ion. For instance, small ions having a high field strength and a tendency to assume low coordination numbers with respect to oxygen, may surround themselves by a number of WO_4 monomers, which possess a high field strength compared with larger anionic groups. In that way the degree of disproportionation will be raised.

This dependence of disproportionation on the nature of the alkali ion can also be observed in the work of Westman [7-4], who determined the chain-length distribution in alkali-phosphate glasses. For example, with an average chain length of 4, the proportion of P atoms occurring in tetramers is 20% in lithium phosphates, 27% in sodium phosphates, and 30% in potassium phosphates.

Both a higher degree of dissociation and a higher degree of disproportionation may favour glass formation.

(c) When the tendency of small alkali ions to create a surrounding of isolated

tetrahedra is very strong, submicroscopical phase separation may occur. Domains containing relatively high proportions of monomers and alkali ions will be formed next to domains containing relatively low proportions of alkali ions and high proportions of larger groups. This tendency will favour nucleation and, therefore, will counteract glass formation.

It can be seen from the results obtained by Gelsing et al.[7-2] and Van der Wielen et al.[7-8] (see sec. 1.2 and fig. 1.1) that, generally, the glass-formation tendency in alkali-tungstate and -molybdate systems increases with decreasing radius of the alkali ion. This indicates that effects (a) and (b) generally dominate effect (c). The only exception to this rule is formed by the Li-tungstate system, suggesting that in this case effect (c) is predominant.

The fact that a similar behaviour is not found in the case of the corresponding molybdate system may be attributed to either (i) effect (a) being stronger in molybdate systems than in tungstate systems, or (ii) the proportion of isolated tetrahedra in molybdate melts being relatively low.

In chapter 1 it was observed that the structures proposed by Gelsing et al.[7-2] and Van der Wielen et al.[7-8] for alkali-tungstate and -molybdate glasses and their melts, being based on a limited amount of experimental data, were highly tentative. It is certainly remarkable that our own ideas on these structures nevertheless correspond to a high degree with those expressed by the above-mentioned authors, the difference being that we have emphasized the presence of large groups in the melts of vitreous alkali molybdates.

7.3. A comparison with similar glasses

For a long time it was thought that the existence of large groups in the melt, giving rise to a high viscosity, was a necessary condition for glass formation. Although the presence of large, irregular groups in the melt certainly favours glass formation, it is becoming more and more clear that even melts containing exclusively small ions can form a glass.

In sec. 2.2.2 the existence of vitreous nitrates has been mentioned. In these systems no large anionic groups are found. It should be noted, however, that Davis et al.[7-9] assume the occurrence of association complexes (e.g. $Na_2NO_3^+$ and $Na(NO_3)_2^-$ ions) in alkali-nitrate melts. These may favour glass formation.

Glasses containing exclusively small anionic groups can also be prepared in the alkali-silicate systems. When the number of bridging oxygen ions per SiO_4 tetrahedron ($= Y$ in the nomenclature of Stevels[7-10]) is considerably lower than 2, a mixture of relatively small chains of tetrahedra is formed. From the work of Havermans et al.[7-5] it is seen that in the K- and NaK-silicate systems glass formation is possible up to compositions approaching that of the ortho-silicates, involving Y values hardly higher than 0.

The glasses which are probably most interesting in this context are alkali-phosphate glasses of high alkali content [7-4], the existence of which has already

been mentioned above. In these glasses the P atoms are tetrahedrally coordinated by oxygen. Glass formation is again possible in regions where only a mixture of relatively short chains is present. By means of paper-chromatographic techniques Westman [7-4]) was able to determine the chain-length distribution. It was already remarked that from the results obtained it can be seen that the chains are subject to stronger disproportionation in the order $K \rightarrow Na \rightarrow Li$.

Vitreous alkali tungstates and molybdates, therefore, are not unique because of the relatively small anions they contain. They are, however, unparalleled because of the phenomenon that, in the vitreous and molten state, coordinations are found which are essentially different from those observed in the crystalline state.

7.4. Final remarks

In sec. 1.5 a number of general glass-formation theories were discussed, none of which, however, appears to have general validity. The reason for this is that the authors of these theories, without exception, try to reduce the problem of glass formation to a matter involving merely one or two simple properties of the glass-forming systems.

It is more likely, however, that a complex of properties influences the tendency to glass formation, the property preventing crystallisation varying from case to case.

Moreover, it may be doubted whether a classification of materials in two groups, the one capable of forming glasses and the other incapable in doing so, is of value until such time as all glass-formation tendencies have been measured quantitatively. In fact, every liquid can form a glass when it is cooled sufficiently rapidly to a sufficiently low temperature.

The first section of this thesis was devoted to a short survey of applications and possible applications of glasses containing appreciable amounts of WO_3 and/or MoO_3. After that section, we restricted ourselves to the investigation of vitreous alkali tungstates and molybdates. Obviously, these glasses are not of commercial interest because of their high critical cooling rates. Perhaps these critical cooling rates can be satisfactorily reduced by a combination of WO_3 and MoO_3 together with various alkali and alkaline-earth oxides. Indications for this can be found in the increased glass-formation tendencies in mixed alkali-tungstate/alkali-molybdate systems, the commercial glasses based on MoO_3, WO_3, MgO and BaO [7-11]) (see sec. 1.1), and the comparable mixed alkali/alkaline-earth nitrate [7-12]), carbonate [7-12]), and silicate (invert) glasses [7-13]).

REFERENCES

[7-1]) E. Kordes and G. Nolte, Z. anorg. allgem. Chem. **371**, 156-171, 1969.
[7-2]) R. J. H. Gelsing, H. N. Stein and J. M. Stevels, Phys. Chem. Glasses **7**, 185-190, 1966.

7-3) A. Navrotsky and O. J. Kleppa, Inorg. Chem. **6**, 2119-2121, 1967.

7-4) A. E. R. Westman, in: J. D. Mackenzie (ed.), Modern aspects of the vitreous state, Butterworths, London, 1960, Vol. 1, pp. 63-92.

7-5) A. C. J. Havermans, H. N. Stein and J. M. Stevels, J. non-cryst. Solids **5**, 66-69, 1970.

7-6) I. Lindqvist, Nov. Acta. reg. Soc. scient. Uppsaliensis, Ser. IV, Vol. 15, No. 1, 1950.

7-7) M. Seleborg, Acta chem. Scand. **21**, 499-504, 1967.

7-8) J. C. Th. G. M. van der Wielen, H. N. Stein and J. M. Stevels, J. non-cryst. Solids **1**, 18-28, 1968.

7-9) W. J. Davis, S. E. Rogers and A. R. Ubbelohde, Proc. Roy. Soc. A **220**, 14-24, 1953.

7-10) J. M. Stevels, Glass Ind. **35**, 657-662, 1964.

7-11) Brit. Pat. Spec. 1,444,153; No. 23872/66.

7-12) H. Rawson, Inorganic glass-forming systems, Academic Press, London, 1967.

7-13) H. J. L. Trap and J. M. Stevels, Glastechn. Ber. **32K**, VI, 31-52, 1959.

Summary

Glass formation in alkali-molybdate and -tungstate systems (M_2MoO_4–MoO_3 and M_2WO_4–WO_3, where M = alkali ion) was found by previous authors in relatively narrow composition regions round 50 mole% MoO_3 and WO_3 respectively. Structures for these glasses have been proposed, which, however, are based on a limited amount of experimental data. The investigations described in this paper try to approach the structures of these glasses from various points of view.

— Determination of the temperatures at which crystallisation sets in when the melt is slowly cooled or the glass slowly heated.

— The regions of glass formation were extended by application of the splat-cooling technique, involving cooling rates of the order of 10^6 °C s^{-1}. This permitted an extensive infrared-spectroscopic study.

— Determination of densities (by the buoyancy method), surface tensions (by the ring method) and viscosities (by the oscillating-hollow-cylinder method) of the molten systems as a function of composition and temperature, based on the concept that there will not be an essential difference between the structures of glass and melt.

Analysis of the results obtained shows that alkali-tungstate glasses contain averagely short chains of WO_4 tetrahedra, which have undergone significant disproportionation. Alkali-molybdate glasses also contain small groups, such as MoO_4^{2-} monomers, in addition to which, however, larger groups are found, comprising Mo atoms with coordination numbers higher than 4. The structures of the glasses essentially differ from those found in crystalline alkali molybdates and tungstates in the glass-formation regions, which contain infinite-chain-type anions. Both groups of glasses have low-viscous melts (1–20 cP). Mixing of either two different alkali species or Mo and W atoms strongly decreases the value of the critical cooling rate and, therefore, favours glass formation.

SAMENVATTING

Eigenschappen van glasvormige en gesmolten alkalimolybdaten en -wolframaten

Uit de literatuur is bekend, dat in de pseudobinaire systemen M_2MoO_4–Mo_3 en M_2WO_4–WO_3 (M = alkali metaal) glasvorming mogelijk is, zij het in nauwe samenstellingsgebieden.

De neiging tot glasvorming is afhankelijk van:

(a) het gehalte aan MoO_3 of WO_3 (in het algemeen: trioxide) met dien verstande, dat glasvorming het gemakkelijkst optreedt rond de samenstellingen 50 mol % M_2MoO_4/50 mol % MoO_3 en 50 mol % M_2WO_4/50 mol % WO_3.

(b) de aard van het alkali-ion, met dien verstande, dat in het algemeen de neiging tot glasvorming daalt in de richting Li→Cs.

Een kwantitatieve maat voor de neiging tot glasvorming is de waarde van de kritische afkoelsnelheid (CCR, in °C/s), d.i. de afkoelsnelheid waarbij juist geen kristallisatie meer optreedt. De laagste CCR, gemeten in alkalimolybdaat- en -wolframaatsystemen is van de orde van grootte van 10 °C/s.

De kristalstrukturen van een aantal verbindingen, voorkomend in de onderzochte systemen, zijn bekend.

De verbindingen M_2MoO_4 en M_2WO_4 zijn, onafhankelijk van de aard van het alkali-ion, opgebouwd uit geïsoleerde MoO_4 resp. WO_4 tetraeders. In de trioxiden zijn de Mo resp. W atomen omringd door zes zuurstofatomen. De MoO_6 oktaeders vormen vlakken, terwijl de WO_6 oktaeders een driedimensionaal netwerk vormen.

In het tussenliggende samenstellingsgebied zijn kristalstrukturen bekend waarin oneindig lange anionketens voorkomen, die zijn opgebouwd uit polyeders met gemengde zuurstofomringing, hetzij oktaeders en tetraeders, hetzij oktaeders en polyeders met vijfomringing.

Het struktuuronderzoek van glasvormige alkalimolybdaten en -wolframaten behelsde tot nu tot voornamelijk een qua samenstellings- en frekwentiegebied beperkt gebleven infraroodonderzoek. Op grond daarvan meenden Gelsing et al., dat alkaliwolframaatglazen een mengsel van gemiddeld korte tetraederketens bevatten. Van der Wielen et al. waren van mening, dat glasvormige alkalimolybdaten ketens van vervormde tetraeders bevatten. Beide struktuurhypothesen houden in dat de grote aniongroepen, voorkomende in de kristallijne verbindingen, dissociëren bij het smelten. Steun hiervoor kan gevonden worden in de kryometrische studie van Kordes en Nolte, die aantoont, dat in gesmolten $Na_2W_2O_7$ geïsoleerde WO_4 tetraeders voorkomen.

Vergelijking met de diverse theorieën over glasvorming in anorganische oxidische systemen leert, dat alkalimolybdaten en -wolframaten enerzijds een hogere, anderzijds een lagere neiging tot glasvorming vertonen, dan op grond van deze theorieën verwacht.

Het in dit proefschrift beschreven onderzoek had tot doel meer aanwijzingen te verkrijgen over de struktuur van glasachtige molybdaten en wolframaten. Daarmee werd tevens een onderzoek ingesteld naar de fundamentele mechanismen die de vorming van glas beheersen.

In hoofdstuk 2 wordt aangetoond dat het mogelijk is, de eerder gevonden glasvormingsgebieden uit te breiden met behulp van de spatkoelmethode: enkele mg gesmolten molybdaat of wolframaat worden door een krachtige luchtstoot uitgespat over een relatief koud oppervlak. De bereikte afkoelsnelheid wordt geschat op 10^6 °C/s. Met deze methode konden de glasvormingsgebieden aanzienlijk worden uitgebreid, met name in de richting van grotere MoO_3-gehalten (tot 100 mol% MoO_3) en WO_3-gehalten (tot 70 mol% WO_3).

Bovendien werd geconstateerd, dat door het mengen van molybdaat en wolframaat en/of twee soorten alkali-oxide een aanmerkelijke vergroting van de neiging tot glasvorming kan worden verkregen. De laagste CCR welke werd bereikt, was 1 °C/s.

De temperaturen waarbij de eerste kristallisatie optreedt bij langzaam afkoelen van de smelt en bij langzaam verwarmen van het glas (resp. t_{CM} en t_{CG}) werden bepaald. In het algemeen komt de samenstelling van minimale t_{CM} overeen met die van minimale CCR, maar *niet* met de eutektische samenstelling.

In hoofdstuk 3 wordt een infrarood spectroscopisch onderzoek beschreven van een groot aantal kristallijne en glasvormige monsters in het frekwentiegebied 1200–300 cm^{-1}. Er bestaat een grote mate van analogie tussen de spectra van de glasvormige wolframaten, ongeacht de aard van het aanwezige alkali-ion of het trioxide-gehalte. Bij de molybdaatglazen is de onderlinge overeenkomst tussen de spectra veel geringer.

De voornaamste conclusie die uit het infraroodonderzoek getrokken kan worden is, dat een zodanig onderzoek onmogelijk de basis kan vormen van een struktuurhypothese, o.a. omdat de afwezigheid van *long-range order* de absorptiebanden van het glas sterk vervormt.

Aanwijzingen over de struktuur van een glasvormig systeem kunnen vaak afgeleid worden uit het verband tussen bepaalde fysische eigenschappen en de samenstelling van het systeem. In de beschouwde systemen kan slechts in nauwe samenstellingsgebieden een redelijke hoeveelheid glas worden verkregen. Daarom is in ons geval de indirekte methode gekozen van de bepaling van fysische eigenschappen in de gesmolten toestand, gebaseerd op de gedachte dat de struktuur van een vloeistof niet essentieel zal verschillen van die van het overeenkomstige glas.

De systemen die werden uitgekozen voor deze metingen zijn de Li, Na en K

molybdaat- en wolframaatsystemen, alsmede enkele gemengde alkalioxide- en molybdowolframaatsystemen.

Achtereenvolgens werden van deze systemen de dichtheid, oppervlakte-spanning en viskositeit als functie van temperatuur en samenstelling bepaald.

In hoofdstuk 4 worden metingen van de dichtheid beschreven. De gebruikte methode was die van het bepalen van de opwaartse kracht uitgeoefend door de vloeistof op een platina dompelgewicht.

Het molair volume bij 950 °C is voor de wolframaatsystemen lineair af-hankelijk van de samenstelling, uitgedrukt in mol % trioxide. Bij de molybdaat-systemen worden positieve afwijkingen t.o.v. een lineair gedrag gevonden. Deze verschijnselen kunnen, voor wat de wolframaten betreft, in verband worden gebracht met een struktuur, waarin de W atomen uitsluitend voorkomen in tetraedrische omringing. Evenzo kan het gedrag van de molybdaten gecorre-leerd worden met een struktuur waarin grote aniongroepen voorkomen met Mo atomen omringd door méér dan vier zuurstofatomen.

Hoofdstuk 5 behandelt de metingen van de oppervlaktespanning, verricht door middel van het bepalen van de maximale trekkracht op een platina ring welke ondergedompeld is in de vloeistof.

Toevoeging van MoO_3 aan gesmolten M_2MoO_4 verlaagt de waarden van oppervlaktespanning en molaire vrije oppervlakte-energie aanzienlijk meer dan de toevoeging van WO_3 aan gesmolten M_2WO_4. Dit verschijnsel kan verklaard worden met de aanname dat in gesmolten wolframaat alleen kleine anionen voorkomen, opgebouwd uit WO_4 tetraeders, terwijl in gesmolten molybdaat ook grotere anionen worden aangetroffen, waarin Mo atomen in hogere om-ringingssituaties voorkomen.

In hoofdstuk 6 wordt de bepaling van de viskositeit van gesmolten alkali-molybdaten en -wolframaten beschreven. Hiertoe werd gebruik gemaakt van de methode van de oscillerende holle cylinder.

De resultaten tonen aan dat voor alle gemeten samenstellingen en tempera-turen de viskositeitswaarde ligt in het gebied 1–20 cP, hetgeen voor een glas-vormende smelt uitzonderlijk laag is. Dientengevolge is het onmogelijk dat er in de gesmolten molybdaten en wolframaten *uitsluitend* grote aniongroepen voorkomen.

Er blijkt geen verband te bestaan tussen de waarde van de viskositeit en de neiging tot glasvorming.

De aanwijzingen die ten aanzien van de struktuur van glasvormige en ge-smolten alkalimolybdaten en -wolframaten afgeleid kunnen worden uit litera-tuurgegevens en uit eigen meetresultaten, zijn samengevat in hoofdstuk 7.

De voornaamste conclusies zijn:

(a) De grote aniongroepen welke voorkomen in kristallijne alkalimolybdaten en -wolframaten in de glasvormingsgebieden, dissociëren bij het smelten in een groot aantal kleinere groepen.

(b) Naast geïsoleerde tetraeders, bevatten glasvormige en gesmolten alkalimolybdaten relatief grote aniongroepen, waarin Mo atomen voorkomen met omringingsgetallen groter dan 4; in de corresponderende wolframaten zijn deze grote groepen afwezig.

(c) De relatief kleine aniongroepen, die in glasvormige en gesmolten alkaliwolframaten voorkomen zijn onderhevig aan een disproportioneringsevenwicht volgens reakties van het type $2\,W_2O_7^{2-} \rightleftarrows WO_4^{2-} + W_3O_{10}^{2-}$.

Levensbericht

Robert Georg Gossink werd op 8 juni 1945 te Eindhoven geboren. In 1963 behaalde hij het diploma gymnasium β aan het Gemeentelijk Lyceum te Eindhoven. Vervolgens werd hij ingeschreven als student aan de Technische Hogeschool in diezelfde stad. In 1966 behaalde hij met lof het kandidaatsexamen in de afdeling der scheikundige technologie en in 1968, eveneens met lof, het ingenieursexamen. Zijn afstudeeronderzoek verrichte hij onder leiding van Prof. Dr. J. M. Stevels in de groep silikaatchemie van de sektie anorganische chemie.

Na zijn ingenieursexamen trad hij in dienst van het Natuurkundig Laboratorium van de N.V. Philips' Gloeilampenfabrieken. De directie hiervan stelde hem in staat zijn afstudeeronderzoek te continueren aan de Technische Hogeschool Eindhoven in de vorm van een promotie-onderzoek.

Op 19 maart 1970 trad hij in het huwelijk met mej. E. H. Schaafsma. Sinds 1 maart 1971 is hij werkzaam in het Natuurkundig Laboratorium te Waalre in de groep Glas.

STELLINGEN

R. G. GOSSINK

STELLINGEN

I

De kryoskopische verschijnselen, zoals deze door Kordes en Nolte zijn waargenomen bij $Na_2W_2O_7$, kunnen behalve met het door hen als enig juist beschouwde dissociatieschema ook verklaard worden met een dissociatie in een mengsel van gemiddeld korte tetraederketens.

<div align="right">E. Kordes en G. Nolte, Z. anorg. allgem. Chem. 371, 156, 1969.</div>

II

De relatief lage waarden van de verhouding tussen aktiveringsenergie van viskeuze stroming (E_η) en aktiveringsenergie van specifiek geleidingsvermogen (E_κ) voor gesmolten alkalimonomolybdaten en -monowolframaten berusten eerder op lage waarden van E_η dan op hoge waarden van E_κ.

III

Het in het veelgebruikte naslagwerk ,,Phase diagrams for ceramists'' opgenomen fasediagram van het systeem K_2MoO_4-MoO_3 is niet met de nodige kritische zin geselekteerd.

<div align="right">E. M. Levin, C. R. Robbins en H. F. McMurdie, Phase diagrams for ceramists, American Ceramic Society, Columbus, 1964/1969.</div>

IV

Gesmolten $Ag_2Mo_2O_7$ vormt glas, mits afgekoeld met een snelheid van meer dan $200\,^\circ C\ s^{-1}$.

V

De boriumtrioxide-anomalie heeft in de glasliteratuur aanzienlijk meer aandacht gekregen dan de grotendeels analoge germaniumdioxide-anomalie.

<div align="right">H. Rawson, Inorganic glass-forming systems, Academic Press, Londen, 1967.</div>

VI

De natchemische methode van glasbereiding biedt uitzicht op het verkrijgen van aanzienlijk homogener en zuiverder glazen dan tot nu toe mogelijk is volgens de klassieke methode.

VII

De veronderstelling, dat de hallucinogene werking van d-lysergzuur diethyl amide (LSD 25) berust op de anti-serotonergische aktiviteit van deze stof in het centrale zenuwstelsel, is gerechtvaardigd.

R. J. Boakes et al., Br. J. Pharmac. **40**, 202, 1970.
J. M. van Ree, persoonlijke mededeling.

VIII

Het onjuiste gebruik van het begrip entropie door Jevgenij Zamjatin illustreert het gevaar van het toepassen van dit begrip buiten de thermodynamica.

Jevgenij Zamjatin in: Teken van leven, Meulenhoff, Amsterdam, 1969, pp. 134-141.

IX

Met het heengaan van S. Vestdijk heeft de Nederlandse romankunst vrijwel opgehouden te bestaan.

X

Het toepassen van de „sticks-regel", zoals dit gebruikelijk is op de Nederlandse hockeyvelden, geeft aan de arbitrage een element van willekeur.

XI

Het verdient aanbeveling dicht bij elkaar geplaatste telefoontoestellen te voorzien van verschillende, karakteristieke wektonen.

Eindhoven, 29 juni 1971   R. G. Gossink